E-20-673
5

USEPA Great Lakes Mid-Atlantic Hazardous Substance Research Center

FINAL PROGRESS REPORT

For the Period:
June 1, 1998 – September 30, 2002

Deliverable #5
(Due December 31, 2002)

TRAC II: SUBPROJECT IV:
Development of the Density Modified Displacement (DMD) Method for Efficient Recovery of DNAPLs from Contaminated Aquifers: Experimental Evaluation and Mathematical Modeling

February 22, 2002

Point of Contact: Kurt D. Pennell, Ph.D.
School of Civil & Environmental Engineering
Georgia Institute of Technology
311 Ferst Drive
Atlanta, GA 30332-0512
Tel: 404-894-9365
Fax: 404-894-8266
E-mail: kpennell@ce.gatech.edu

(I) PROJECT TITLE: Development of the Density Modified Displacement (DMD) Method for Efficient Recovery of DNAPLs from Contaminated Aquifers: Experimental Evaluation and Mathematical Modeling

(II) INVESTIGATORS: Principal Investigator: Kurt D. Pennell, Associate Professor, School of Civil & Environmental Engineering, 311 Ferst Drive, Georgia Institute of Technology, Atlanta, GA 30306-0512.

(III) PROJECT GOALS:

The overall objective of this project is to refine specific aspects of the DMD technology and develop a numerical model capable of simulating the DMD process in heterogeneous subsurface systems. The anticipated products of this research include a system of experimental protocols for DMD technology implementation and numerical simulator to be used for DMD remedial design. Specific objectives of the project are listed below.

(1) *Screen and select alcohols and other miscible compounds for in-situ density modification of* pure and mixed DNAPLs;
(2) Measure the phase behavior (ternary phase diagrams) and mass transfer of alcohols in selected surfactant/alcohol/DNAPL systems;
(3) Evaluate the DMD technology and develop optimal flushing strategies in two-dimensional aquifer cells; and
(4) Develop and validate a mathematical simulator to be used for DMD design and performance predictions at the field scale.

(IV) RATIONALE:

Surfactant-induced displacement of DNAPLs has been shown to be an extremely efficient means for recovering DNAPLs from laboratory soil columns (Pennell et al., 1994; 1996). Utilization of this approach in the field, however, could lead to uncontrolled migration of the mobilized free product. This is of particular concern for DNAPLs, which tend to travel downward through an aquifer formation until a confining layer is encountered. To overcome this limitation, a Density Modified Displacement (DMD) method has been developed by Dr. Pennell which incorporates (1) *in-situ* conversion of DNAPLs to LNAPLs using alcohols and (2) displacement of the resulting LNAPL by low interfacial tension surfactant solutions. In the DMD system, alcohol is introduced in a pre-flush solution (prior to surfactant flushing), as an additive to the surfactant solution, or both. When properly implemented, the DMD technique results in upward displacement and recovery of the NAPL phase. To date, a limited number of proof-of-concept experiments have been completed as part of previous GLMAC HSRC research activities (Thrust Area II: Spring '97 SAC meeting). Based on these results, a provisional patent application was filed in April 1997, followed by a full patent application in April 1998. On August 8, 2000, U.S. Patent No. 6,099,206 was issued for "Density Modification Displacement To Remediate Contaminated Aquifers". Although the DMD technology holds great promise, detailed experimental and mathematical modeling work is required to extend the method to a wider range of DNAPLs and to address issues related to implementation in heterogeneous subsurface systems. The research project has been structured to couple detailed experimental

work with mathematical model development and testing. A matrix of batch, column and 2-D aquifer cell experiments will be conducted to refine and test the DMD method. Experimental results will be used as the basis for mathematical model development and simulator testing. It is anticipated that this research will lead to the development of an extremely efficient method for DNAPL recovery from contaminated aquifers.

(V) APPROACH:

To achieve the research objectives, the project has been organized around three main tasks that are summarized below. The project involves direct collaboration with other GLMAC investigators, including Dr. Linda Abriola who will develop and test a mathematical model to simulate the DMD process described in Task 3. In addition, Dr. Kim Hayes will conduct a series of complementary batch experiments designed to investigate the mass transfer of alcohols into DNAPL droplets and the corresponding conversion of DNAPLs to LNAPLs (Subproject I). The experimental matrix will include four DNAPLs of varying density (PCE, TCE, DCB and CB) and a DNAPL/LNAPL mixture selected by TRAC II members. Properties of the four representative DNAPLs are given in Table 1. Bachman aquifer material will be used as the solid phase for the 2-D column and aquifer cell studies. The initial surfactant formulations to be considered will consist of 4% solution of Aerosol MA-100/Aerosol OT-100 (4:1) and a 4% solution of Aerosol MA-100, both with 500 mg/L $CaCl_2$ as a background electrolyte.

Table 1. Relevant properties of the DNAPLs selected for study.

DNAPL	MW (g/mole)	Solubility (mg/L)	Density (g/cm^3)	Viscosity (mN/m^2)	VP (mm Hg)	IFT (water) (dyne/cm)
Tetrachloroethene (PCE)	165.8	200	1.62	0.90	14	47.5
Trichloroethene (TCE)	131.4	1100	1.46	0.57	60	34.5
Dichlorobenzene (DCB)	147.2	100	1.31	1.41	1	23.2
Chlorobenzene (CB)	112.6	500	1.11	0.80	12	37.4

Task 1. Selection of Partitioning Alcohols and Surfactant Formulations

The first phase of this work involves detailed testing of alcohols and other partially-miscible compounds that have the potential to modify the density of DNAPLs *in-situ*. Initially, a matrix of batch experiments will be conducted with three alcohols (n-butanol, n-pentanol, and tert-butanol) and four DNAPLs (PCE, TCE, DCB and CB). Ternary phase diagrams, density, viscosity, and interfacial tension measurements will be completed for all of the systems investigated. In selecting an appropriate partitioning alcohol or solute, it will be necessary to consider (1) the tendency for the compound to partition into the DNAPL, (2) aqueous phase solubility, and (3) any unusual phase behavior (e.g., formation of gels) that may occur.

Task 2. Aquifer Cell Testing of DMD

The second phase of this work will involve small and medium-scale rectangular (2-D) aquifer cell experiments. The small cells will be constructed from rectangular borosilicate glass

columns (5 cm H X 15 cm L X 2.5 cm W) equipped with custom made rectangular endplates. The columns will be packed with air-dried Bachman aquifer material in 1 cm increments under vibration. After the rectangular endplates have been secured, the soil column will be saturated with CO_2 gas to facilitate rapid and complete saturation of the column with water. A Rainin HPLC pump, equipped with a pulse damper and back pressure regulator to minimize pulsing, will be used to saturate the column with water. After complete water saturation, DNAPL will be injected into the column in an up-flow mode using a Harvard Apparatus Model 22 syringe pump, followed by downward flushing with water to achieve a uniform residual saturation of DNAPL. The rectangular column will then be oriented in a horizontal position. DMD formulations containing alcohol and surfactant (selected based upon the results of Task 1) will then be flushed through the contaminated soil columns. Various DMD flushing strategies will be evaluated in these experiments, including flow interruption and alcohol preflushing. The rate of alcohol mass transfer into the NAPL phase will also be evaluated in a series of alcohol flushing experiments. Based on the results of the small-scale rectangular columns, a limited number (~10) of medium-scale aquifer cell (40 cm H X 60 cm L X 1.5 cm W) experiments will be conducted. These studies will allow for the evaluation of the DMD approach on a larger scale and in the presence of heterogeneity (low-permeability lenses). Data collected from both the small- and medium-scale 2-D cells will be utilized in Task III to develop and evaluate a numerical simulator for use in DMD remedial design and performance evaluation.

Task 3. Development and Evaluation of a Numerical Simulator for DMD

The success of the DMD technology in the field will ultimately depend upon our ability to predict and control DNAPL displacement and transport in a three-dimensional setting. The performance of DMD depends on the complex interplay of buoyancy, viscous, and capillary forces. In natural systems, however, these forces will be spatially and compositionally dependent, precluding any simple *a priori* predictions of system behavior. Modeling tools will, thus, be required to design, monitor, and predict the performance of this technology in the field. The DMD model to be developed in this task will be based upon a full two-phase compositional non-equilibrium formulation. An existing code, MISER (Abriola *et al.*, 1997), a two-phase reactive transport model originally developed for unsaturated zone remediation, will be extensively adapted for this purpose. MISER will be adapted to simulate the two-phase flow of surfactant solution and organic liquid based on the solution of phase mass balance equations. A parametric model for the capillary retention and relative permeability functions is developed in a manner similar to that presented by Kaluarchchi and Parker (1992). The retention function will be represented with either the standard Brooks-Corey or van Genuchten type expression, and the model will account for full hysteresis in the retention function and organic liquid relative permeability function. Effects of flow behavior caused by changes in the aqueous/organic interfacial tension will be accounted for by Leverett-type scaling of the two-phase retention function in proportion to the ratio of interfacial tensions. Additionally, the total trapping number concept will be employed to quantify the trapping and mobilization of the organic liquid as a function of capillary and buoyancy forces. A two-dimensional model will be developed initially, and experiments conducted under Task 2 will be used to validate and refine the two-dimensional simulator. The model will then be extended to three dimensions, facilitating the analysis of complex field-scale behavior.

(VI) RESULTS:

The following sections summarize experimental results obtained during the period June 1, 1998 through September 30, 2002. The work performed under Task 1 involved a large matrix of batch experiments that were designed to select and evaluate partitioning alcohol and surfactant formulations for use in the DMD process. In Task 2, a series of 2-D box experiments were performed to evaluate the DMD process for recovery of representative DNAPLs (e.g., CB, TCE, PCE) and selected DNAPL mixtures. In situ density conversion of the DNAPL was realized by flushing with either an aqueous solution containing 6% butanol or a surfactant-stabilized macroemulsion containing 15% butanol. Subsequent displacement of the density-modified DNAPL was then achieved by flushing with a low-IFT surfactant formulation consisting of either 4% Aerosol MA/OT (4:1) + 20% butanol + 0.500 g/L $CaCl_2$.or 10% Aerosol MA + 15% butanol + 15 g/L NaCl + 1 g/L $CaCl_2$. Mathematical model development and testing results (Task 3) are not described in this report because this work was conducted under a separate subcontract to Dr. Linda Abriola at the University of Michigan by.

Task 1. Selection of Partitioning Alcohol and Surfactant Formulation

Task 1.A. DNAPL Density Conversion Using n-Butanol in Aqueous Solutions

In previous experiments, the partitioning of butanol into several chlorinated solvents has been shown deviate from ideality, yielding partitioning curves that were nonlinear. These results demonstrated that under equilibrium conditions more alcohol was present in the aqueous phase than was anticipated based on ideal phase behavior. Despite this nonlinear partitioning behavior, it is still possible to develop surfactant-alcohol flushing solutions that will achieve *in situ* density conversion of DNAPLs. Along with the desired density reduction, however, the partitioning of alcohol into a DNAPL can lead to significant changes in viscosity and interfacial tension. Furthermore, little or no attention has been directed toward the partitioning of water into the DNAPL phase, which occurs concurrently with alcohol partitioning, and may alter relevant physical and chemical properties of the resulting NAPL. Therefore, the purpose of the batch experiments conducted during the past six months was to quantify the effects of butanol partitioning on the water content, density, interfacial tension and viscosity of two DNAPLs, chlorobenzene (CB) and trichloroethylene (TCE).

Phase Behavior

The results of the CB and TCE phase behavior studies are described using ternary phase diagrams (Figures 1 and 2, respectively). These diagrams indicate both the CB/n-butanol/water and TCE/n-butanol/water systems exhibit type II phase behavior resulting from two partially miscible pairs (CB or TCE/water and n-butanol/water) and one miscible pair (CB or TCE/n-butanol) in each system. It is important to note that both the CB and TCE diagrams contain two single-phase regions, although the single aqueous phase region (lower right corner) is very small and this boundary is not distinguishable. Measured tie lines slope downward toward the water apex (lower right) for both CB and TCE, indicating substantial partitioning of n-butanol into the organic liquid phase. Although g^E models typically have difficulty predicting ternary liquid-liquid equilibrium, calculated UNIQUAC phase behavior (boundaries and tie line slopes) were found to be in relatively good agreement with experimental data (Figures 1 and 2). The UNIQUAC calculated tie lines shown in both phase diagrams provide an indication of the predicted tie line slope in the proximity of each experimental tie line.

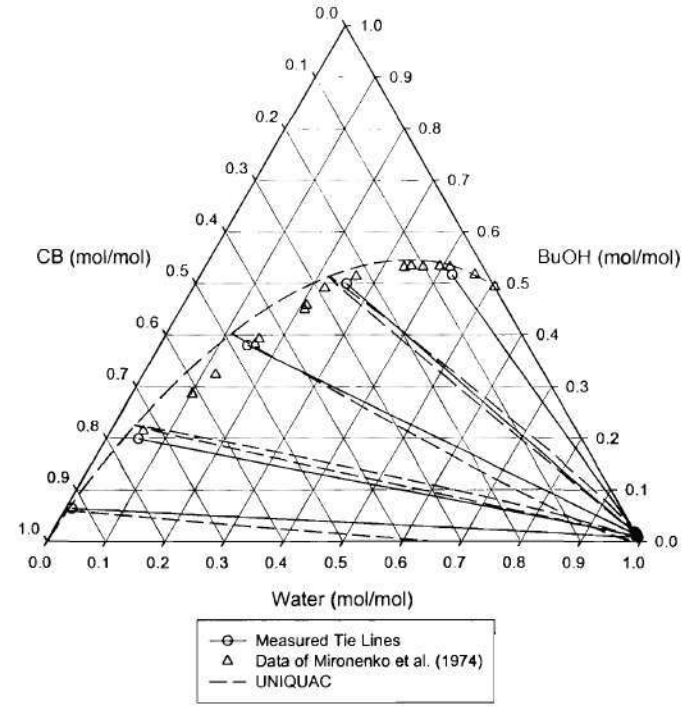

Figure 1. Ternary phase diagram for the CB/BuOH/Water system.

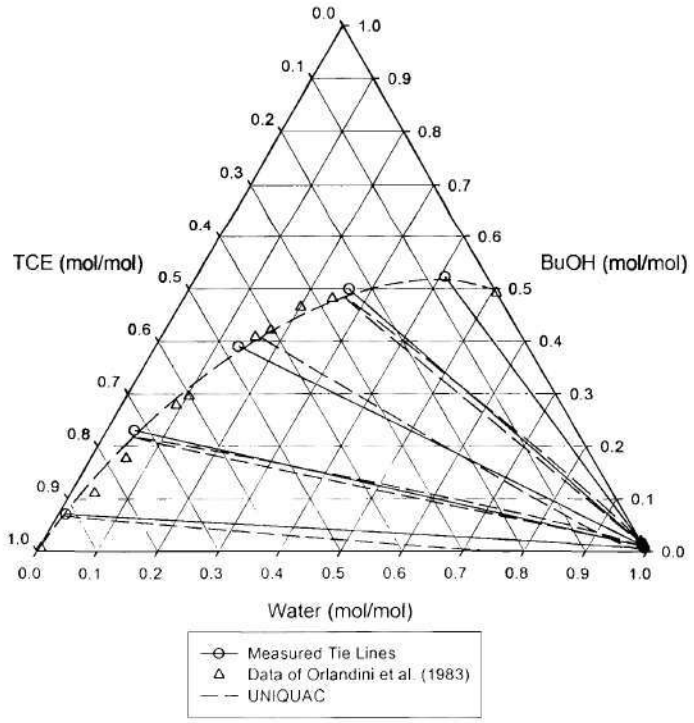

Figure 2. Ternary phase diagram for the TCE/BuOH/water system.

The tie lines represent lines of constant composition within the two-phase envelope. Any mixture composition residing on a tie line will separate into two phases with compositions described by the end points of the tie line. A significant application of this concept, in regard to DMD, is that there exists one tie line that represents DNAPL to LNAPL density conversion. Regions in which equilibrated sample mixtures contained two phases are labeled as DNAPL and LNAPL, and are separated by a tie line corresponding to density conversion (Figure 3). The location of the DNAPL-LNAPL boundary is a function of contaminant density and extent of n-butanol and water partitioning. While the exact location of this boundary may be altered by changes in aqueous phase density (e.g., the addition of salts) the intent here was to assess density conversion resulting from n-butanol partitioning. The location of the density transition boundary, and consequently the area of the LNAPL region are governed largely by the initial (pure component) NAPL density. For CB, the DNAPL-LNAPL boundary coincided with smaller mole fractions of n-butanol, resulting in a relatively larger LNAPL region (Figure 3). In contrast, the DNAPL-LNAPL boundary for TCE occurred at a higher mole fraction of n-butanol, resulting in a much smaller LNAPL region. These results illustrate the increased difficulty associated with density conversion of relatively dense NAPLs. In practice, relatively larger amounts of n-butanol will be required to modify the density of DNAPLs, such as TCE or PCE. Preflood solutions for these relatively heavy DNAPLs must contain high concentrations of n-butanol (i.e., near the solubility limit), and several pore volumes may be required to achieve in situ density conversion.

Alcohol Partitioning

The equilibrium partitioning of n-butanol in the ternary system consisting of CB/n-butanol/water and TCE/n-butanol/water was investigated over the entire range of organic phase n-butanol mole fractions. Experimental and calculated (UNIQUAC) aqueous phase n-butanol concentrations (g/L) are plotted against organic liquid, n-butanol mole fractions (X_{BuOH}) in Figure 4. Partitioning of n-butanol in these systems was observed to be nonlinear (non-ideal), which is consistent with the findings of previous studies (see Trac II Subproject I and IV Progress Reports, Fall 2000). UNIQUAC calculations were likely affected by the interaction parameters for the miscible contaminant/n-butanol pairs. These parameters were regressed from binary vapor-liquid equilibrium, and therefore do not fully account for the interactions of the complex ternary system.

The sigmoidal trend of the n-butanol partitioning data and lower range (<0.6) of X_{BuOH} are due to the incorporation water into the organic liquid phase. To illustrate this point, the data used in Figure 4 are shown in Figure 5 neglecting the water content of the organic phase (an assumption made in previous studies see Trac II Subproject I and IV Progress Reports, Fall 2000). Under the assumption of a binary NAPL system (Figure 5), alcohol partitioning was examined over the entire range of organic phase n-butanol mole fractions. While the general n-butanol partitioning trends of these data are similar at lower X_{BuOH} (<0.3), there is a marked difference for X_{BuOH} above 0.3. At relatively high X_{BuOH}, an increase in aqueous phase n-butanol concentration has little effect on the composition of the NAPL (Figure 4). The limited effect of n-butanol partitioning on the NAPL n-butanol mole fraction is due to lower contaminant mole fraction (NAPL) in this range, for which the mixture approached a binary n-butanol/water system.

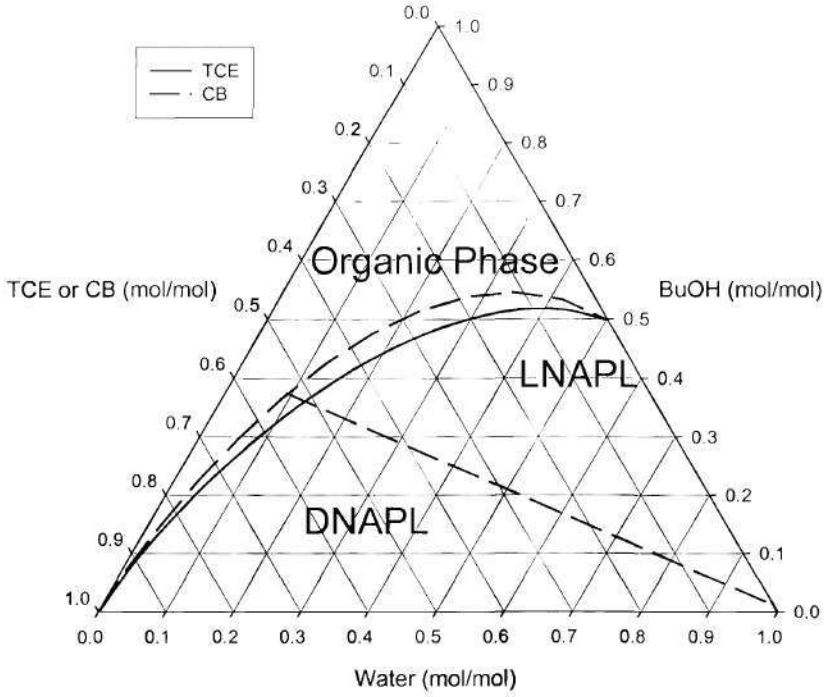

Figure 3. Density transformations inside the two-phase region.

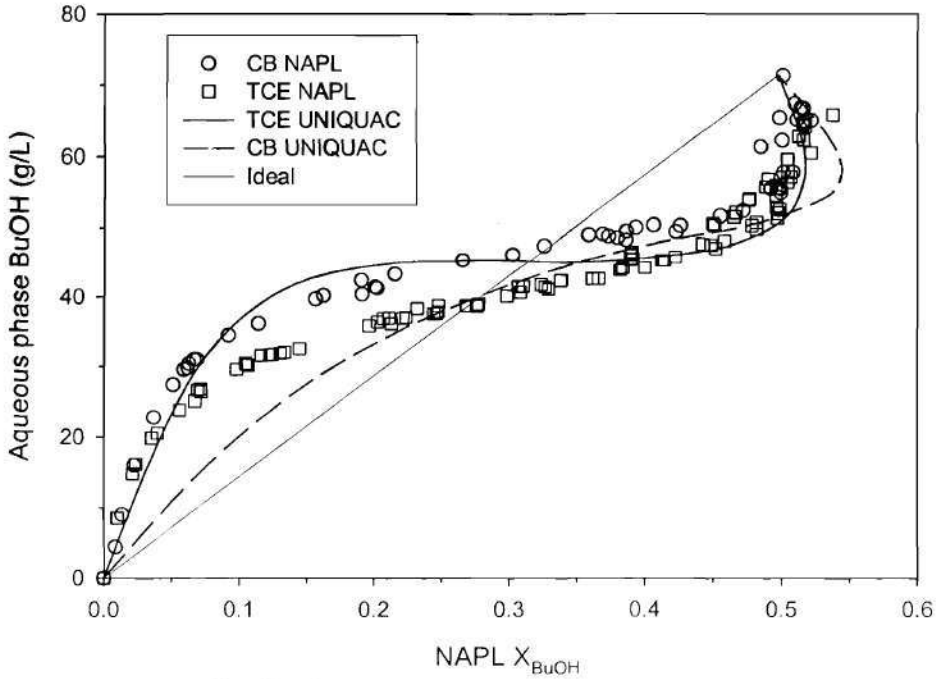

Figure 4. n-butanol distribution between the aqueous phase and NAPL.

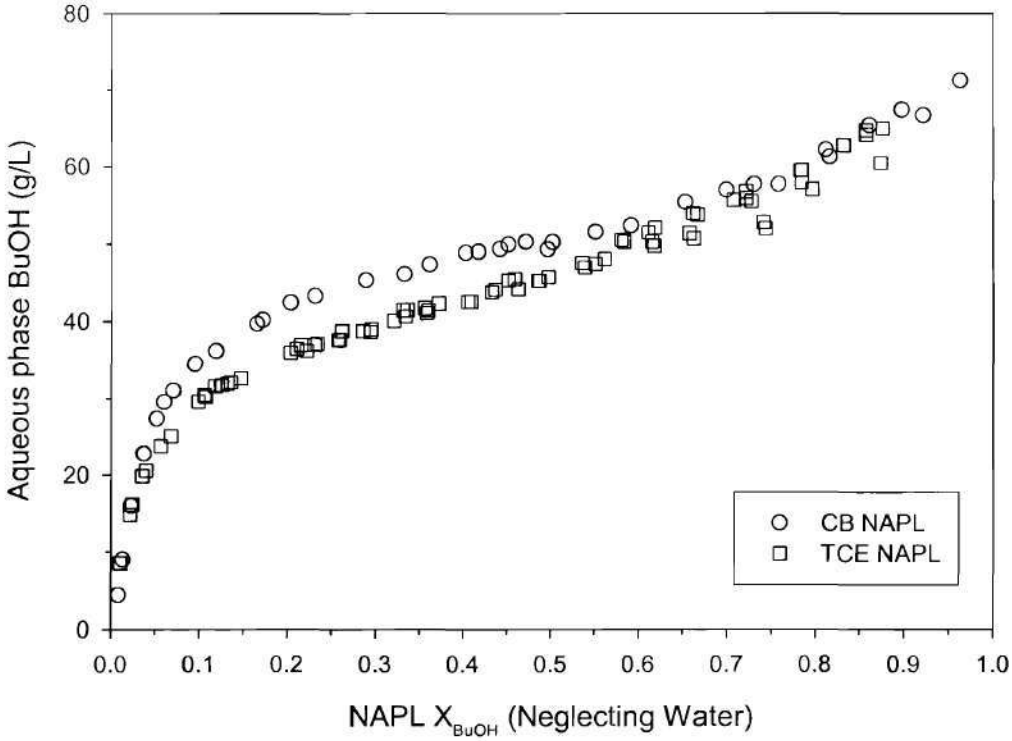

Figure 5. n-butanol distribution neglecting the water content of the NAPL.

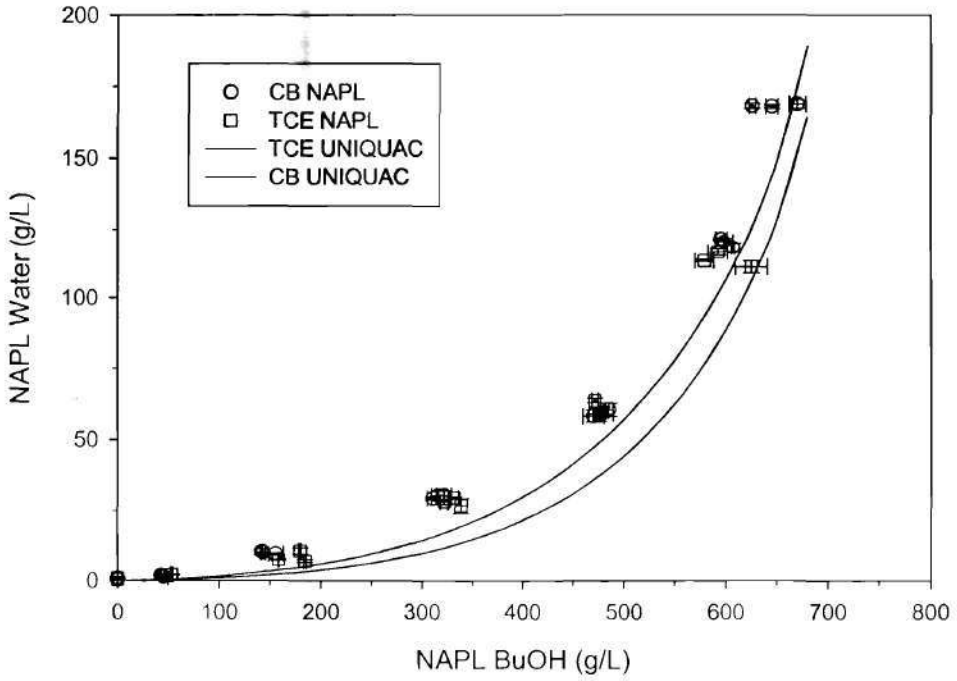

Figure 6. Water content of CB-NAPL and TCE-NAPL with increasing BuOH content.

The solubility of water is relatively low in both CB and TCE (0.033 and 0.32 wt% respectively). In contrast, the solubility of water in n-butanol is 20% (wt.), which corresponds to a water mole fraction of 0.515 for a binary system of water and n-butanol. This large tendency for water to dissolve into n-butanol necessitates the determination of NAPL water content for systems containing n-butanol. The water contents of CB-NAPL and TCE-NAPL are presented as a function of NAPL n-butanol concentration (Figure 6). An increase in the concentration of n-butanol in the NAPL resulted in a corresponding increase in the water content of the NAPL. The tendancy for water to be incorporated in the n-butanol containing NAPL is an extension of the water incorporation observed in the binary n-butanol-water system. When considered on a concentration basis, the experimental data for CB and TCE coincide, further demonstrating that water incorporation was due to the presence of n-butanol (Figure 6). The results from the UNIQUAC calculations are also shown in Figure 6. These predictions accurately captured the trend of the data because the n-butanol/water binary interaction parameter was based on mutual solubilities (liquid-liquid equilibrium) and the interactions between the contaminant and water were negligible, as evident by their nearly immiscible nature.

DNAPL Density Conversion

The dissolution of water into the NAPL acts to buffer further density alteration, and in practice could prohibit attainment of the necessary buoyancy force for upward displacement in porous media. The measured and predicted (from UNIQUAC compositional calculations) densities of CB and TCE as a function of increasing X_{BuOH} are shown in Figure 7. The density of water at the same temperature is also shown in Figure 7 as a point of reference. As n-butanol partitioning increased, the incorporation of the water initially helps to lower the density of the DNAPL, however, at and above NAPL X_{BuOH} sufficient for density conversion, the incorporation of water had a less beneficial impact. The point of density conversion (approximately X_{BuOH} of 0.38 for CB and 0.50 for TCE relative to water at 22±2°C) is also dependent upon the aqueous phase density. Several options exist for both the preflood and displacement flood solutions, however, without careful consideration for the solution density, upward displacement may not occur. It is, however, important to note that attainment of neutral buoyancy (between the NAPL and resident flushing solution) may be an acceptable end point for the DMD process. The possibility of horizontal displacement of density modified NAPL may be especially important for heavier DNAPLs, which will require the incorporation of substantial n-butanol mass to approach the density of water. The sharp inflection in the TCE density data at X_{BuOH}=0.5 occurred at substantially higher n-butanol mole fractions than was observed for CB density conversion, but very near to the n-butanol mole fraction necessary for TCE density conversion. The observed inflection in density corresponded to the sharp upward turn in the partitioning data (Figure 4), and in both cases corresponds to systems approaching binary mixtures of n-butanol and water.

DNAPL Viscosity

NAPL viscosity is an important physical property affecting many source-zone remediation technologies, and is particularly important to flushing based schemes designed to displace NAPL as free product. If the NAPL is or becomes highly viscous, significant head losses and instability/fingering of the displacing fluid may occur. In practice, this could make it much more difficult to displace the NAPL from a porous medium, regardless of density. The viscosity of CB and TCE as a function of butanol mole fraction were determined at 20°C using a Haake RS75 Rheometer (Figure 8). The viscosities of both CB and TCE increased asymptotically to a

maximum value of approximately 3.0 centipoise (cP) as the butanol mole fraction was increased. The observed increase in NAPL viscosity was expected since the viscosity of pure n-butanol is approximately 3.0 cP. In most scenarios, NAPLs with viscosities of less than 3.0 cP should flow through unconfined aquifer systems without substantial head loss. However, the effect of both NAPL and displacing fluid viscosity on flow must be carefully considered prior to implementation of DMD.

Interfacial Tension

The interfacial tension between the organic liquid and aqueous phases is closely related to the displacement of NAPLs from porous media. For the DMD process to be successfully implemented, two considerations are important regarding interfacial tension: a) preventing premature NAPL mobilization during *in situ* density conversion; and b) providing for complete NAPL mobilization during the displacing surfactant flood. Endpoint equilibrium NAPL-water interfacial tensions were measured for binary systems of butanol/water, CB/water and TCE/water. Organic-aqueous phase interfacial tensions were then determined as a function of increasing X_{BuOH} for both preflood solution (6% butanol) and displacement solution (4% 4:1 Aerosol MA/OT + 20% butanol + 500 mg/L $CaCl_2$). For the preflood solution, the IFT for CB and TCE decreased from approximately 13 dyne/cm to 3 dyne/cm, indicating that significant mobilization of free product would not be anticipated for most systems even at the maximum butanol loading. For the displacing surfactant solution the IFT increased from approximately 0.1 dyne/cm to 0.4 dyne/cm, indicating that NAPL displacement would occur for most systems.

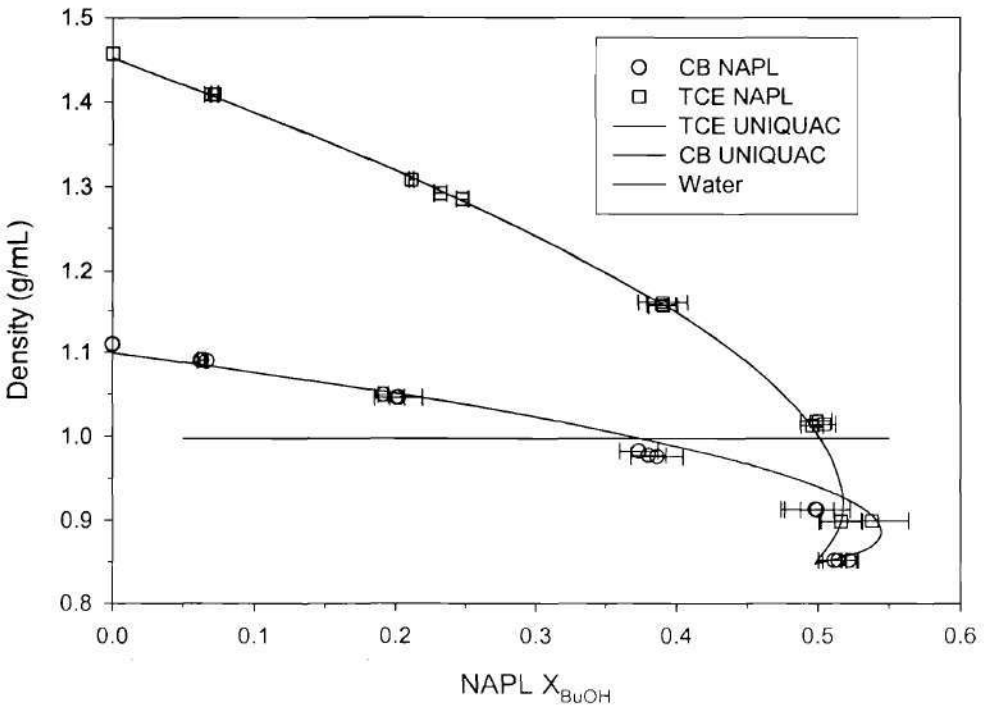

Figure 7. CB- and TCE-NAPL density with increasing n-BuOH content.

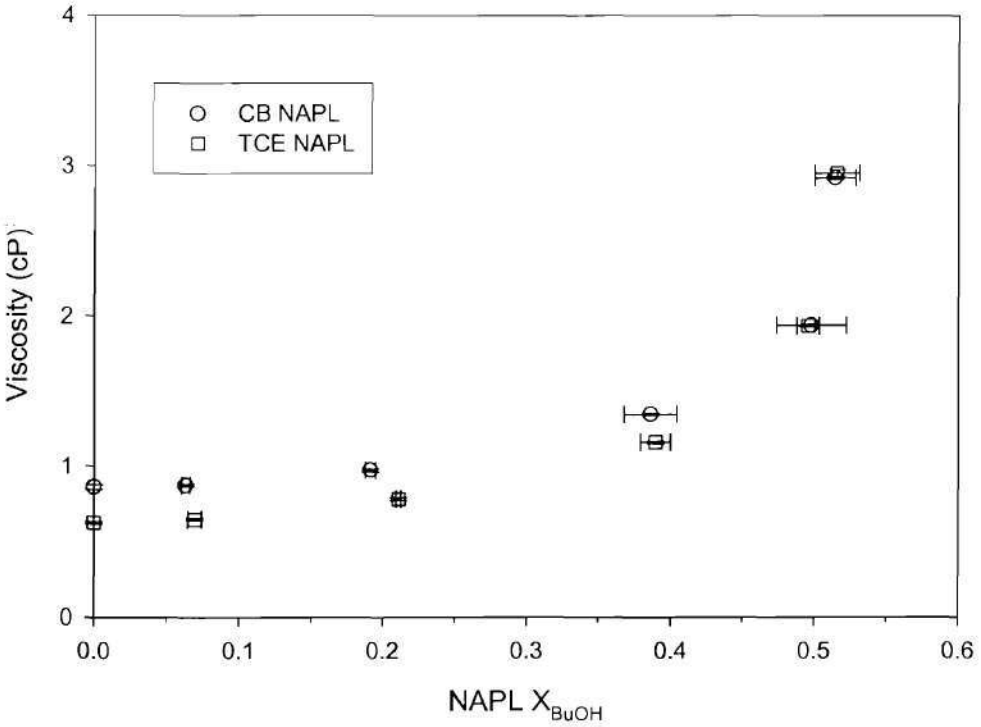

Figure 8. CB- and TCE-NAPL viscosity with increasing BuOH content.

Task 1.B. Development of Macroemulsion Formulation for n-Butanol Delivery

Emulsions are defined as dispersions of one liquid in another incompletely miscible liquid. Typically, emulsions are subdivided into microemulsions and macroemulsions, with the chief distinction being that the former is thermodynamically stable. Macroemulsion systems are thermodynamically unstable because of their larger surface area per drop, resulting in an excess free energy that cannot be balanced by entropic contributions. Many macroemulsions exhibit kinetic stability (i.e., stability for a given period ranging from hours to months to years) lending themselves to industrial and commercial applications.

Initial qualitative screening of Tween 80 + Span 80 + n-butanol mixtures indicated favorable macroemulsion stability (i.e., stability on the order of hours) with a combination of 4.7% (vol) Tween 80 + 1.3% (vol) Span 80. Macroemulsion viscosity and IFT in the presence of TCE, are also important factors to be considered in emulsion development as an increase in viscosity, or decrease in IFT may lead to premature NAPL mobilization during the density conversion preflood. Thus density, viscosity and IFT measurements were used to design a macroemulsion that was relatively kinetically stable and compatible with the solution developed for the low-IFT displacement of the density converted NAPL. The developed emulsion was subsequently tested in two-dimensional aquifer cell experiments to assess the feasibility of an emulsion delivery (preflood) approach for the DMD method.

A series of batch experiments were conducted with 4.7% (vol) Tween 80 + 1.3% (vol) Span 80 emulsions of increasing n-butanol content to assess emulsion stability, viscosity and interfacial tension in the presence of TCE-NAPL. Results obtained from these experiments were used to perform a total trapping number (N_T) analysis. The purpose of the N_T analysis was to select a macroemulsion formulation that would not displace residual TCE during the in-situ density conversion flood.

Macroemulsion Batch Experiments

Tween 80 and Span 80 were initially selected as possible emulsifying agents due to their synergistic effects. An emulsion of 4.7% (vol) Tween 80 + 1.3% (vol) Span 80 was developed with n-butanol fractions of up to 35% (vol). Photographs of emulsions with increasing volume fraction of n-butanol were taken over 48 hours (Figure 9). These pictures provide a qualitative assessment of stability as a function of n-butanol content, and indicate greater stability with greater n-butanol volume fraction. This was a favorable result, as the motivation for emulsion development was to deliver high butanol concentrations to entrapped and pooled DNAPL. The effects of IFT and viscosity, however, must also be considered in the formulation of a flushing emulsion.

The viscosity and IFT of the 4.7% (wt) Tween 80 + 1.3% (wt) Span 80 + n-butanol macroemulsion was measured over a range of n-butanol volume fractions (nominally 0-0.30) (Figures 10 and 11, respectively). For each n-butanol fraction the viscosity of the emulsion was found to be dependent on shear rate, indicating that the emulsion was non-Newtonian. Consequently, viscosity was measured at two shear rates, 200 s^{-1} and 1000 s^{-1}, over the indicated range of n-butanol volume fractions (Figure 7-2). While the viscosity was determined to be shear thinning (i.e., decreasing viscosity with increasing shear rate) over these shear rates, the magnitude was relatively small at 20°C (0.2 to 0.8 cP). Since many subsurface systems are lower in temperature (~10°C), the viscosity was also measured at 10°C, and was found to increase from 2.1 to 7.6 cP as the n-butanol content increased from 0% to 30% (vol). Interfacial tension between the emulsion and TCE decreased from 14.3 dyne/cm at 0% (vol) n-butanol to 3.6 dyne/cm at 30% (vol) n-butanol (Figure 11). The observed reduction in interfacial tension was

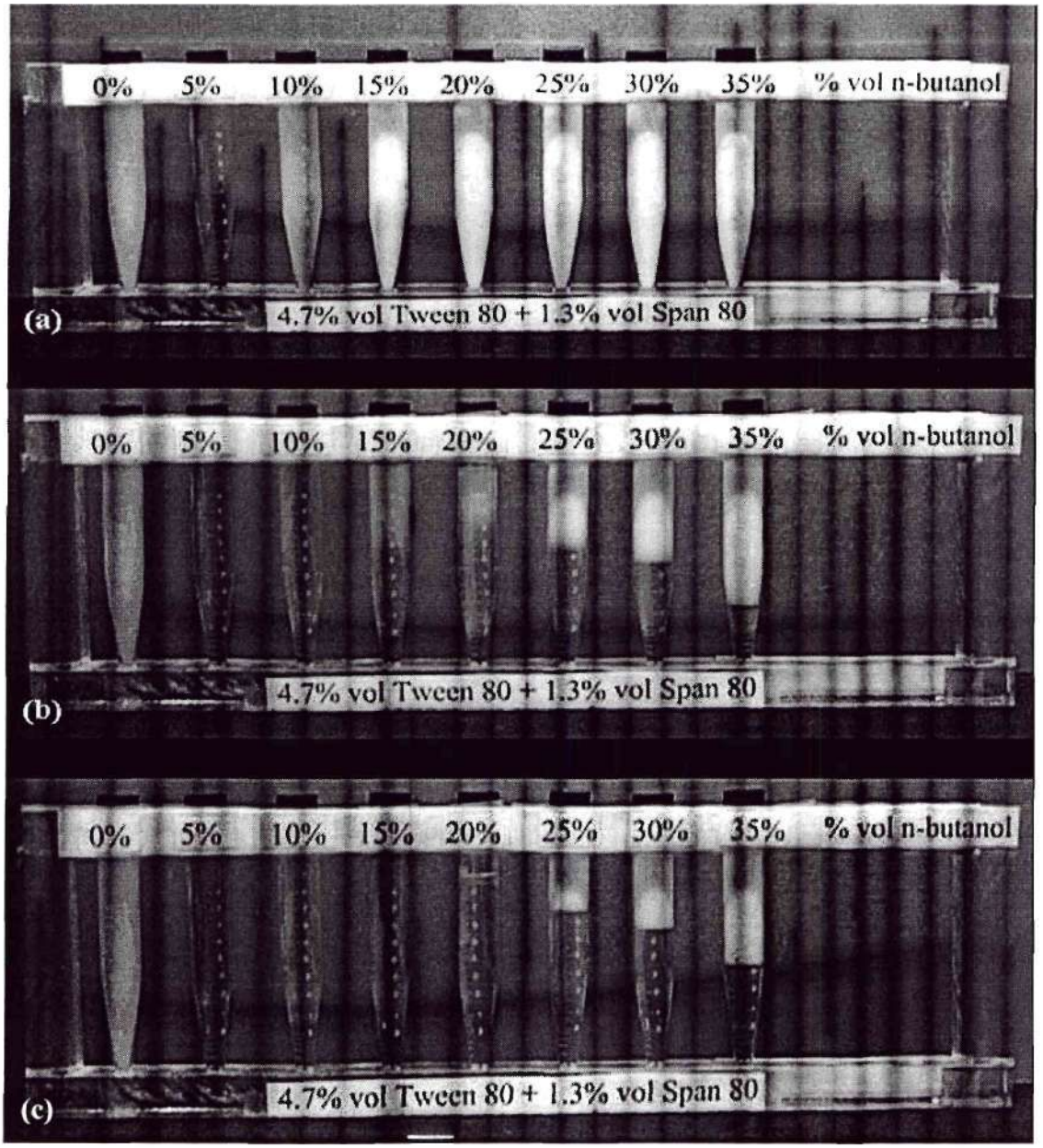

Figure 9. Time series of photographs of 4.7% (vol) Tween 80 + 1.3% (vol) Span 80 macroemulsion with increasing (left to right) volume fractions of n-butanol (a: initial, b: 24 hr, c: 48 hr)

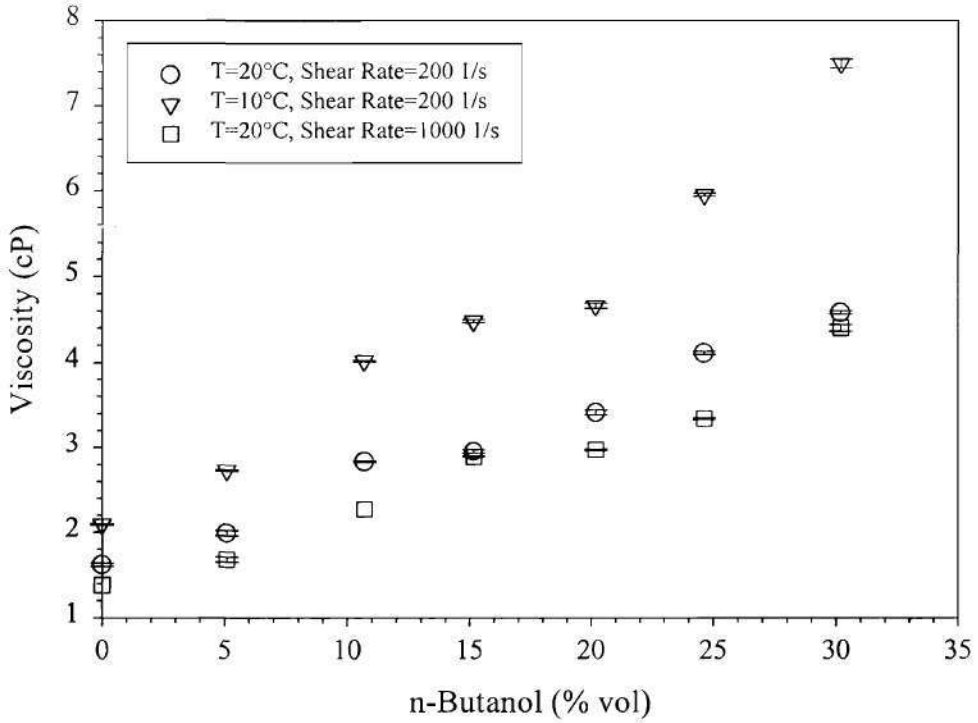

Figure 10. Emulsion viscosity as a function of increasing n-butanol content.

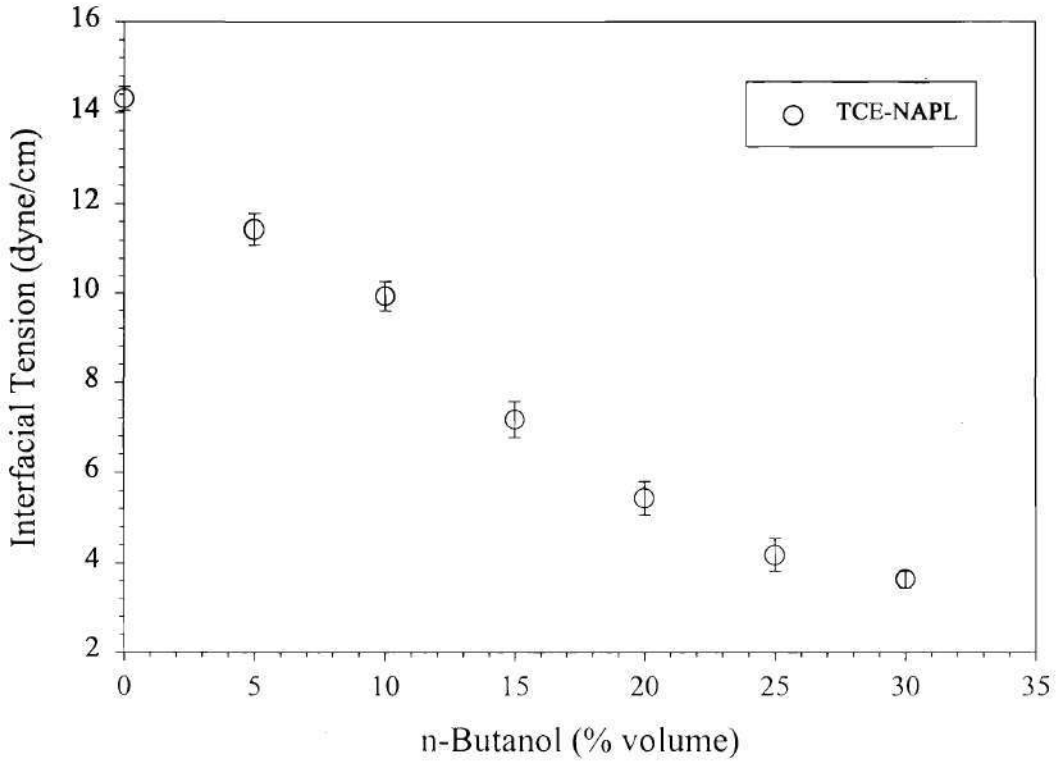

Figure 11. Interfacial tension between emulsions of increasing n-butanol content and TCE-NAPL.

attributed to the increasing organic nature of the macroemulsion as the n-butanol fraction was increased (0% to 30% vol).

To minimize the potential for premature mobilization of the TCE in the 2-D aquifer cell experiment, the total trapping number concept (Pennell et al. 1996) was utilized in the development of the final emulsion formulation. Capillary (N_{Ca}), Bond (N_B, absolute value), and total trapping (N_T) numbers were calculated using properties from 2-D aquifer cell studies, and are shown as a function of macroemulsion n-butanol content (% vol) in Figure 12. Viscosities measured at 200 s^{-1} and 1000 s^{-1} were used in the capillary number calculation to illustrate the effect of macroemulsion rheology on the potential for NAPL mobilization. While the macroemulsion viscosity varied with shear rate, the effect on the capillary number was minimal. Furthermore, the Bond number dominated the total trapping number, due primarily to the large density contrast ($\Delta\rho$ = 0.48 g/mL) between the TCE-NAPL and macroemulsion. Pennell et al. (1996) reported the onset of PCE mobilization at a total trapping number of 2 x 10^{-5}, and complete mobilization of PCE at total trapping numbers in excess of 1 x 10^{-4}. To avoid possible premature mobilization of TCE, a 4.7% (vol) Tween 80 + 1.3% (vol) Span 80 macroemulsion containing 15% (vol) n-butanol (N_T = 2.1 x 10^{-5}) was selected for use. Additionally, the 15% n-butanol content emulsion exhibited relatively low viscosity (~4 cP at 10°C). Relevant physical properties of the macroemulsion developed for *in situ* density conversion are given in Table 2.

As a first-order approximation of macroemulsion stability, time to visible coalescence of the 4.7% (vol) Tween 80 + 1.3% (vol) Span 80 + 15% (vol) n-butanol emulsion was evaluated (~4 hours). Based on a Stoke's law analysis of the creaming rate (i.e., the rising of n-butanol droplets and resulting coalescence), n-butanol droplets were estimated to be on the order of 10 microns. The macroemulsion was found to be polydisperse when under 200X magnification (Figure 13), indicating a need for measurement of the droplet size distribution (Figure 14). The droplet size distributions obtained from two measurement techniques, coulter counter and image analysis, indicated that the emulsion droplets ranged in size from 1 μm to 20 μm, with the majority of droplets having diameters less than 5 μm. It is important to note that measurement of concentrated emulsions is problematic, as traditional light scattering techniques yield ambiguous results without dilution of the emulsion. Dilution of emulsions, however, may alter the droplet size distribution. Moreover, measurement techniques may alter emulsion droplet size distributions depending on the mechanism of measurement (e.g., shear in flowing systems, contact with interfaces for visualization, etc.). Thus, the distributions presented herein should only be used as an indication of probable droplet sizes, while recognizing that the distribution will change with time.

Table 2. Properties of DMD flushing solutions at 22±2 °C.

Solution	Density (g/mL)	Viscosity (cP)	IFT with TCE (dyne/cm)
Water	0.998	0.95	35.2±0.3
Macroemulsion	0.979±0.001	2.52±0.05	7.2±0.4
Displacement Solution	1.015±0.001	2.99±0.06	0.51±0.02

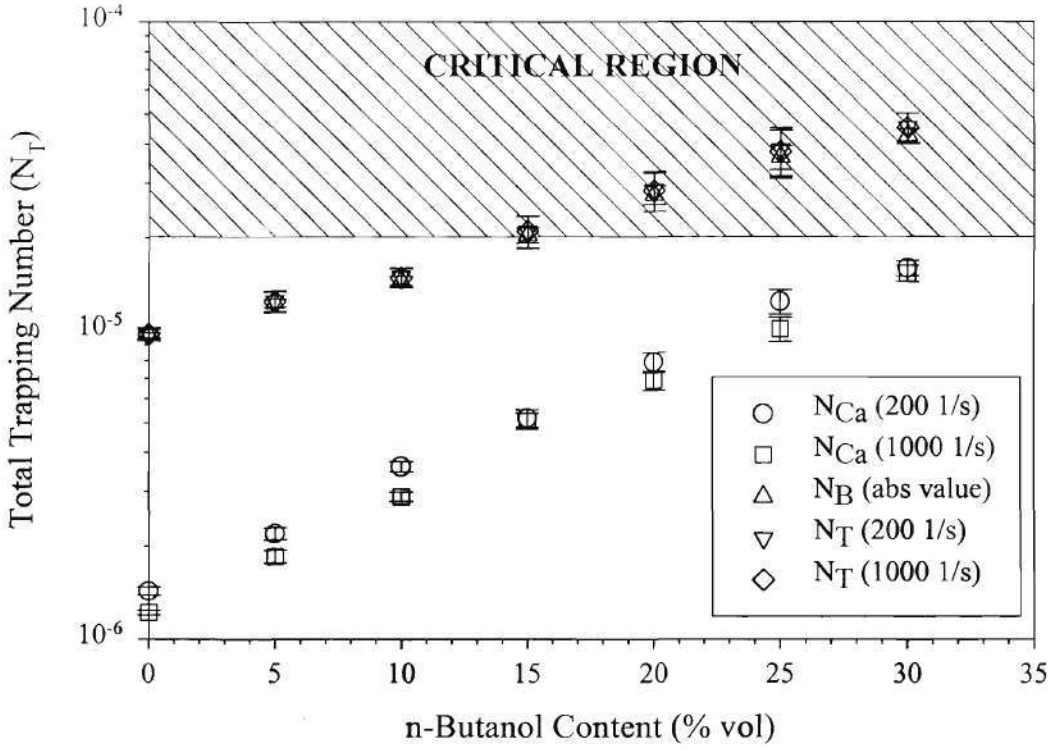

Figure 12. Capillary, Bond and total trapping numbers for an emulsion preflood in the DMD of TCE-NAPL.

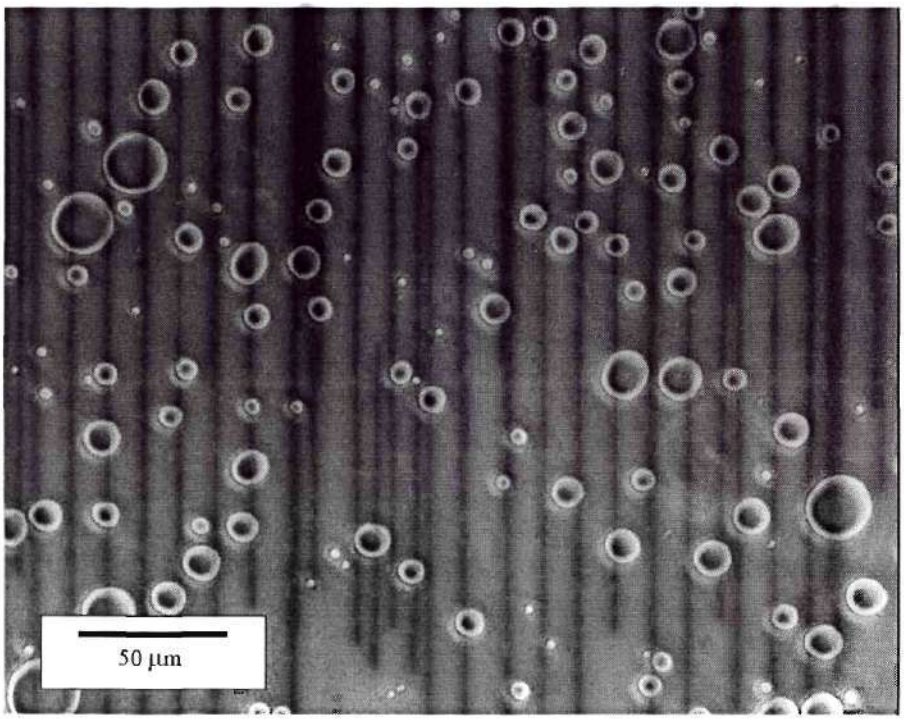

Figure 13. Representative photograph of the 15% (vol) n-butanol emulsion under 200X magnification.

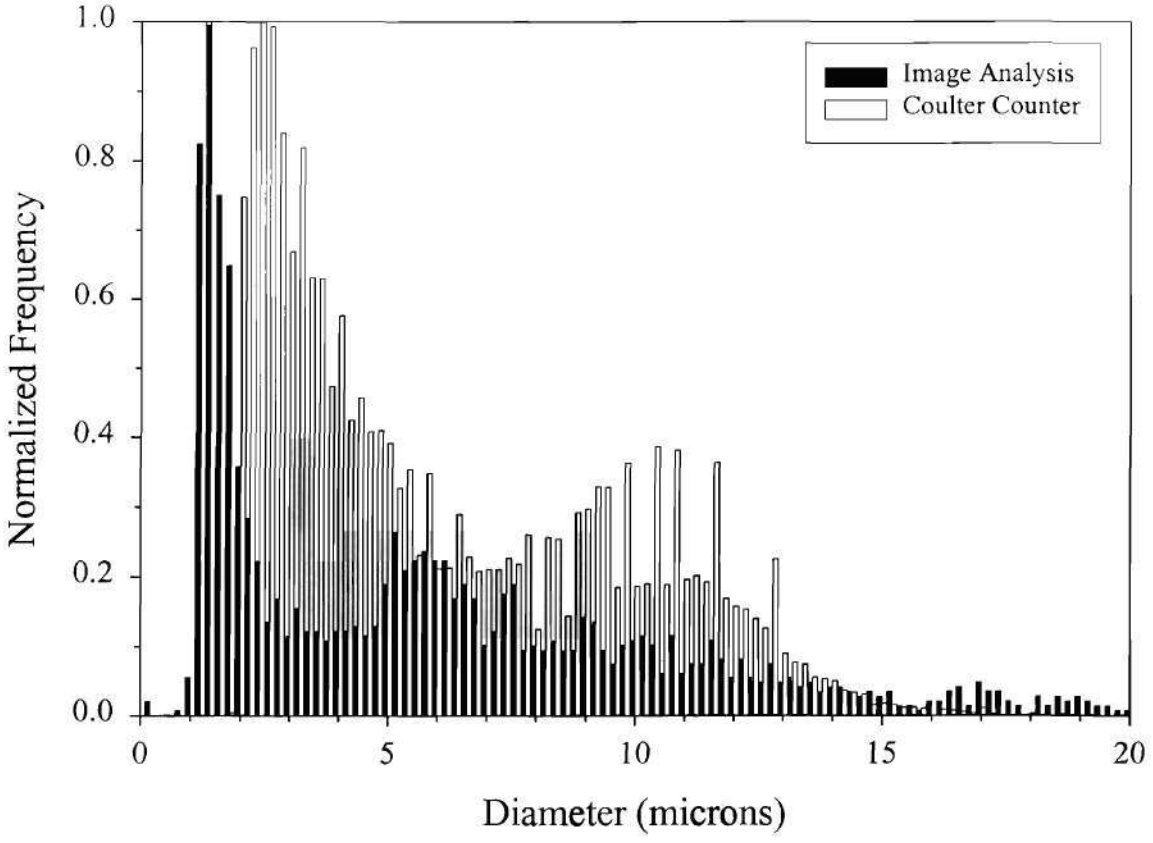

Figure 14. Droplet size distributions of the influent emulsion.

Task 1.C. Refinement of the Low-IFT Surfactant Solution used for NAPL Displacement

During tests of the DMD method in 2-D aquifer cells (see Task 2), TCE displaced as a result of the low-IFT surfactant flood (10% Aerosol MA-80 + 5% butanol + 15 g/L NaCl + 1 g/L $CaCl_2$) appeared to move at a slower rate than injected solution. In addition, the color of the NAPL changed from red to a deep purple, indicating that a significant amount of the low IFT surfactant solution (dyed blue) had partitioned into the NAPL. These effects were observed in both the control experiment (without density conversion) and in DMD experiments, using either 6% butanol in water or a macroemulsion solution (4.7% (vol.) Tween 80 + 1.3% (vol.) Span 80 + 15% butanol) to achieve density conversion of TCE.

In order to investigate this phenomenon in more detail and to develop more efficient low-IFT displacement solutions, phase behavior experiments were conducted for 8% (wt.) Aerosol MA-80 and TCE as a function of electrolyte composition and concentration (NaCl and $CaCl_2$.) and butanol concentration. To date, four phase behavior studies have been completed for TCE and 8% Aerosol MA-80 with; a) 0-15 g/L NaCl, b) 0-10 g/L $CaCl_2$, c) 0-15 g/L NaCl + 1 g/L $CaCl_2$, and d) 0-15 g/L NaCl + 1 g/L $CaCl_2$ + 5% butanol. The actual experiments were conducted in 10 mL graduated centrifuge tubes. Initially, each centrifuge tube was filled with 5 mL of TCE (dyed red) and 5 mL of 8% (wt.) Aerosol MA-80 containing the appropriate concentration of salt and butanol. The resulting solutions contained in the centrifuge tubes were mixed for a minimum of 72 hours on an oscillating shaker, and then allowed to settle for a period of 48 hours or until no additional phase separation occurred. The final phase volumes were recorded, and aliquots were taken from each distinct phase to be analyzed for TCE and Aerosol MA concentrations using either GC or HPLC methods, respectively.

The results of the 0 to 15 g/L NaCl scan for TCE and Aerosol MA-80, represented in terms of a volume fraction diagram, are shown in Figure 15. At salt concentrations below approximately 8 g/L NaCl two distinct phases existed. TCE liquid resided at the bottom of the centrifuge tube, below an oil-in-water microemulsion (Winsor Type I system). As shown in Figure 16, the concentration of TCE in the Type I microemulsion increased from 55 g/L to 220 g/L over a NaCl concentration range of 0 to 8 g/L. Although these are relatively high TCE concentrations, the visible volume of TCE decreased only slightly over this range, as one would expect based on mass balance calculations. For salt concentrations between 8 g/L and 12 g/L NaCl, three distinct phases were observed, identified in Figure 1 as an "aqueous" (water-rich) phase, a middle-phase microemulsion, and TCE. Middle- phase microemulsions are referred to as Winsor Type III systems, and consist of a surfactant- and organic-rich phase. The middle-phase microemulsion contained extremely high concentrations of TCE, ranging from 476 g/L to 1100 g/L. At NaCl concentrations above 12 g/L, two phases were again observed, a water-rich "aqueous phase" and a Winsor Type II microemulsion. The Winsor Type II system represents a water-in-oil microemulsion (i.e., reverse micelles), in which water was solubilized within the TCE liquid phase. For this system, essentially all of the TCE resided in the Type II microemulsion. Hence, measured concentrations of TCE remained relatively constant, at a value of approximately 1150 g/L. This concentration almost completely accounts for the volume or mass of TCE originally added to the system (i.e., 5 mL).

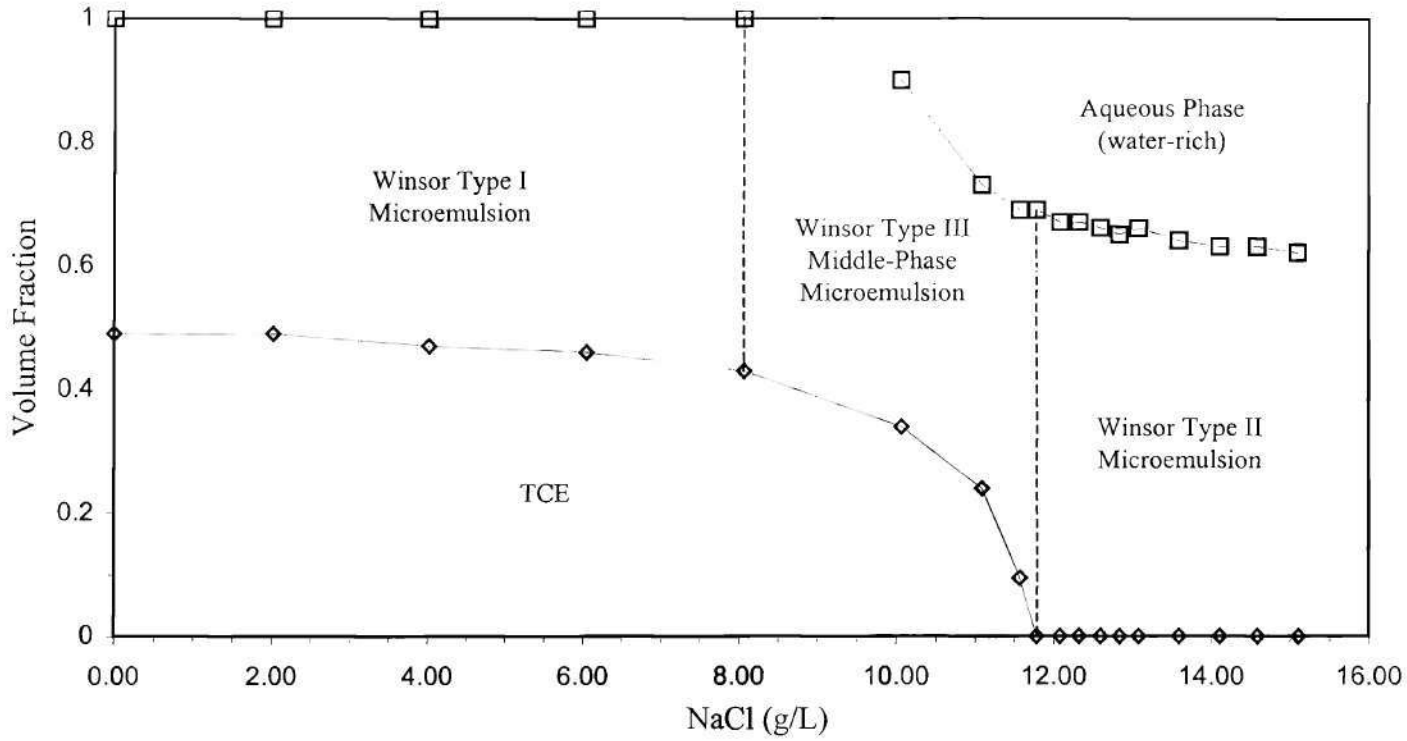

Figure 15. Volume fraction diagram for 8% (wt.) Aerosol MA-80 and TCE as a function of NaCl concentration.

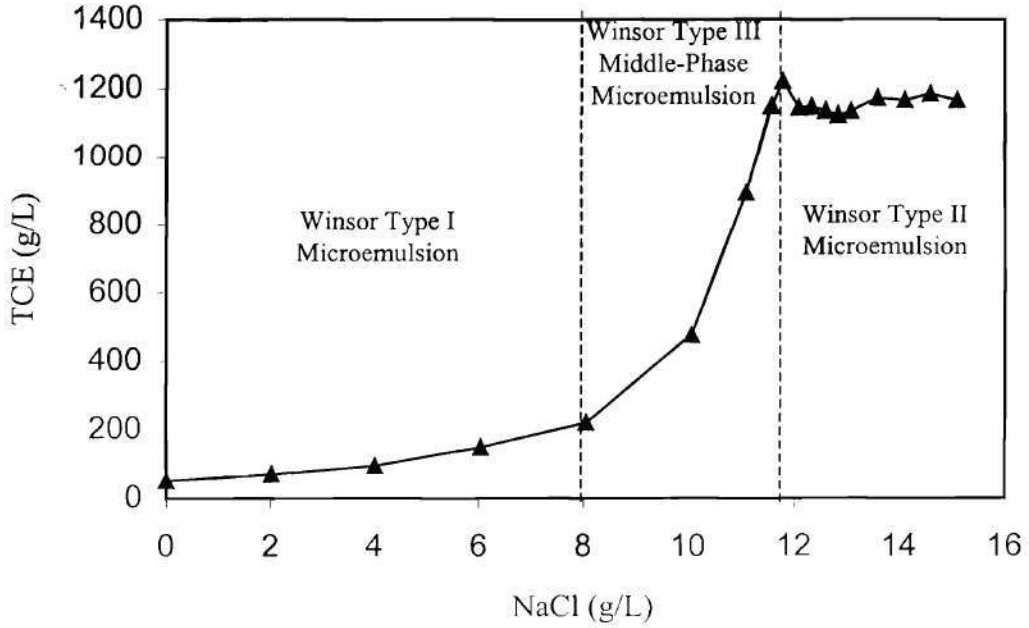

Figure 16. Concentrations of TCE in the Type I, Type III and Type II microemulsions as a function of NaCl concentration.

Concentrations of TCE and Aerosol MA-80 in the water-rich aqueous phase were also measured by GC and HPLC analysis, respectively (Figure 17). The concentration of Aerosol MA-80 in the aqueous phase ranged from approximately 6.4 g/L to 5.3 g/L, indicating that a large fraction (e.g., 46% at 15 g/L NaCl) of the Aerosol MA-80 existed in both the Type III middle-phase microemulsion and the Type II microemulsion observed at high NaCl concentrations. Furthermore, the concentration of TCE in the water-rich aqueous phase was approximately 1.6 g/L, only slightly above the aqueous solubility of TCE in water (1.1 g/L). These data are consistent with the analysis presented previously, which indicated that essentially all of the TCE existed in the Type II microemulsion at high NaCl concentrations.

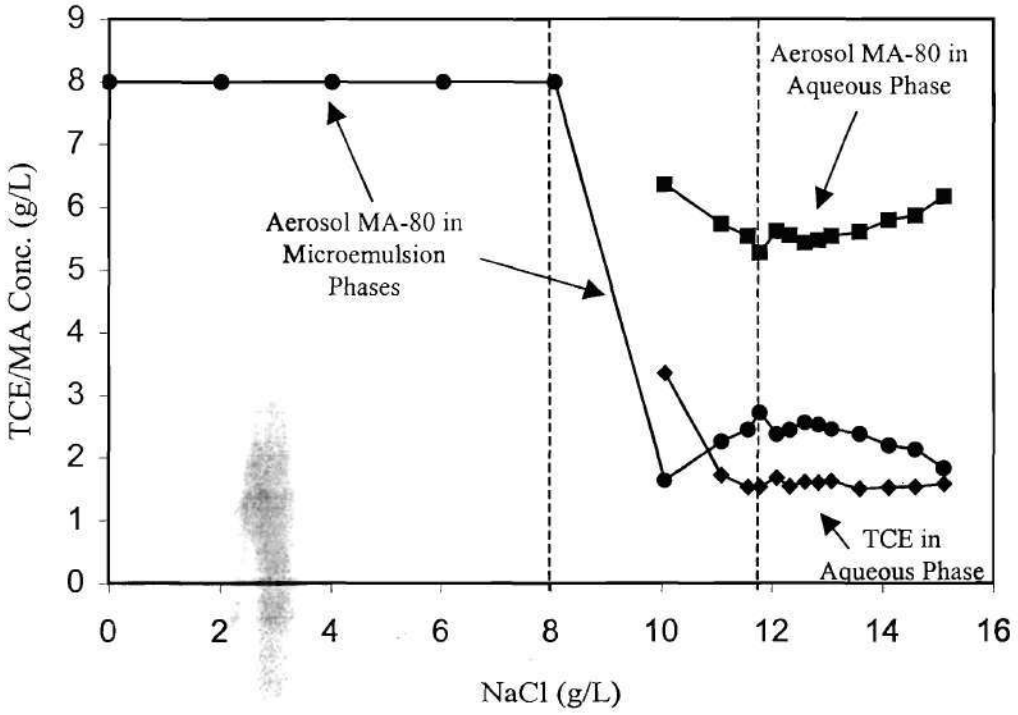

Figure 17. Concentrations of TCE and Aerosol MA 80 in the water-rich aqueous phase, and concentrations of Aerosol MA-80 in all microemulsion phases as a function of NaCl concentration.

Phase behavior experiments were also conducted for TCE and Aerosol MA-80 in the presence of 0-15 g/L NaCl + 1 g/L $CaCl_2$, 0-10 g/L $CaCl_2$, and 0-15 g/L NaCl + 1 g/L $CaCl_2$ + 5% butanol. The addition of 1 g/L $CaCl_2$ to the NaCl systems resulted in the appearance of the Type III middle-phase microemulsion at approximately the same total salt concentration (8 g/L), but the transition to Type II microemulsion occurred at a lower total salt concentrations (10 g/L versus 11.8 g/L). The volume fraction diagram for the NaCL + 1 g/L $CaCl_2$ system is given in Figure 18. A photograph of centrifuge tubes containing TCE, Aerosol MA-80, and 0-15 g/L NaCl + 1 g/L $CaCl_2$ is shown in Figure 19, arranged from left to right in order of increasing NaCl concentration.

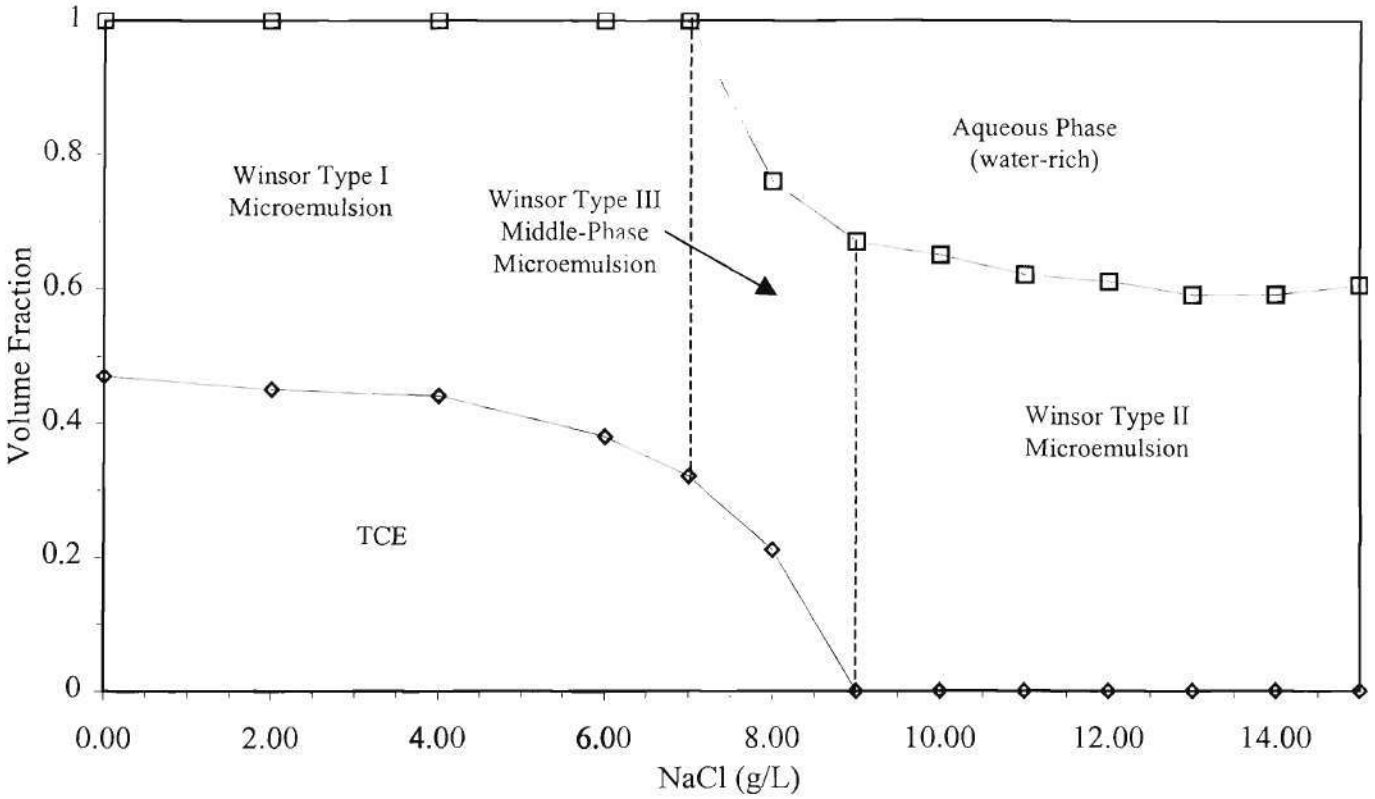

Figure 18. Volume fraction diagram for 8% (wt.) Aerosol MA-80, TCE and 1 g/L $CaCl_2$ as a function of NaCl concentration.

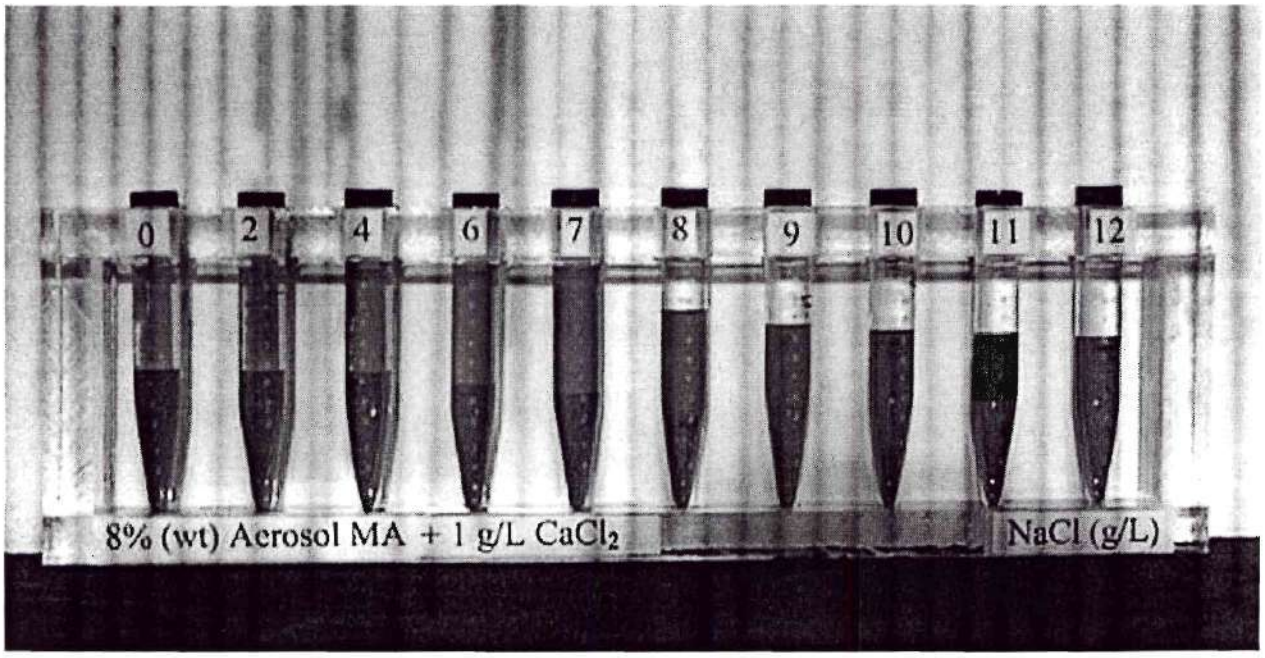

Figure 19. Photograph of the TCE, Aerosol MA-80, and 1 g/L $CaCl_2$ system as a function of NaCl concentration.

The addition of 5% butanol to the TCE, Aerosol MA-80, 1 g/L $CaCl_2$, and 0-15 g/L NaCl system shifted the volume fraction diagram to the left (lower NaCl concentrations), resulting in the appearance of a three phase system at a NaCl concentration of 2 g/L (data not shown). The subsequent transition to a two-phase, Winsor Type II system occurred at a NaCl concentration of only 3 g/L. Similar phase behavior and volume fraction transition points were observed for the TCE, Aerosol MA-80, 0 – 10 g/L $CaCl_2$ system (data not shown).

To achieve efficient displacement of NAPLs as an "oil bank", it is desirable to utilize surfactant formulations that exhibit a) sufficiently low IFTs to displace the NAPL (based on the total trapping number concept) and b) Winsor Type I behavior (oil-in-water microemulsion) rather than Winsor Type III and Winsor Type II systems. The latter condition is important because many of the Type III and Type II systems lead to the formation of liquid gels or viscous NAPL solutions that may be extremely difficult to remove from the subsurface. Although a middle-phase system may be desirable in some situations, particularly if high solubilization capacity is desired, it will be far easier to implement surfactant formulations for which the NAPL remains as a separate, relatively pure (free of surfactant) phase. Therefore, future 2-D aquifer cell tests of the DMD method will employ a low-IFT surfactant solution containing salt concentrations just below those corresponding to Type III behavior. Based on the results of the phase behavior studies reported herein, a solution of 8% Aerosol MA 80 + 6 g/L NaCl + 1 g/L $CaCl_2$ has been selected (shown in Figures 18 and 19).

Task 2.A. Aquifer Cell Testing of DMD Method: Aqueous Delivery of n-Butanol

The 2-D aquifer cell experiments were designed to assess delivery of DMD preflood and displacing solutions to the DNAPL source-zone, conversion of DNAPL to LNAPL using an aqueous butanol solution, and upward displacement and recovery of the NAPL. The 2-D aquifer cell used in these studies has dimensions of 63.5 cm (height) x 38 cm (length) x 1.4 cm (thickness). The end chambers were screened over the entire height of the aquifer cell. The cell was packed under water-saturated conditions with Ottawa Federal Fine sand as the background matrix. Two regions of lower permeability lenses, consisting of F-70 Ottawa sand, were emplaced to increase heterogeneity and simulate potential field heterogeneities. The first layer of lenses was located up to 3 cm above the bottom-confining layer (F-70) and covered the entire length of the cell, while the second layer of lenses was emplaced 19 to 21.5 cm above the bottom confining layer and 19 cm from either end chamber. An influent well, constructed from 0.32 cm O.D. 316 stainless steel tubing and screened over the bottom 5.2 cm, was packed in the cell matrix to simulate a partially-screened well. This injection well was used minimize the potential effects of density override of the resident solution by lower density injection solutions, thereby increasing contact between the flushing solutions and the entrapped or pooled DNAPL.

Chlorobenzene Box Experiment

Following redistribution of CB within the box, a 6% butanol preflood solution (1575 mL, dyed blue-green) was introduced through the screened well at an average flow rate of 4.5 mL/min. A representative photograph at early time (~350 mL injected) is shown in Figure 20a. The lower density preflood solution (0.988 g/mL versus 0.997 g/mL for resident aqueous solution) flowed slightly upward from partially screened through the zone of CB contamination. The preflood solution was also present in the upper left-hand portion of the cell because the end chamber was fully screened, which allowed for mixing within and subsequent flow from the end-chamber. At later time (~1560 mL injected), the resident pore water was completely displaced by the preflood solution as seen in Figure 20b. The CB-NAPL was now swollen due to alcohol and water partitioning, which resulted in upward migration of CB-NAPL, as well as some downward migration of the CB. The downward migration of CB-NAPL was very slow, occurring over a period of approximately 4 hours. This problem was mitigated by the end of the preflood period, at which time sufficient butanol had partitioned into the NAPL to achieve density conversion.

Following a flow interruption period of 17 hours, 1524 mL of displacing surfactant solution (4% 4:1 Aerosol MA/OT + 20 % butanol + 500 mg/L $CaCl_2$) was introduced through the partially screened well at an average flow rate of 4.2 mL/min. Representative images of this phase of the DMD process are shown in Figures 6a and 6b. After approximately 0.26 pore volumes of displacing solution (not dyed) were introduced, upward CB-NAPL displacement occurred, which appeared as a bank of free product that formed along the front interface (Figure 21a). At later time (~840 mL injected), the NAPL migrated upward through the region of low permeability lenses and moved toward the water table at the upper right-hand portion of the cell (Figure 21b). Aqueous phase effluent concentration data for the CB box experiment are shown in Figure 22. During the preflood, the effluent concentration of butanol increased to approximately 45 g/L, which was substantially lower than the injected concentration of 60 g/L. These data indicate that butanol partitioned readily into CB-NAPL, and indicate that the NAPL X_{BuOH} was approximately 0.5. This value is greater than the X_{BuOH} of 0.41 necessary for density conversion of CB-NAPL.

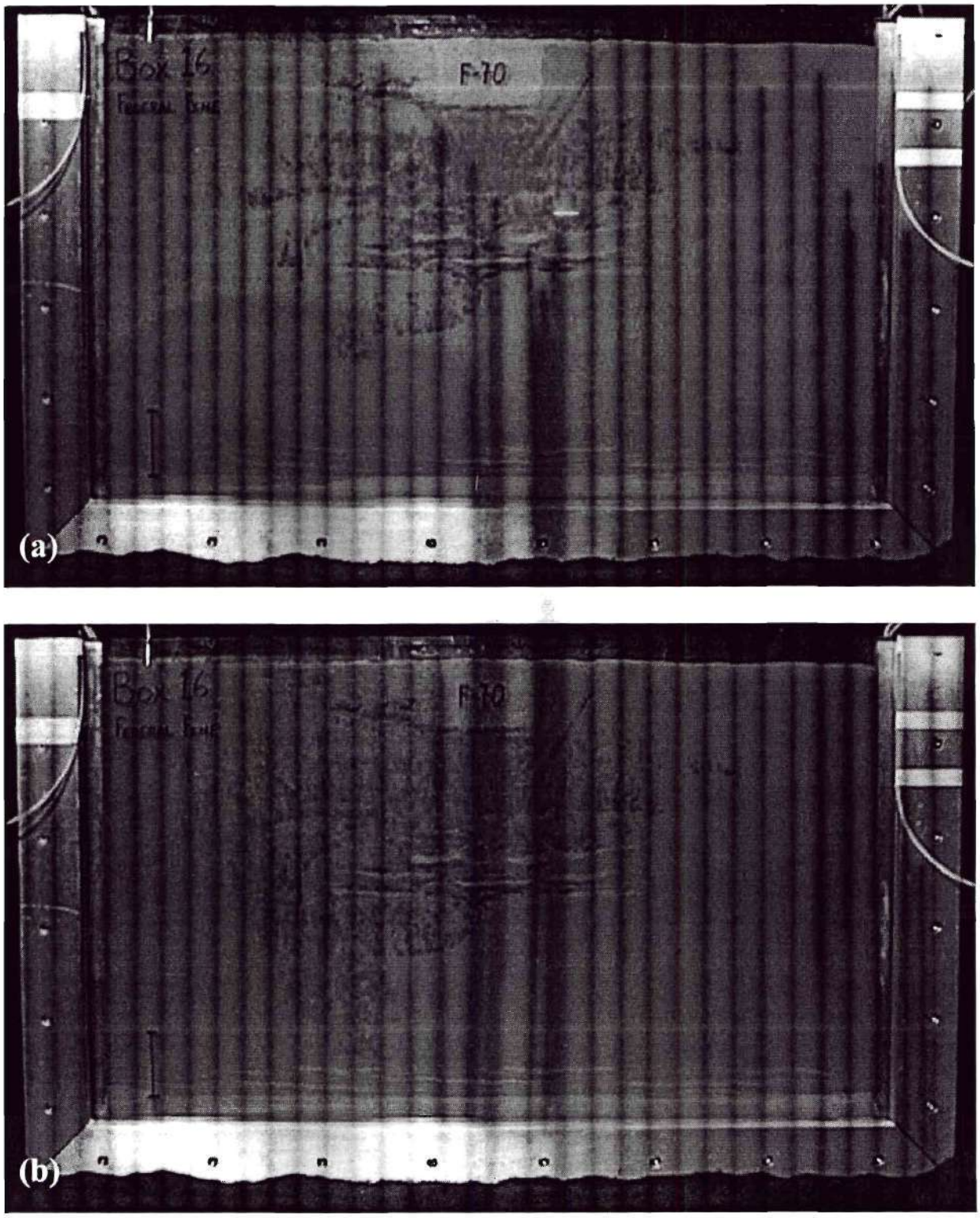

Figure 20. Representative early (a) and late (b) time photographs of the 6% butanol preflood in the CB-NAPL box experiment.

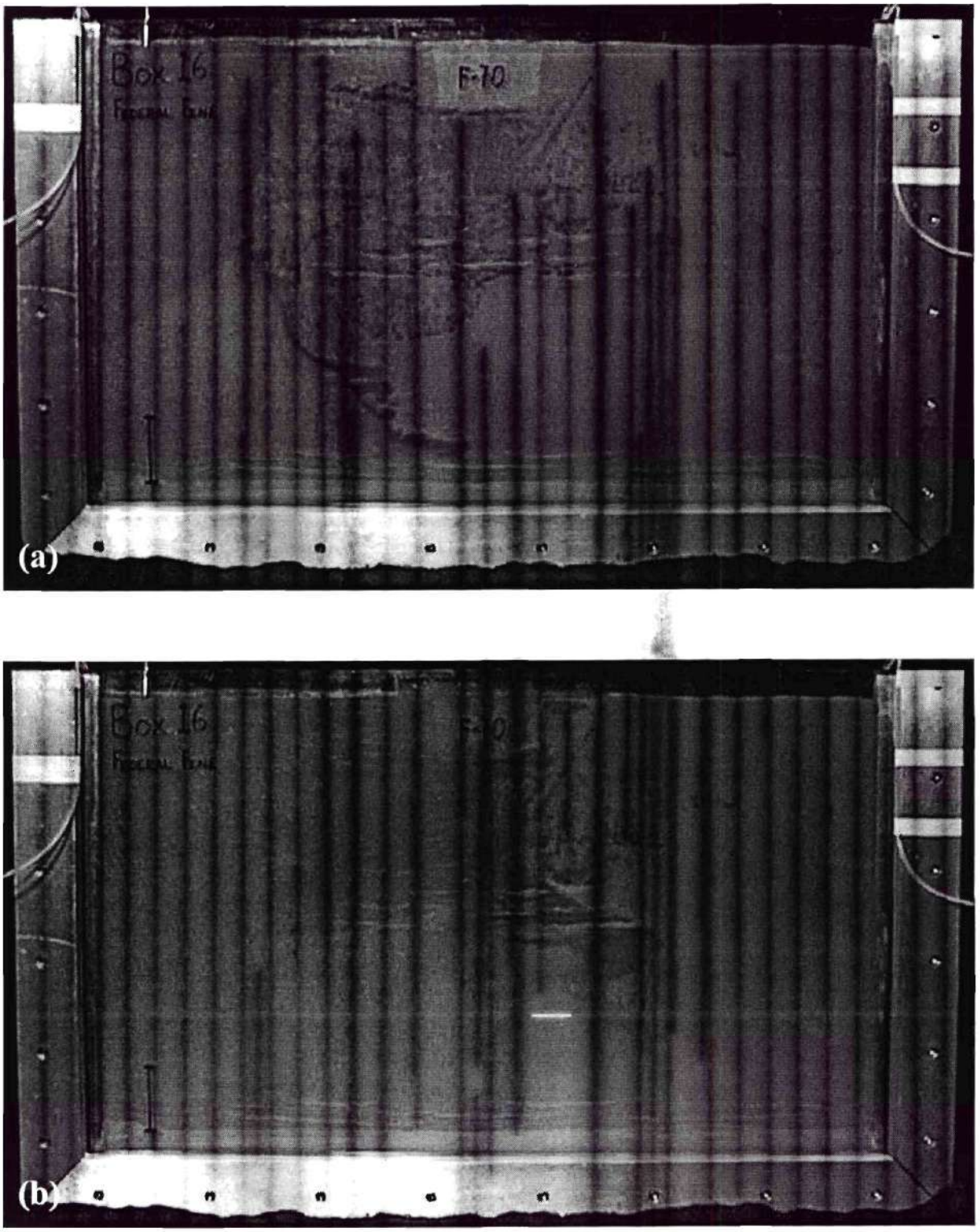

Figure 21. Representative early (a) and late (b) time photographs of the displacing surfactant flood in the CB-NAPL box experiment.

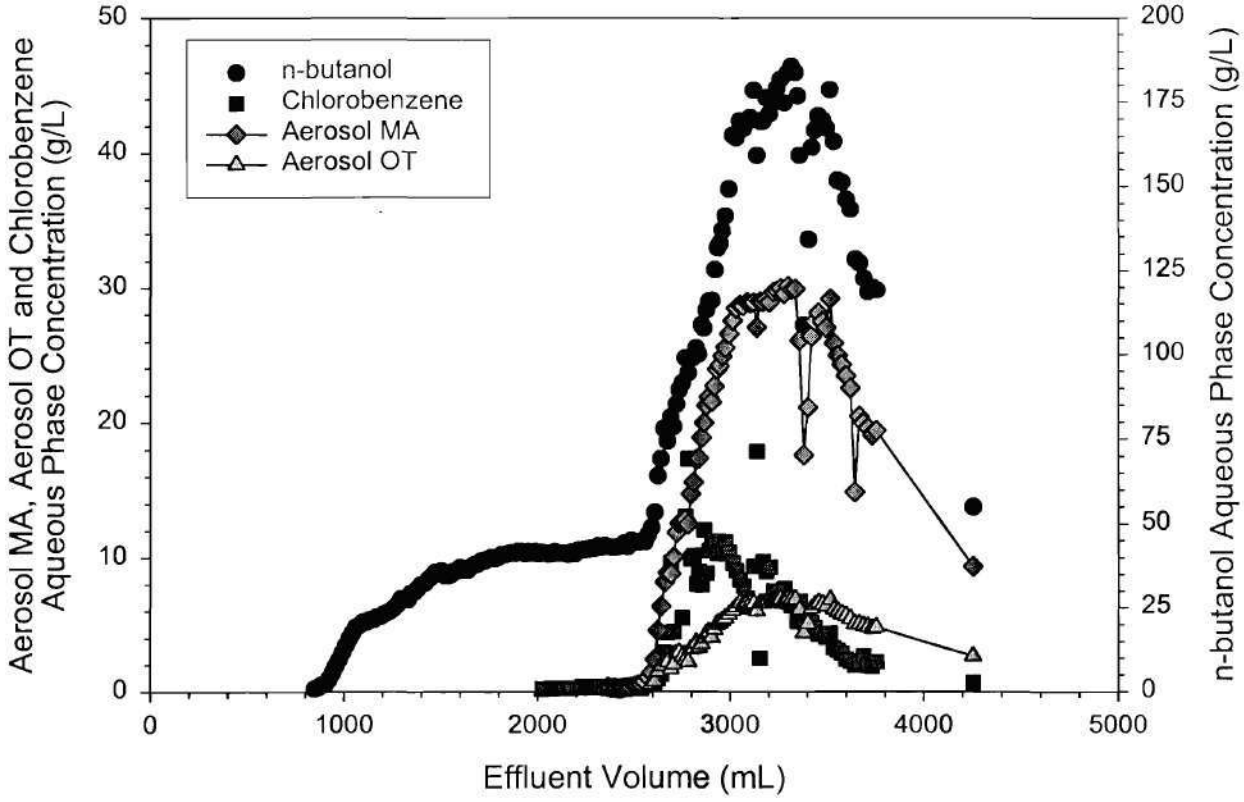

Figure 22. Aqueous effluent concentrations of butanol, CB, Aerosol MA and Aerosol OT from the CB-NAPL box experiment.

Appearance of the displacing surfactant solution in the effluent occurred at 2500 mL, and corresponded with a sharp increases in the effluent concentrations of butanol and CB. The butanol concentration approached the influent value of 193 g/L, while the CB concentrations increased to approximately 12 g/L, a 25-fold increase over the aqueous solubility. Effluent NAPL densities ranged from 0.96 to 0.90 g/mL, all of which were less than the corresponding aqueous phase densities.

Trichloroethylene Box Experiment

Following the injection and redistribution of 30.6 mL of TCE, an extended butanol preflood (6253 mL) was conducted at an average flow rate of 4.7 mL/min. At early time (~330 mL injected), the 6% butanol preflood solution front (dyed blue-green) contacted TCE near the lower confining layer, did not induce free product displacement (Figure 23a). At later time (~5990 mL injected), significant swelling of the NAPL was observed (Figure 23b), accompanied by some upward and horizontal migration of TCE-NAPL. After a flow interruption of 18 hours, 1500 mL of displacing surfactant solution (not dyed) were introduced into the cell through the partially screened well at an average flow rate of 4.4 mL/min. Representative early and late time images of the surfactant flood are shown in Figures 24a and 24b. Upward displacement and recovery of TCE-NAPL are shown in Figure 9a after approximately 270 mL of displacing solution had been injected. After approximately 1000 mL of displacing solution were introduced, upward and

horizontal displacement TCE-NAPL was observed (Figure 24b). At no time did the displaced TCE-NAPL migrate downward.

Aqueous phase effluent concentration data for the TCE box are shown in Figure 25. The preflood effluent concentration of butanol increased to approximately 55 g/L, compared to the influent preflood concentration of 60 g/L, indicating alcohol partitioning. The aqueous phase butanol concentration of 55 g/L corresponded with an equilibrium X_{BtOH} of approximately 0.5, the mole fraction required for TCE density conversion in the batch systems. The aqueous phase concentrations of TCE during the butanol preflood fluctuated around 300 mg/L, but increased to 14 g/L during the displacement flood. Similarly, effluent concentrations of butanol increased to a value of 206 g/L during the displacement flood. This is greater than the influent butanol concentration of 193 g/L, and was likely a result of NAPL (containing butanol) solubilization. Effluent NAPL densities ranged from 0.95-0.92 g/L, and all were less than the density of the corresponding aqueous phase densities.

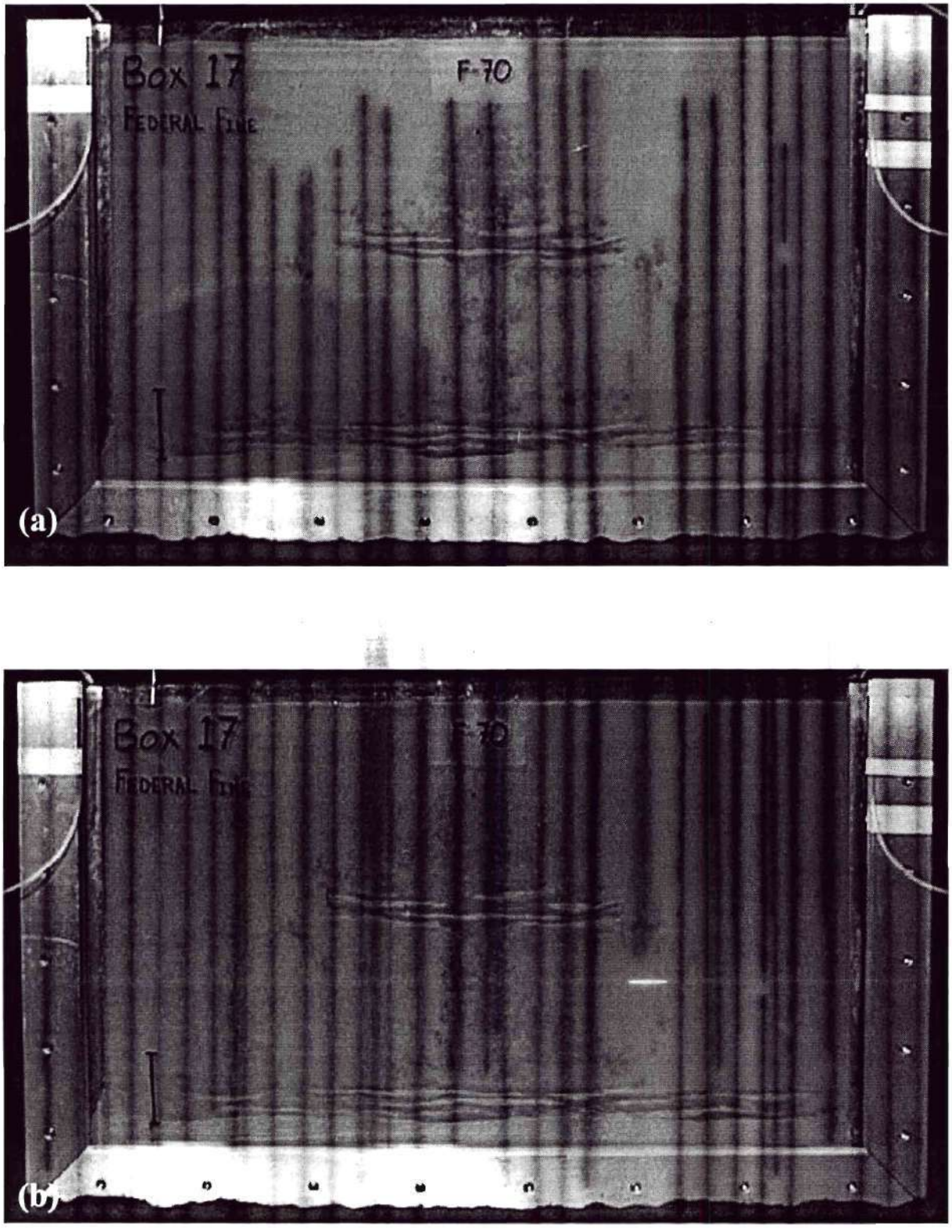

Figure 23. Representative early (a) and late (b) time photographs of the 6% butanol preflood in the TCE-NAPL experiment.

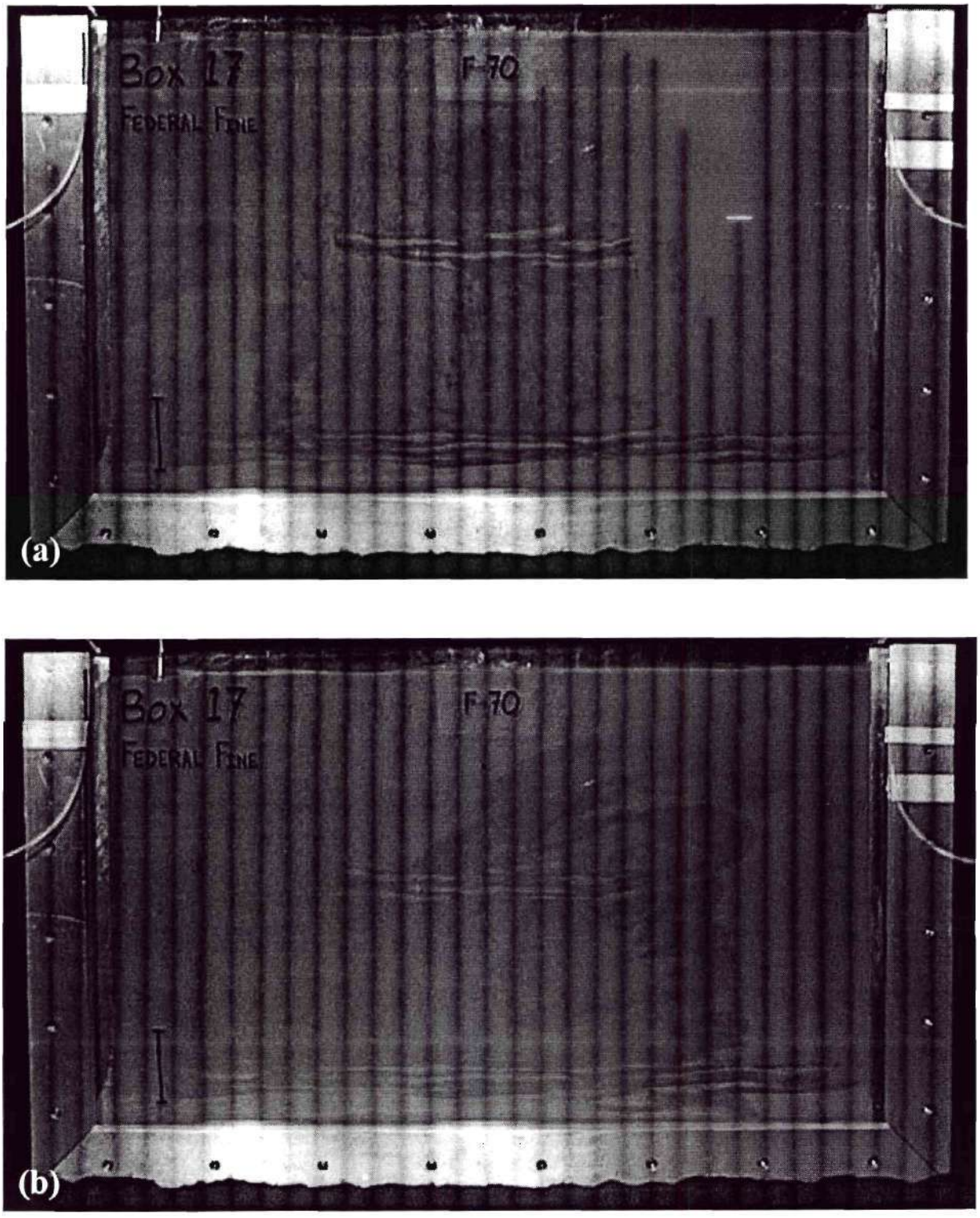

Figure 24. Representative early (a) and late (b) time photographs of the displacing surfactant flood in the TCE-NAPL box experiment.

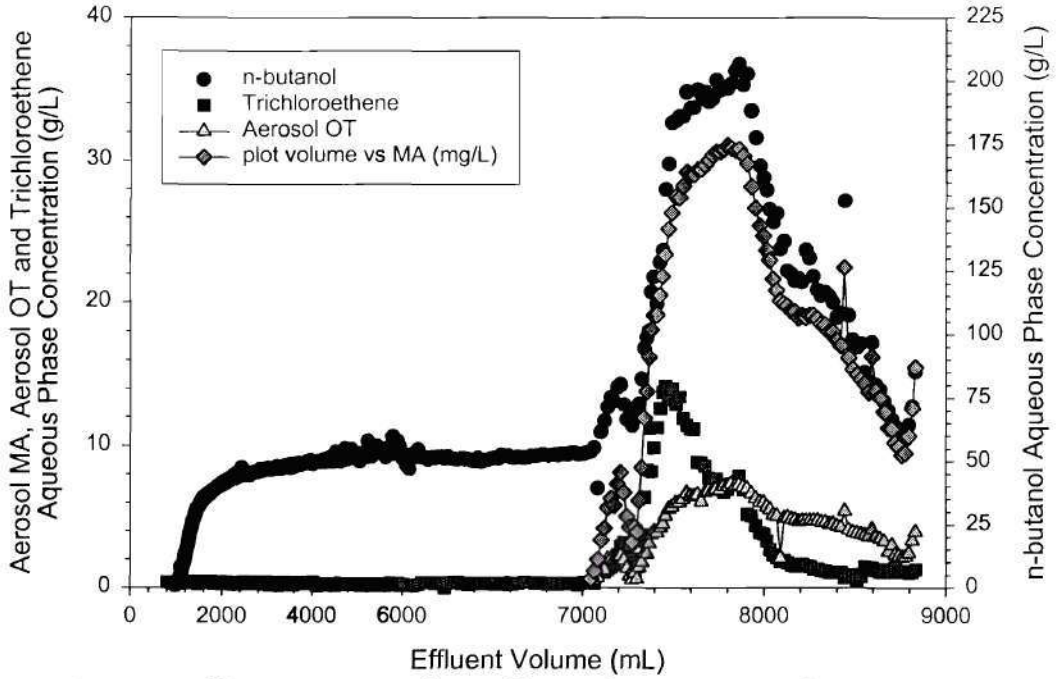

Figure 25. Aqueous effluent concentrations of butanol, TCE, Aerosol MA and Aerosol OT from the TCE-NAPL box experiment.

Task 2.B. Aquifer Cell Testing of DMD Method: Macroemulsion Delivery of n-Butanol

In Task 2A it was demonstrated that an aqueous solution of 6% (wt) n-butanol could effectively convert CB and TCE into LNAPLs prior to low-IFT displacement and recovery. The amount of preflood solution required, however, was significantly greater in the case of TCE (~5 pore volumes preflooding) than of CB (~1 pore volume), limiting the efficiency of the DMD method for relatively heavier DNAPLs (TCE and PCE). The efficiency of the DMD method may be improved if alcohol can be delivered in greater quantities during the preflood. However, attempts to increase n-butanol delivery in a micellar surfactant solution indicated that the presence of surfactants alters (unfavorably) equilibrium partitioning behavior of n-butanol. Consequently, the overall objective of this study was to develop and evaluate a macroemulsion for the delivery of n-butanol in the DMD of TCE.

The 2-D aquifer cell experiments conducted as part of Task 2B were designed to assess delivery of DMD preflood and displacing solutions to the DNAPL source-zone, conversion of DNAPL to LNAPL using an aqueous butanol solution, and upward displacement and recovery of the NAPL. The 2-D aquifer cell had dimensions of 63.5 cm (height) x 38 cm (length) x 1.4 cm (thickness). The end chambers were screened over the entire height of the aquifer cell. The cell was packed under water-saturated conditions with Ottawa Federal Fine sand as the background matrix. Two regions of lower permeability lenses, consisting of F-70 Ottawa sand, were emplaced to increase heterogeneity and simulate potential field heterogeneities. The first layer of lenses was located up to 3 cm above the bottom-confining layer (F-70) and covered the entire length of the cell, while the second layer of lenses was emplaced 19 to 21.5 cm above the bottom confining layer and 19 cm from either end chamber. An influent well, constructed from 0.32 cm O.D. 316 stainless steel tubing and screened over the bottom 5.2 cm, was packed in the cell matrix to simulate a partially-screened well. This injection well was used minimize the potential effects of density override of the resident solution by lower density injection solutions, the reby increasing contact between the flushing solutions and the entrapped or pooled DNAPL.

The selected emulsion was evaluated in three aquifer cell experiments (Boxes 7-A through 7-C) to assess the ability of the emulsion to deliver n-butanol for *in situ* density conversion of TCE from a DNAPL to an LNAPL. Properties of each aquifer cell are given in Table 3. Box 7-A represents a preflood of shorter duration (0.95 pore volumes versus 1.2 pore volumes), demonstrating significant reduction in TCE-NAPL density, but incomplete density modification. Two replicate aquifer cell experiments (Boxes 7-B and 7-C) were conducted in which the emulsion preflood successfully converted the TCE-NAPL to an LNAPL prior to displacement and recovery. A more complete chemical analysis of effluent solutions was performed for Box 7-C and will therefore be discussed in greater detail than Box 7-B.

Table 3. Overview of 2-D aquifer cell experiments (Boxes 7-A, 7-B, and 7-C).

Parameter	Box 7-A	Box 7-B	Box 7-C
Pore Volume (mL)	1335	1180	1185
Permeability ($cm^2 \times 10^7$)	5.6±0.4	4.5±0.1	4.6±0.2
TCE Released (mL)	32	36	26
Overall TCE-NAPL Saturation (%)	2.4	3.0	2.2
Volume of Preflood (mL)	1250	1310	1410
Preflood Flow Rate (mL/min)	3.7±0.3	4.1±0.1	3.6±0.4
Volume of Displacement Flood (mL)	1520	1120	1400
Displacement Flood Flow Rate (mL/min)	3.7±0.3	3.6±0.5	3.5±0.2

After the injection and redistribution of 32 mL of TCE (2.4l% overall saturation), a total of 1250 mL of 15% n-butanol emulsion (not dyed) was introduced into Box 7-A through the partially screened influent well at an average flow rate of 3.7 ± 0.3 mL/min. Prior to commencement of the emulsion preflood, the water (dyed blue-green) was introduced for visualization purposes. The aquifer cell had a pore volume of 1335 mL and overall intrinsic permeability of 5.6 (±0.4) x 10^{-7} cm^2. At early time (~370 mL) the emulsion front contacted the TCE-NAPL near the confining layer and did not induce mobilization of free product (Figure 26a). At later time (~960 mL) the emulsion contacted the region of higher TCE saturations and became milky-white in color (Figure 26b). Both the injected n-butanol emulsion and the emulsion formed upon contact with TCE-NAPL were observed to be readily transported through the porous medium (Figure 26b). Upon completion of the emulsion preflood (1250 mL), 1520 mL of the low-IFT displacement solution (dyed blue-green) were introduced through the partially screened well at an average flow rate of 3.7±0.3 mL/min. Representative middle (~555 mL) and late (~1250 mL) time photographs of the displacement flood are shown in Figure 27. Downward migration and infiltration of TCE-NAPL into the confining layer (F-70 Ottawa sand) was observed, indicating incomplete density modification.

Aqueous phase concentrations of TCE, n-butanol and Aerosol MA in Box 7-A are shown as a function of effluent volume collected in Figure 28. The vertical lines in Figure 11 indicate the introduction of emulsion, displacement solution, and water into the influent injection well. Significant concentrations of TCE (~40 g/L) were observed upon breakthrough of the emulsion, as approximated by the appearance of n-butanol. These high concentrations of TCE are indicative of in situ emulsification, consistent with visual observations of the aquifer cell (Figure 26) and effluent samples. Concentrations of n-butanol in the effluent samples increase sharply at approximately 1100 mL, but did not reach the concentration of n-butanol in the influent emulsion, indicating partitioning of n-butanol into the TCE-NAPL. Upon breakthrough of the displacement solution, as evidenced by the appearance of Aerosol MA in the effluent, concentrations of n-butanol decreased to near 80 g/L before rebounding to near 105 g/L. This second increase in n-butanol concentration resulted from emulsion destabilization and mixing, and solubilization of n-butanol-rich NAPL. The latter is apparent when trends in effluent TCE concentration are compared to those in effluent n-butanol concentration. Increased TCE concentrations resulted from NAPL solubilization, however, the NAPL uder going solubilization included n-butanol.

Aqueous and non-aqueous phase effluent sample densities collected from Box 7-A are reported in Figure 29. Here again, vertical lines represent introduction of the emulsion, displacement solution and post treatment water into the partially screened influent well, while horizontal lines represent the density of influent solutions. A reduction in TCE-NAPL density from 1.47 g/mL to a minimum effluent NAPL density of 0.90 g/mL was the result n-butanol partitioning facilitated by the delivery of the emulsion. Density conversion relative to the corresponding aqueous phase samples, however, was only observed for a limited number of samples. Unconverted DNAPL densities were significant, ranging from 1.05 g/mL to 1.13 g/mL. Insufficient density reduction suggests emulsion prefloods of greater than 0.95 pore volumes should be used for the DMD of TCE.

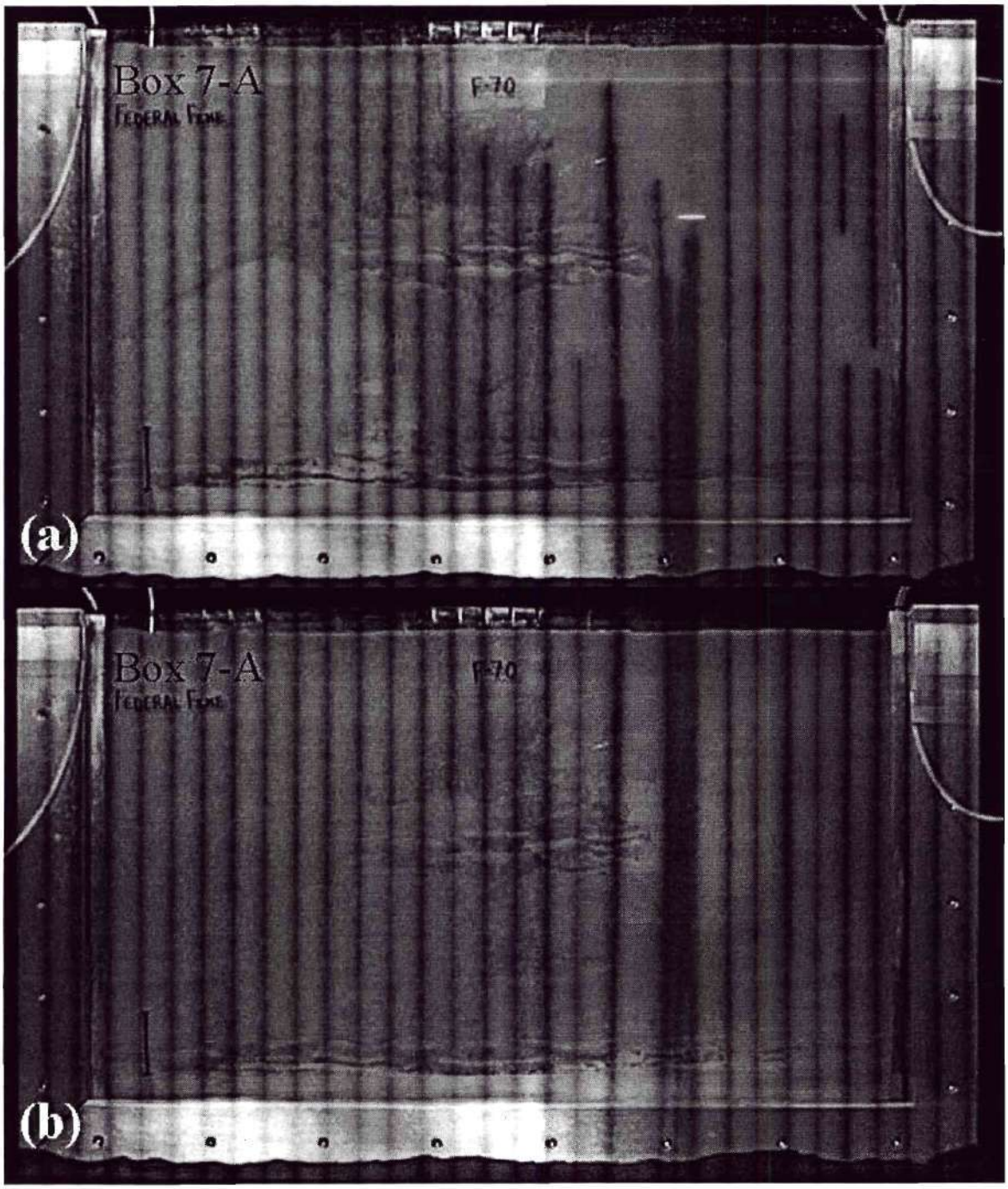

Figure 26. Representative early (a: ~370 mL) and late (b: ~960 mL) time photographs of the emulsion preflood during Box 7-A.

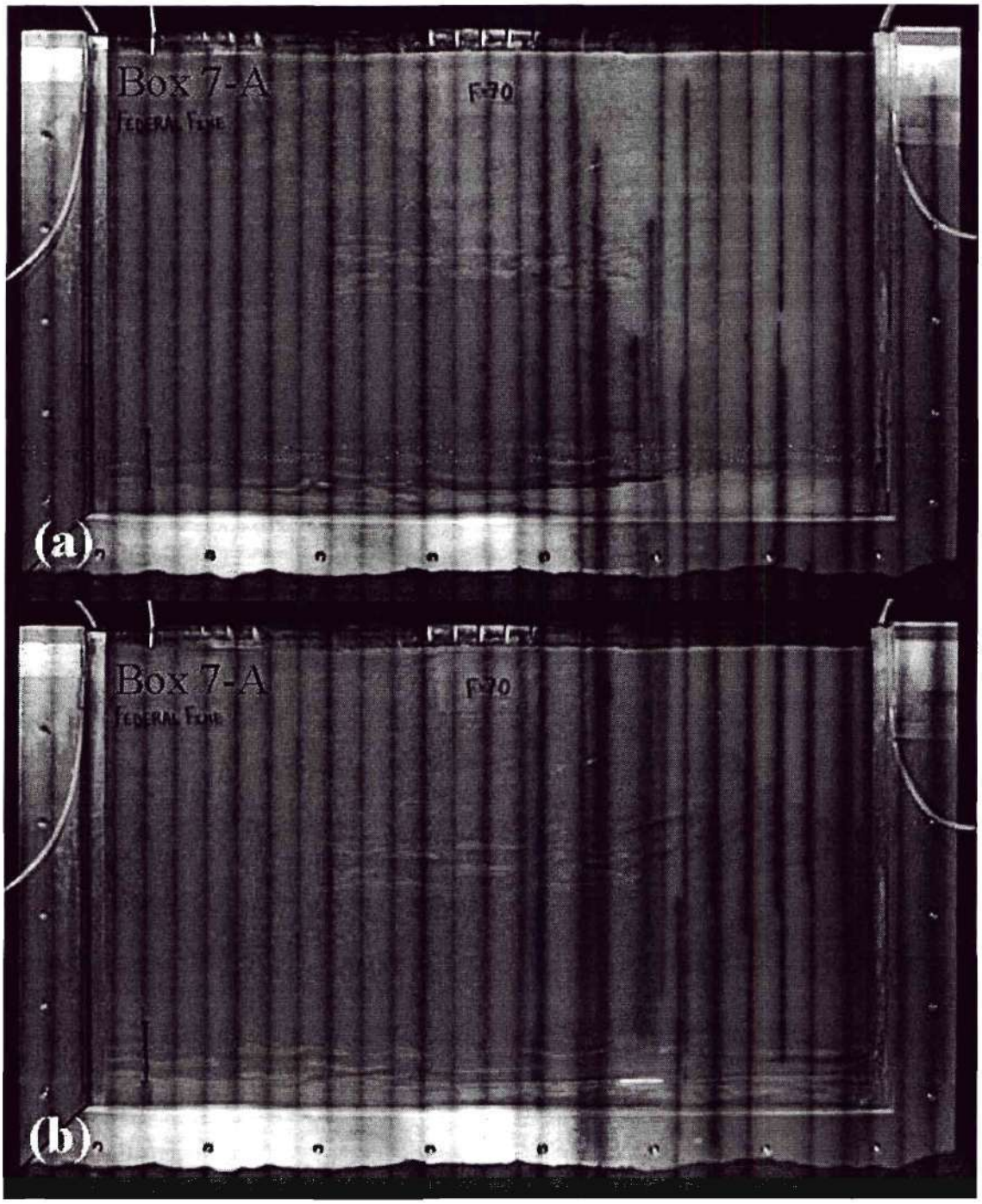

Figure 27. Representative middle (a: ~555 mL) and late (b: ~1250 mL) time photographs of TCE-NAPL displacement in Box 7-A.

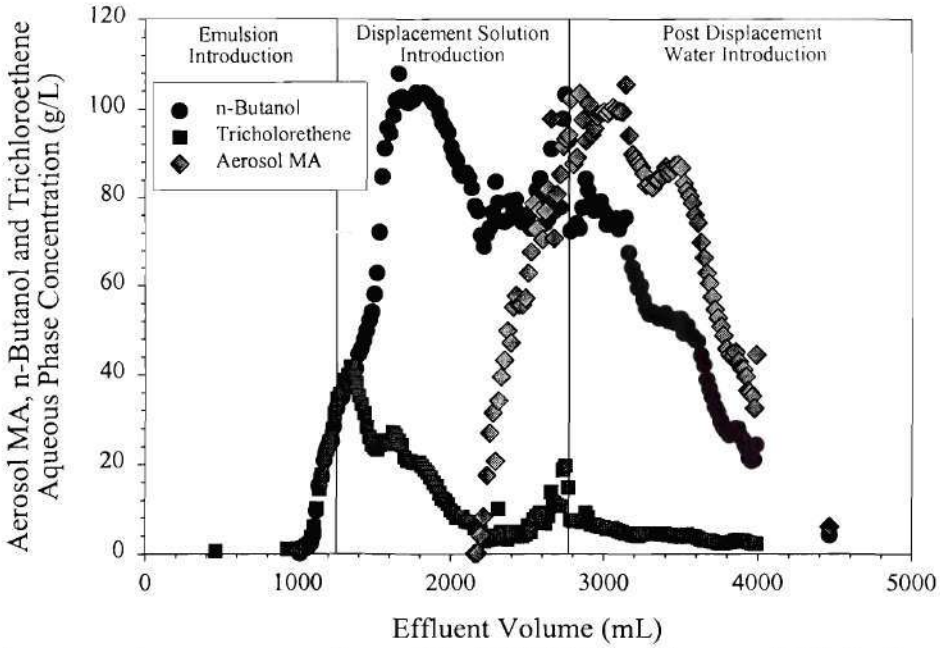

Figure 28. Aqueous phase concentrations of BuOH, TCE, and Aersosol MA in the effluent of Box 7-A. Vertical lines represent the introduction of flushing solutions into the influent.

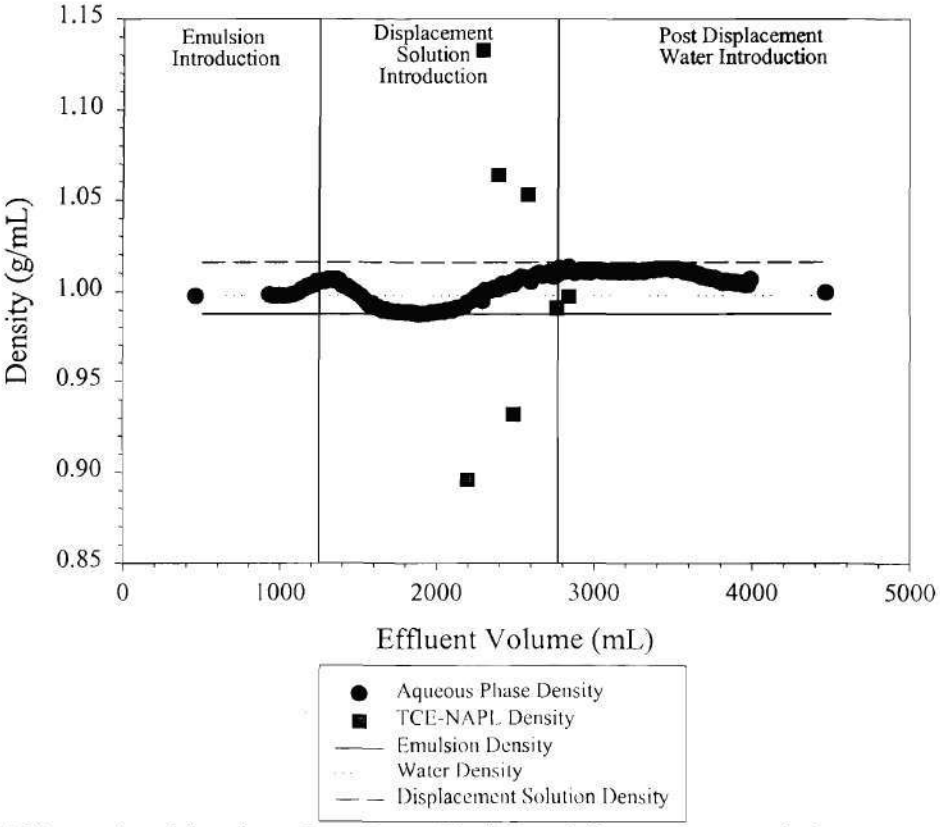

Figure 29. Effluent densities from Box 7-A. Horizontal lines represent influent solution densities, and vertical lines represent the introduction of flushing solutions into the influent.

A longer (1.2 pore volume) emulsion preflood was used Box 7-B, which had a pore volume of 1182 mL and an overall intrinsic permeability of 4.6(±0.2) x 10^{-7} cm^2. The volume of TCE remaining within the cell after release and redistribution was 36 mL, corresponding to an overall saturation of 3%. A total of 1307 mL of the 15% (vol) n-butanol emulsion (not dyed) was introduced through the partially screened well at an average flow rate of 4.1±0.1 mL/min. As the preflood macroemulsion passed through regions of high TCE saturation, the aqueous phase became milky-white in color, characteristic of emulsified TCE and surfactant (Figures 30a and 30b). Following the preflood, a total of 1120 mL of low interfacial tension solution (10% (vol) Aerosol MA + 6% (vol) n-butanol + 15 g/L NaCl + 1 g/L $CaCl_2$, dyed blue-green) was flushed through the aquifer cell to mobilize the density modified NAPL. The average flow rate during the displacement flood was 3.6±0.5 mL. At the completion of the low-IFT displacement flood, a final water flood was used to produce the remaining surfactant solution from the cell. Representative images, shown in Figures 31a and 31b, demonstrate the upward migration of the density-modified TCE upon mobilization. Although NAPL mobilization was observed, free product was not collected in the effluent samples as a result of the high solubilization capacity of the 10% Aerosol MA solution. In effect, the displaced free product was solubilized as it migrated toward, and resided in, the effluent end chamber.

Effluent concentrations of TCE and n-butanol are shown as a function of effluent solution volume collected in Figure 32. The vertical lines in Figure 15 represent the introduction of each flushing solution into the partially screened injection well. The appearance of n-butanol in the effluent was delayed relative to the TCE spike, and was substantially lower in concentration relative to the injected concentration of 120 g/L. These trends are consistent with strong partitioning of n-butanol into resident TCE. Effluent n-butanol concentrations were found to decrease over the course of the low IFT displacement flood, eventually falling below the injected concentration (50 g/L). Also evident in Figure 32 is the considerable mass of TCE (53%) that was recovered during the macroemulsion preflood. The large increase in effluent TCE concentrations at 1200 mL were attributed to the breakthrough of the milky-white TCE/surfactant macroemulsion observed during the preflood. The second increase in the TCE effluent concentration at 2200 mL corresponded with the breakthrough of the low-IFT displacement flood. Subsequent concentrations of TCE varied considerably, which was consistent with non-uniform free-product migration into the end chamber. The tailing observed after flushing with ~3300 mL was largely the result of viscous instabilities, which led to partial breakthrough of the post displacement water flood. The combination of the DMD macroemulsion preflood and low-IFT displacement (total 2427 mL flooded) resulted in an overall TCE recovery of 92%.

Densities of effluent aqueous phase samples over the course of the experiment are shown in Figure 33. Breakthrough of the macroemulsion preflood corresponded to the increase in effluent density at ~1200 mL. These increased densities resulted from the large mass (~50%) of TCE incorporated in the macroemulsion and the partitioning of n-butanol into the residual TCE-NAPL. Upon introduction of the low-IFT solution the effluent density rose, but did not reach the influent value of 1.02 g/mL. This effect was attributed to the solubilization of density-modified TCE. Density data substantiate the upward displacement observed during the low-IFT displacement flood (Figure 31). The subsequent decrease and scatter in aqueous phase densities resulted from the non-uniform front of the post mobilization water flood.

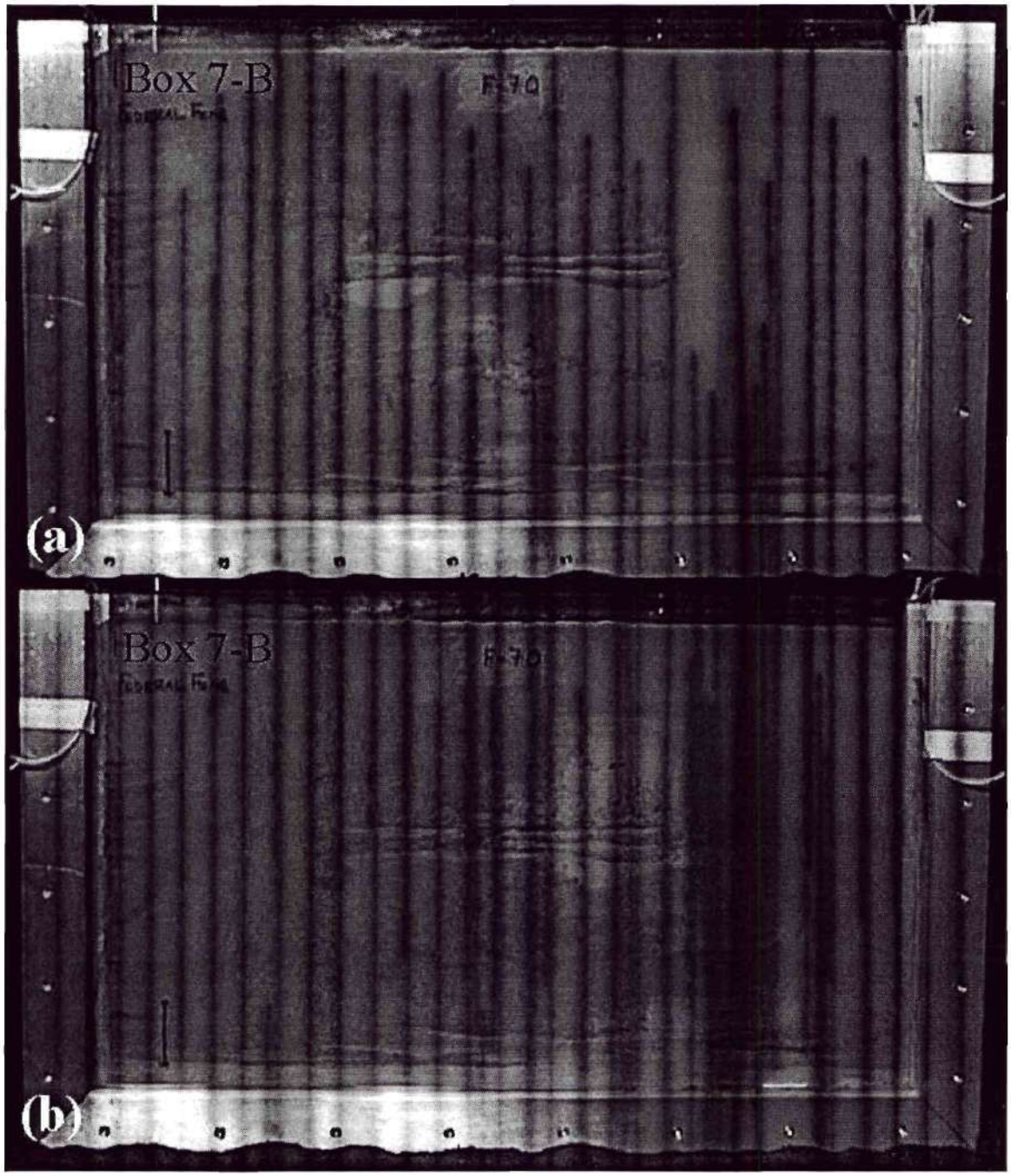

Figure 30. Representative early (a: ~530 mL) and late (b: ~950 mL) time photographs of the emulsion preflood during Box 7-B.

Figure 31. Representative early (a: ~650 mL) and late (b: ~1050 mL) time photographs of TCE-NAPL displacement in Box 7-B.

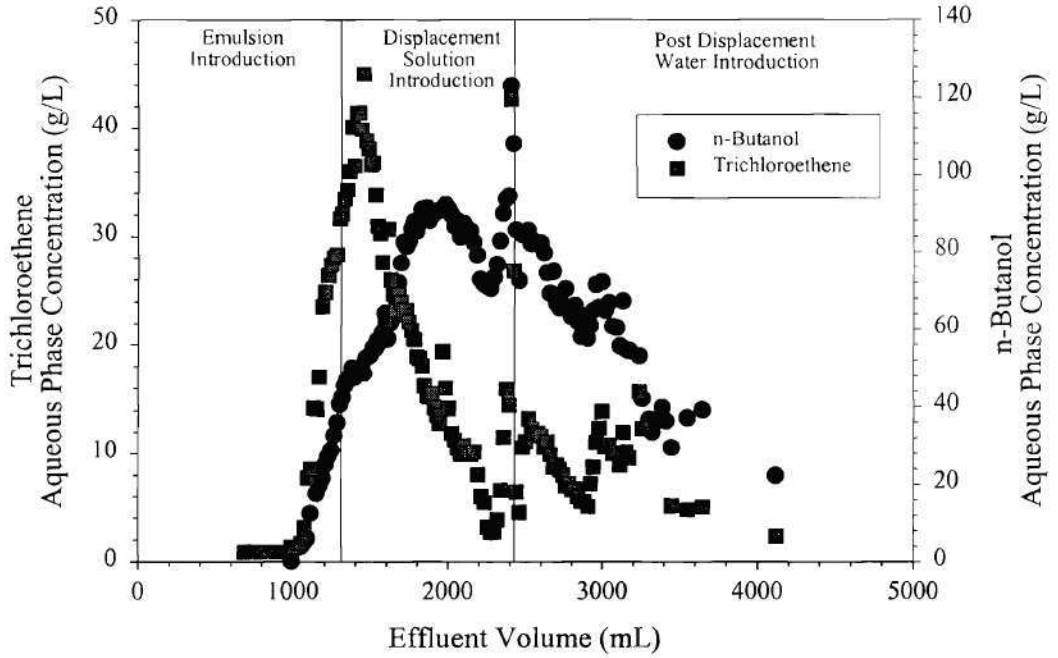

Figure 32. Effluent aqueous phase concentrations of BuOH, TCE and Aerosol MA from Box 7-B. Vertical lines represent the introduction of flushing solutions in the influent.

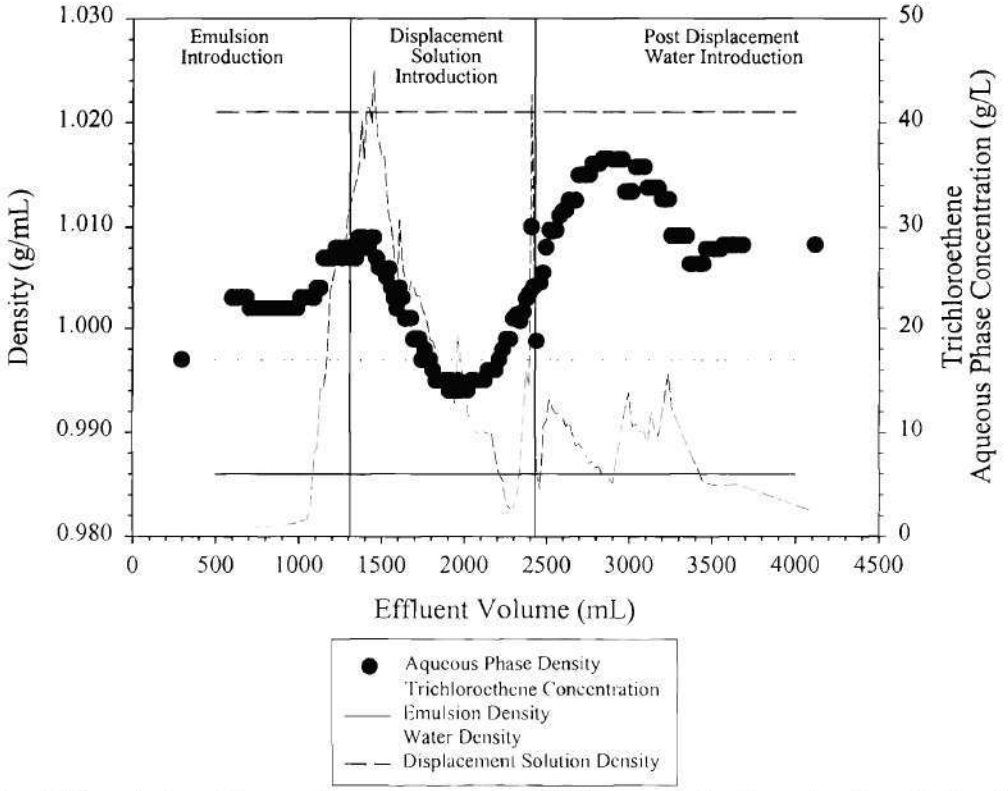

Figure 33. Effluent densities and aqueous phase TCE concentrations in Box 7-B. Horizontal lines represent influent solution densities, and vertical lines represent solution introduction.

In an effort to reproduce the *in situ* density conversion process using an emulsion of 15% (vol) n-butanol, a replicate aquifer cell study was conducted (Box 7-C). Box 7-C represents a more comprehensive investigation of the emulsion flood and subsequent displacement of TCE-NAPL, including Aerosol MA concentrations, effluent viscosities and head loss measurements. A total of 1410 mL of the 15% (vol) n-butanol emulsion preflood was introduced into Box 7-C through the partially screened well, at an average flow rate of 3.6±0.4 mL/min. At early time (~430 mL), the macroemulsion (not dyed) flow front contacted TCE-NAPL near the lower confining layer and did not induce free product mobilization (Figure 34a). As the preflood macroemulsion passed through regions of high TCE saturation (~920 mL), the aqueous phase became milky-white in color, characteristic of emulsified TCE and surfactant (Figure 34b). Based on visual observations, the milky-white macroemulsion migrated through the porous media without significant reduction in flow relative to the injected emulsion front. In general, the formation and transport of a TCE-rich macroemulsion observed in Boxes 7-A (Figure 26) and 7-B (Figure 30) was replicated in Box 7-C (Figure 34).

Immediately following the emulsion preflood, a total of 1400 mL of low IFT solution (dyed blue-green) were introduced into Box 7-C through the partially screened well, at an average flow rate of 3.5±0.2 mL. Representative middle (~700 mL) and late (~1080 mL) time images illustrate the migration of density-modified NAPL, which consisted primarily of TCE, water and n-butanol (Figure 35). At the completion of the low-IFT displacement flood, a final water flood (not dyed) was used to displace the remaining surfactant solution from the 2-D cell.

Aqueous phase effluent concentrations of TCE and n-butanol are shown as a function of effluent solution volume collected for Box 7-C (Figure 36). The vertical lines shown in Figure 36 correspond to the introduction of the emulsion, displacement solution and post treatment water flooding through the partially screened injection well. Appearance of n-butanol in the effluent was delayed relative to the TCE spike, and was substantially lower in concentration relative to the concentration of n-butanol in the influent emulsion (~120 g/L). These trends are consistent with substantial partitioning of n-butanol into the resident TCE-NAPL. Effluent concentrations of n-butanol were found to decrease over the course of the low-IFT displacement flood, eventually falling below the concentration of n-butanol in the injected displacement solution (53 g/L). The elevated n-butanol concentrations observed during the displacement flood were attributed to the breaking and mixing of the 15% (vol) n-butanol emulsion along the displacement front, as well as solubilization of high n-butanol content TCE-NAPL. A considerable amount of TCE (~60%) was recovered during the macroemulsion preflood in Box 7-C (Figure 36). Significant mass removal (>50%) was also measured during the macroemulsion preflood in Boxes 7-A and 7-B. Recent studies have demonstrated that in situ macroemulsification of NAPLs is an important recovery mechanism, accounting for 30 to 68% of DNAPL removal when conditions are favorable for emulsion transport. The large increase in effluent TCE concentrations at ~1100 mL was due to breakthrough of the milky-white TCE/surfactant macroemulsion. The second increase in the TCE effluent concentration at ~2400 mL corresponded with breakthrough of the low-IFT displacement flood, as indicated by the increase in Aerosol MA concentrations. Concentrations of TCE varied during the displacement process, which was attributed to non-uniform free-product migration into the end chamber. The tailing of effluent n-butanol and Aerosol MA concentrations observed after flushing with ~4000 mL was largely the result of viscous instabilities, which led to partial breakthrough of the post-displacement water flood. Effluent aqueous phase concentrations of n-butanol and TCE measured in Box 7-C were similar those reported in Boxes 7-A and 7-B. Analysis of effluent NAPL samples revealed significant partitioning of the Aerosol MA into the TCE-NAPL, with

Aerosol MA concentrations ranging from 24 to 125 g/L. The high surfactant concentrations are indicative of Winsor Type II behavior and the formation of reverse micelles. The total Aerosol MA mass partitioned into the NAPL, however, amounted to only 3% of the Aerosol MA introduced into the aquifer cell, demonstrating the relatively insignificant loss of surfactant to the NAPL under the experimental conditions.

Effluent densities of both the aqueous and organic phases measured over the course of Box 7-C are shown in Figure 37. Horizontal lines appearing in Figure 37 represent influent solution densities and provide a reference point for density conversion. Vertical lines represent the introduction of each solution into the partially screened influent well. Breakthrough of the macroemulsion corresponded to the increase in effluent density observed at ~1100 mL. The increased aqueous phase densities resulted from the large mass (~60%) of TCE incorporated in the macroemulsion and partitioning of n-butanol into the TCE-NAPL. Without emulsification of TCE-NAPL and the partitioning of n-butanol, the aqueous phase effluent density would have decreased to a value near that of the influent macroemulsion (0.98 g/mL). Effluent TCE-NAPL densities ranged from 0.97-0.99 g/mL, and all were less than their corresponding aqueous phase samples. The relatively low TCE-NAPL densities measured in effluent samples indicate successful in situ density conversion of TCE-NAPL, and substantiate the observed upward NAPL displacement during the low-IFT displacement flood (Figure 35). The subsequent decrease and scatter of the aqueous phase densities resulted from mixing of the post-mobilization water flood with the displacement solution. Effluent aqueous phase samples from Box 7-C corroborate data trends observed for Box 7-B.

The potential for reduction in hydraulic conductivity is an important consideration when flooding with a macroemulsion. Consequently, the drop in head across the aquifer cell (Box 7-C), as well as aqueous and non-aqueous phase viscosities, is plotted as a function of effluent volume in Figure 38. Head loss increased throughout the macroemulsion flood, reaching a maximum of 7.4 cm corresponding to a gradient in head of ~12%. Over the course of Box 7-C, the flow rate was maintained at ~3.5 mL/min until all of the displaced free product was recovered during water flooding, at which time (~3500 mL) the flow rate was increased to ~12 mL/min to expedite recovery of the resident surfactant solution. Given the relatively constant flow rate at early time, the corresponding increase in head loss was attributed to the increased aqueous phase viscosity (Figure 38). Viscosity of the organic liquid phase is an important parameter in low-IFT displacement processes, as both the aqueous and organic phases must to flow through an unconfined domain. Results indicate these NAPL samples had higher viscosities (8-11 cP) than those reported previously. While the NAPL viscosities measured in Box 7-C were high, NAPL viscosities as high as 15.6 cP have been reported during the displacement of complex, multicomponent DNAPLs from a medium of similar intrinsic permeability (2×10^{-7} cm^2). Finally, It is important to note that the viscous instabilities observed during NAPL displacement flood could be reduced with further optimization of the low IFT solution.

Mass recoveries of TCE and n-butanol from both Boxes 7-A through 7-C are shown in Table 4. The high recovery of TCE (~93% in Boxes 7-B and 7-C) was obtained after flushing with a total of 2. 1 and 2.4 pore volumes (macroemulsion and low IFT solution) respectively, indicating the efficiency of the DMD process. SEAR solubilization studies in similar systems have reported using up to 8 pore volumes to recover 70% of the released NAPL. Significant surfactant partitioning was measured in effluent NAPL sample from Box 7-C, however, the total mass of surfactant lost to the NAPL was only 3% of the total surfactant introduced. Overall surfactant recoveries were approximately 87% in Boxes 7-A and 7-C.

Compared to the results of previous DMD studies, use of the 15% (vol) n-butanol emulsion reduced the volume of preflood solution required for in situ TCE density conversion from ~5 pore volumes to ~1.2 pore volumes. This work focused on the use of a macroemulsion to delivery a partitioning alcohol to the entrapped and pooled TCE-NAPL. However, the displacement solution used herein represents one of several possible approaches. For example, displacement following a macroemulsion preflood could be realized using alcohol flooding or a different low-IFT surfactant formulation. Furthermore, a macroemulsion density-conditioning flood employed prior to the introduction of a solution possessing an ultra-high solubilization capacity may reduce the risk of downward displacement and promote neutral buoyancy recovery. In conclusion, the use of an emulsion preflood in the DMD method holds great promise for favorable partitioning of n-butanol and *in situ* density conversion of DNAPLs. This emulsion preflood approach was designed for implementation within horizontal flushing scenarios in aquifer systems without the need for physical confinement of the source zone.

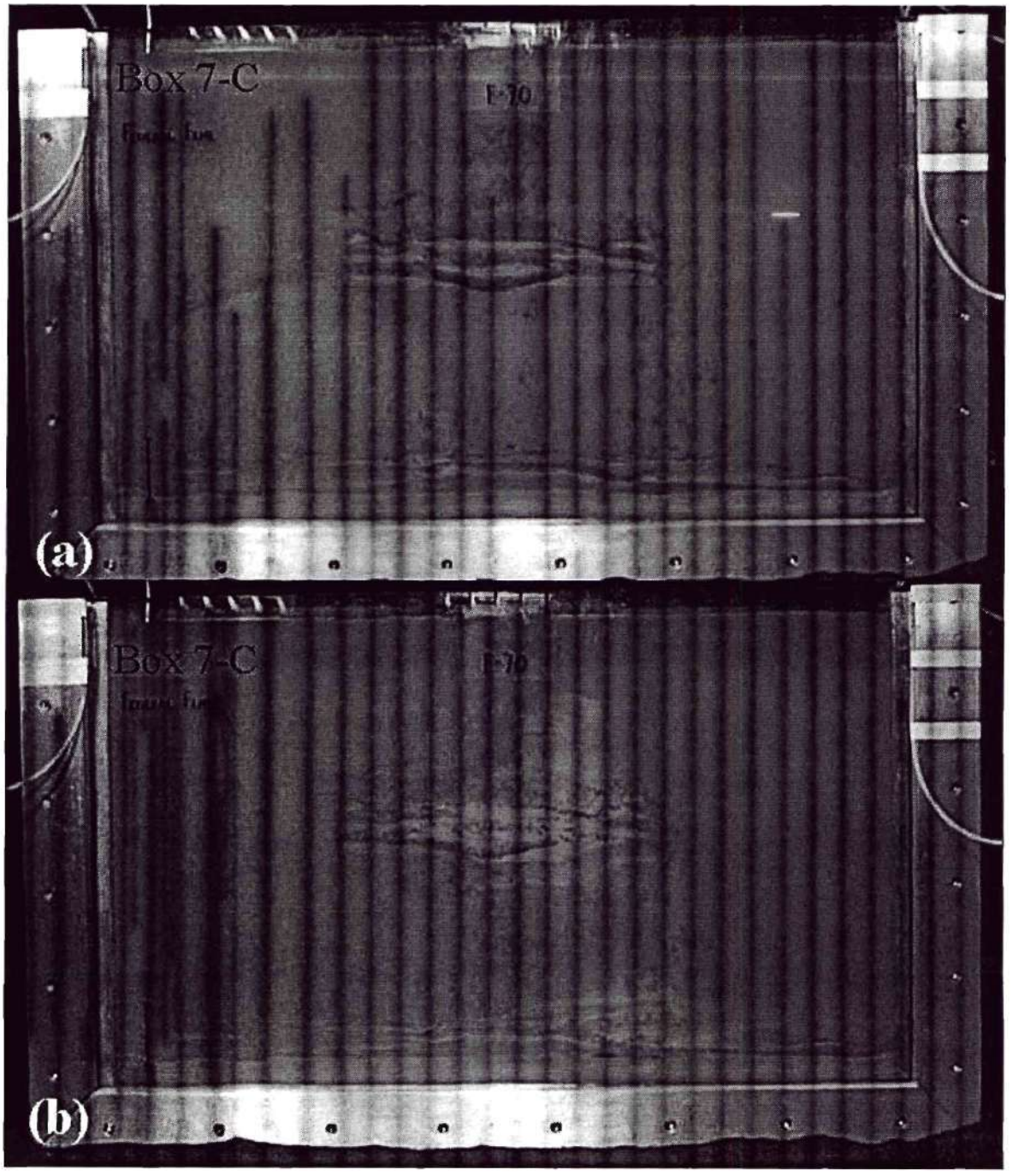

Figure 34. Representative early (a: ~430 mL) and late (b: ~920 mL) time photographs of the emulsion preflood during Box 7-C.

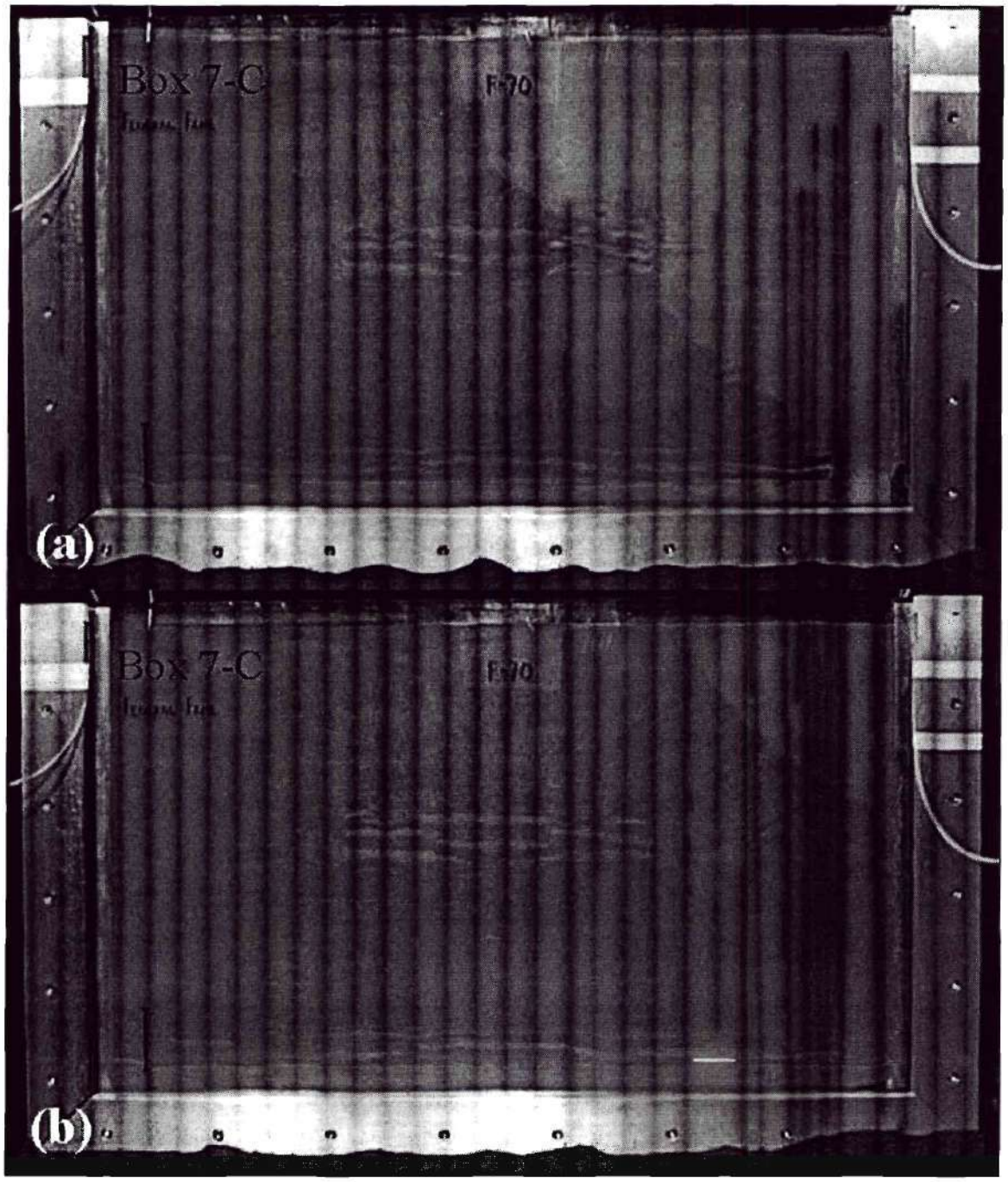

Figure 35. Representative early (a: ~700 mL) and late (b: ~1080 mL) time photographs of TCE-NAPL displacement in Box 7-C.

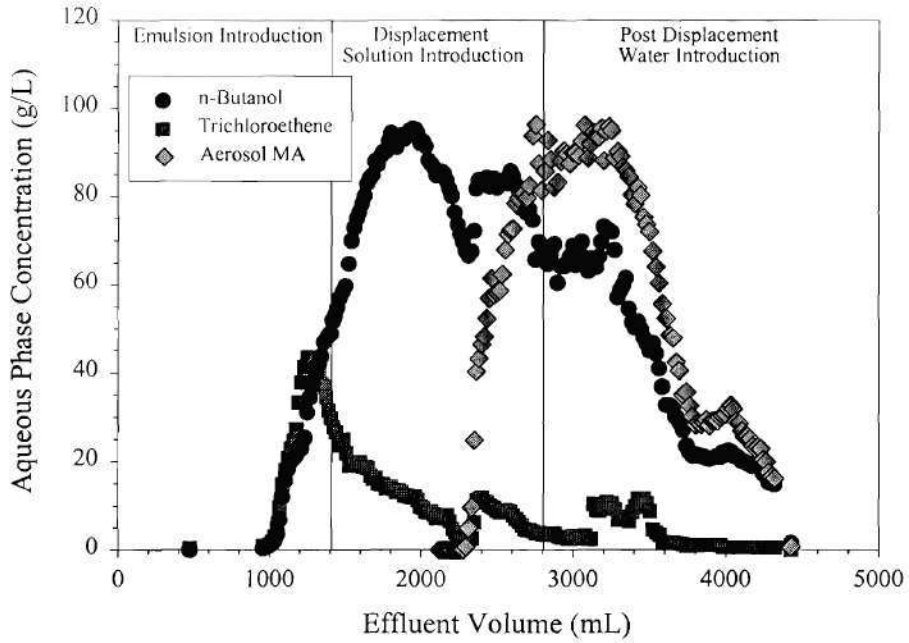

Figure 36. Effluent aqueous phase concentrations of BuOH, TCE and Aerosol MA in Box 7-C.

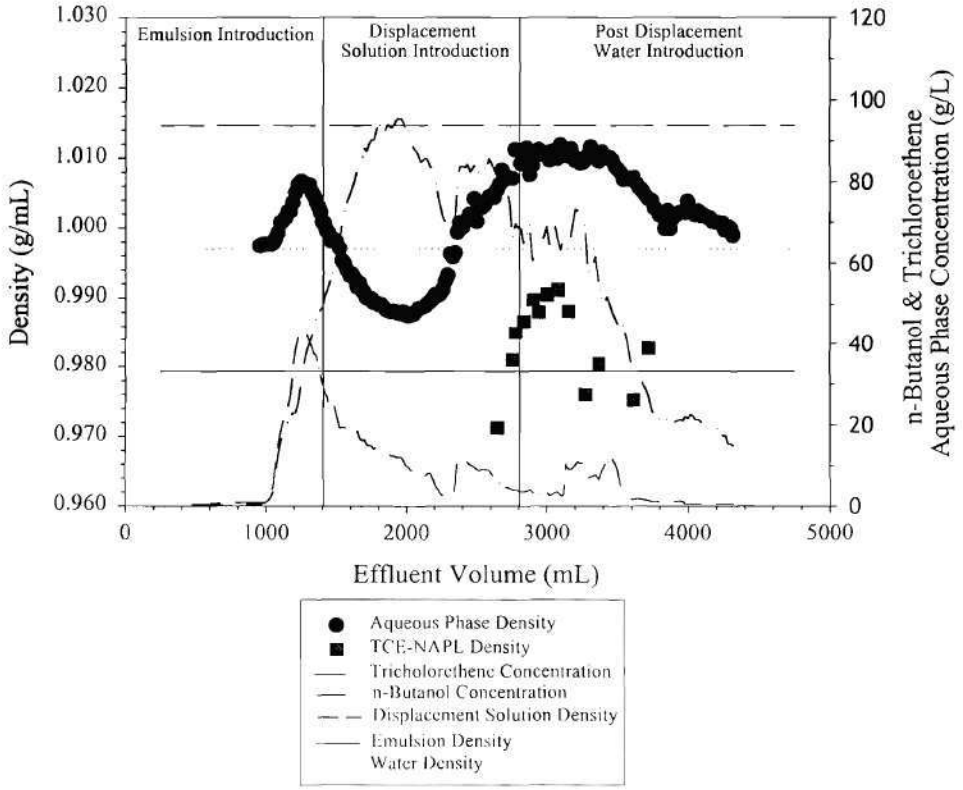

Figure 37. Effluent densities and aqueous phase concentrations of BuOH and TCE from Box 7-C. Horizontal lines represent influent solution densities, and vertical lines represent solution introduction.

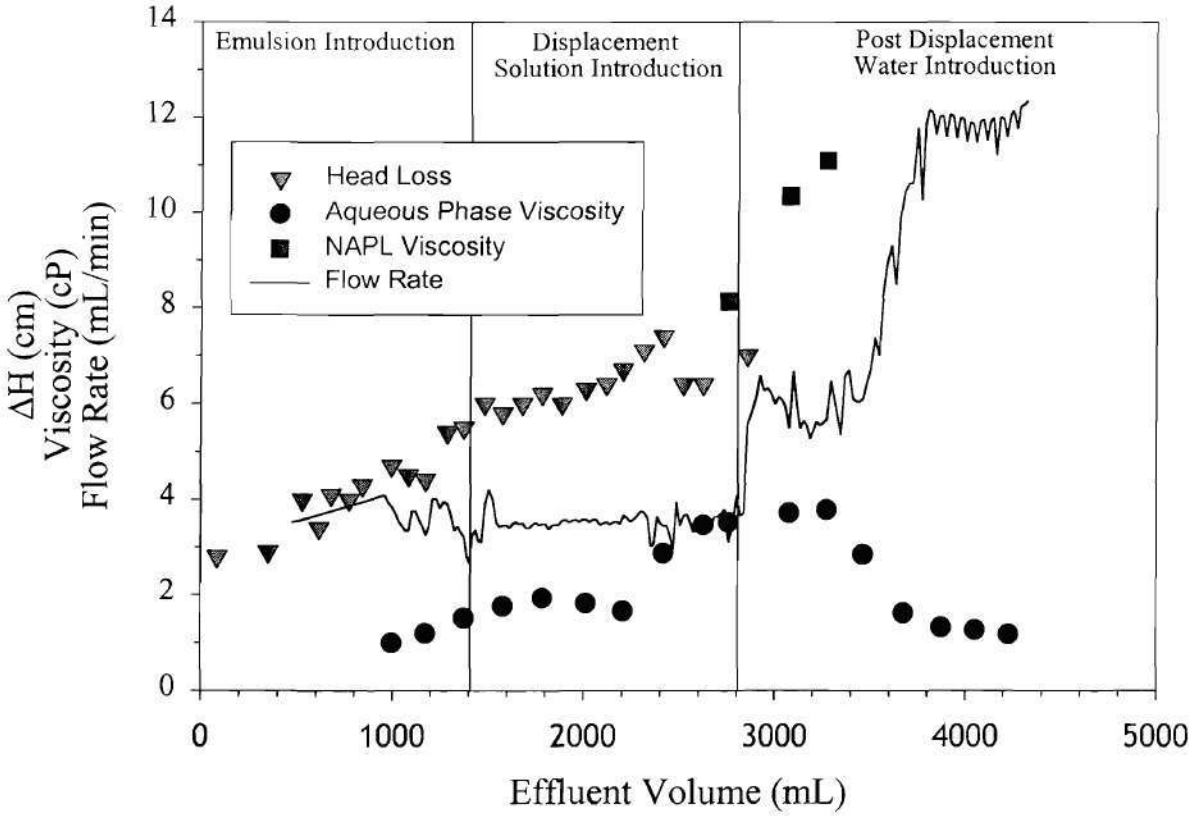

Figure 38. Effluent viscosities, flow rate, and corresponding head loss across the aquifer cell during flooding in Box 7-C. Vertical lines represent the introduction of flushing solutions in the influent.

Table 4. Recoveries of major components from Boxes 7-A, 7-B and 7-C.

Parameter	Box 7-A	Box 7-B	Box 7-C
TCE Available to Flooding (g)	46.2	52.2	37.7
TCE Recovered as NAPL (g)	6.2	4.9	2.3
TCE Solubilized/emulsified (g)	33.5	44.0	32.7
Total TCE Recovered (g)	39.7	48.9	35
Recovery of TCE (%)	86.0	93.6	92.7
n-Butanol Introduced (g)	222	220	240
n-Butanol Recovered in NAPL (g)	5.8	6.3	11.6
n-Butanol Recovered in Aqueous Phase (g)	193	178	185
Total n-Butanol Recovered (g)	199	184	197
Recovery of n-Butanol	89.6	83.8	82.0
Aerosol MA Introduced (g)	153	Not Measured	140
Aerosol MA Recovered in NAPL (g)	Not Measured	Not Measured	4.2
Aerosol MA Recovered in Aqueous Phase (g)	134	Not Measured	117
Recovery of Aerosol MA (%)	87.6	Not Measured	86.6

Task 2.C. Aquifer Cell Testing of DMD Method: DNAPL Mixtures

While the DMD method has been demonstrated for recovery of laboratory-grade DNAPLs (e.g., CB, TCE, and PCE), many field-scale remediation scenarios must treat DNAPLs composed of multiple components (e.g., spent degreasers). Because the DMD method relies upon partitioning large quantities of n-butanol into the organic phase, the effect of DNAPL composition on alcohol partitioning becomes an important consideration. Batch and 2-D aquifer cell experiments were used to evaluate the DMD method for recovery of two binary DNAPL mixtures representative of spent degreasing solvent (TCE+grease). In these binary mixtures, decane was selected as representative of an aliphatic grease component. The composition of the first mixture was chosen such that the resulting DNAPL density was similar to that of CB (~1.1 g/mL). This selection allowed results obtained for the DNAPL mixture to be benchmarked against those obtained for pure CB. The second mixture evaluated had a density between that of CB and TCE (~1.3 g/mL) and represented a relatively heavier mixture, in which changes in the equilibrium alcohol partitioning, arising from the presence of decane, may affect the extent of preflooding required for in situ density conversion.

A 2-D aquifer cell having similar dimensions and containing a similar porous media as used in the pure component experiments was used in a proof-of-concept experiment conducted with the relatively lighter DNAPL mixture. This DNAPL mixture had a density of 1.1 g/mL and consisted of 0.69 mole fraction TCE and 0.31 mole fraction decane. For Box M1, the packed aquifer cell had an overall permeability of $5x10^{-7}$ cm^2 and a pore volume of 1400 mL. After injection and redistribution, 19 mL of NAPL was entrapped, pooled or dissolved within the 2-D cell, yielding an overall DNAPL saturation of 1.3%. In situ density modification of the TCE-decane DNAPL mixture was accomplished using an aqueous solution containing 6% (wt) n-butanol. During the preflood, 1660 mL of 6% (wt) n-butanol solution were introduced through the partially screened well at an average flow rate of 4.3 mL/min. At early time (~680 mL), the 6% n-butanol preflood solution (dyed blue-green) contacted the DNAPL mixture without inducing free-product mobilization (Figure 39a), however some redistribution occurred as a result of the NAPL swelling (i.e., increases in the volume of NAPL due to the partitioning of n-butanol). All preflood and displacement solutions, introduced through the partially screened well, were observed in the upper left-hand portion of the cell shortly after the commencement of flushing. This behavior was attributed to flow of the injected solution into the fully screened end chamber and subsequent mixing and flow back into the aquifer cell. At later time (~1620 mL) significant swelling of the NAPL was observed (Figure 39b), which led to some migration. Immediately following the preflood period, 1490 mL of low-IFT solution consisting of 4% (4:1 wt) Aerosol MA/OT + 20% (wt) n-butanol + 500 mg/L $CaCl_2$ (not dyed) were introduced into the cell through the partially screened well at an average flow rate of 4.3 mL/min. Representative early (~540 mL) and late (~1350 mL) time photographs of the low-IFT surfactant flood show displacement and upward migration of the density converted NAPL (Figure 40).

Effluent concentrations from Box M1 are shown in Figure MIX3 with increasing effluent volume. Here, vertical lines represent the introduction of the preflood, low-IFT displacement flood and post treatment water flood solutions into the partially screened injection well. After the appearance of preflood solution in the effluent, n-butanol concentrations increased to approximately 52 g/L, which was significantly less than the influent value of approximately 59 g/L, and indicated partitioning of n-butanol from the aqueous phase into the NAPL mixture. Similar effluent concentrations were observed during the preflood of Box 13 (Figures 20-23), which was contaminated by pure CB-NAPL (i.e., the same NAPL density as the mixture investigated in Box M1). The concentration approached a plateau value of approximately 52 g/L, as opposed to the influent value of 59 g/L, due to the relatively minor density reduction

needed for density conversion. That is, the amount of n-butanol required for density conversion was far less than the capacity of the TCE-decane mixture for n-butanol. Density conversion for pure CB-NAPL was obtained at an n-butanol mole fraction of 0.38 in the organic phase (Figure 7), and requires an aqueous phase concentration of ~48 g/L. This concentration lies on the portion of the alcohol distribution curve where the slope is the least. Effluent concentrations of n-butanol observed in the CB-NAPL box experiment resulted from partitioning occurring along this portion of the distribution curve, where large increases in the mole fraction of n-butanol in the organic phase resulted from small increases in the aqueous phase concentration of n-butanol. Thus the system never approached the capacity of the NAPL for n-butanol during the preflood. Given the similar densities and effluent n-butanol concentrations, it is reasonable to assume the NAPL mixture exhibited phase behavior similar to that of CB-NAPL. The equilibrium distribution of n-butanol, however, was not measured for this TCE-decane mixture. Effluent concentrations of n-butanol rose significantly with the arrival of the low-IFT surfactant solution in the effluent, and exceeded the influent n-butanol concentration (in the low-IFT solution) of 209 g/L. Concentrations of n-butanol in excess of the influent value were attributed to solubilization of the NAPL, which now contained high concentrations of n-butanol. Effluent concentrations of TCE approached a maximum of 6 g/L, which was significantly lower than concentrations reported for the pure TCE-NAPL box experiment. Lower concentrations of TCE in the effluent of Box M1 may have resulted from a Raoult's law type solubility depression; however, other factors such as NAPL distribution also effect effluent concentrations. Significant concentrations (up to ~3 g/L) of decane were observed in the effluent from Box M1 and indicate the potential for solubilization of large quantities of relatively insoluble (in water) compounds by low-IFT surfactant solutions. As anticipated, Aerosol MA and Aerosol OT concentrations in the effluent approached their influent values of 32 g/L and 8 g/L, respectively.

Effluent densities from Box 1M are shown in Figure 41. Here vertical lines represent the introduction of flushing solutions through the partially screened influent well, and horizontal lines represent the density of the influent solutions. Aqueous phase effluent densities were largely a function of n-butanol aqueous phase concentrations (i.e., the amount of the light component). Aqueous phase densities initially decreased from that of resident water (0.998 g/mL) to near that of the influent preflood solution (0.989 g/mL). A second decrease in effluent density resulted from the large increase in n-butanol concentration upon the arrival of the low-IFT solution (0.968 g/mL) in the effluent. The effluent aqueous phase densities began to rise upon commencement of the post-displacement water flood, and ultimately approached the density of water. Effluent densities of the non-aqueous phase ranged from 0.899 to 0.983 mg/L and were all less than (density conversion) or equal to (neutral buoyancy) that of corresponding aqueous phase samples. This decrease in NAPL density (from 1.10 g/mL) was accomplished with flooding 1658 mL (~1.2 pore volumes) of 6% (wt) n-butanol preflood solution (aq), and compares favorably to the results obtained with pure CB-NAPL in which 1.2 pore volumes of a 6% (wt) n-butanol solution (aq) were used to preflood a similar 2-D box. Results of Box M1 suggest the presence of decane in the NAPL had minimal impacts (with respect to the DMD method) on the partitioning behavior of n-butanol.

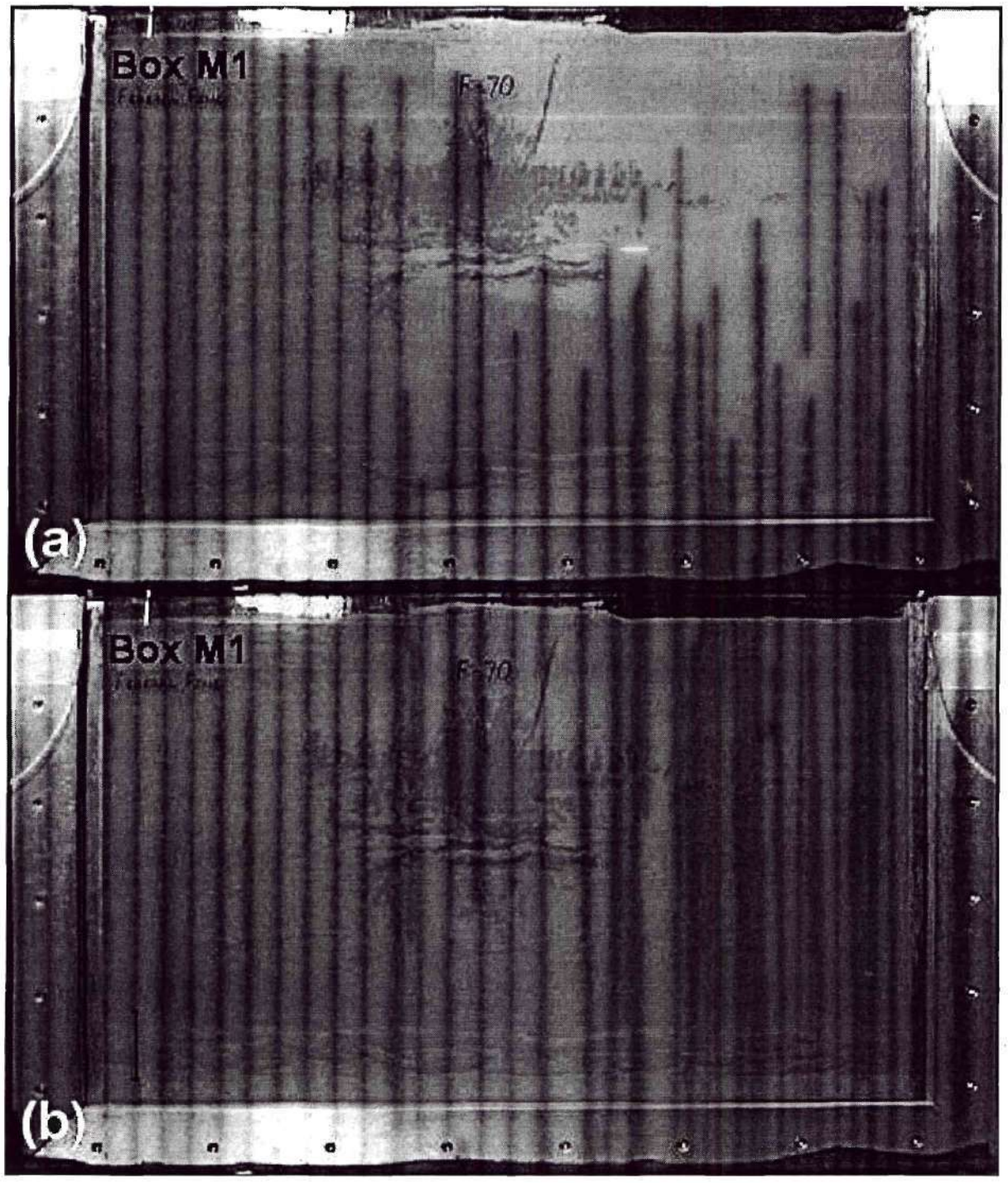

Figure 39. Representative early (a: ~680 mL) and late (b: ~1620 mL) time photographs during the 6% (wt) n-butanol aqueous preflood of Box M1 (initial NAPL composition was 0.69 mole fraction TCE and 0.31 mole fraction decane).

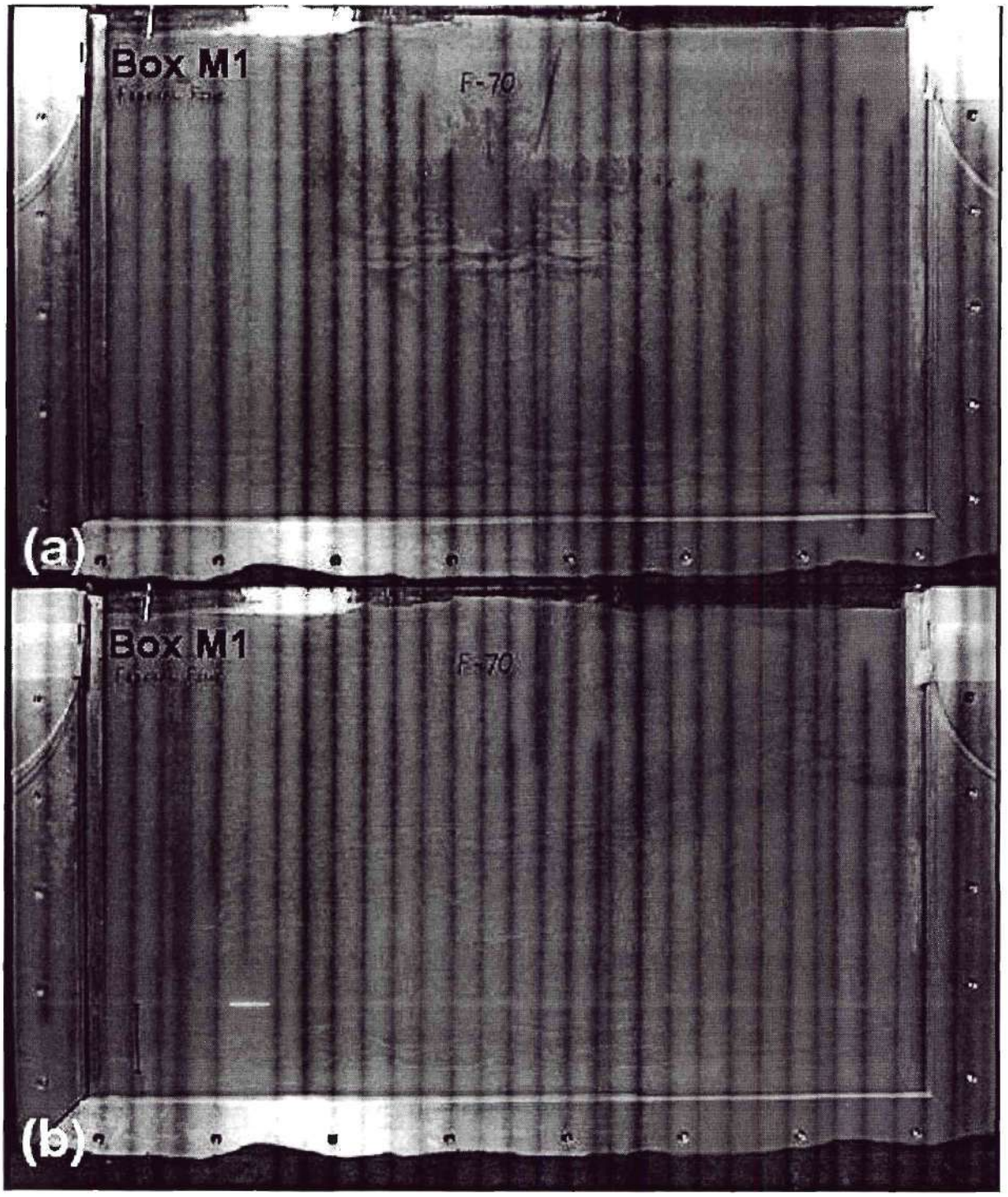

Figure 40. Representative early (a: ~540 mL) and late (b: ~1350 mL) time photographs during NAPL displacement in Box M1 (initial NAPL composition was 0.69 mole fraction TCE and 0.31 mole fraction decane).

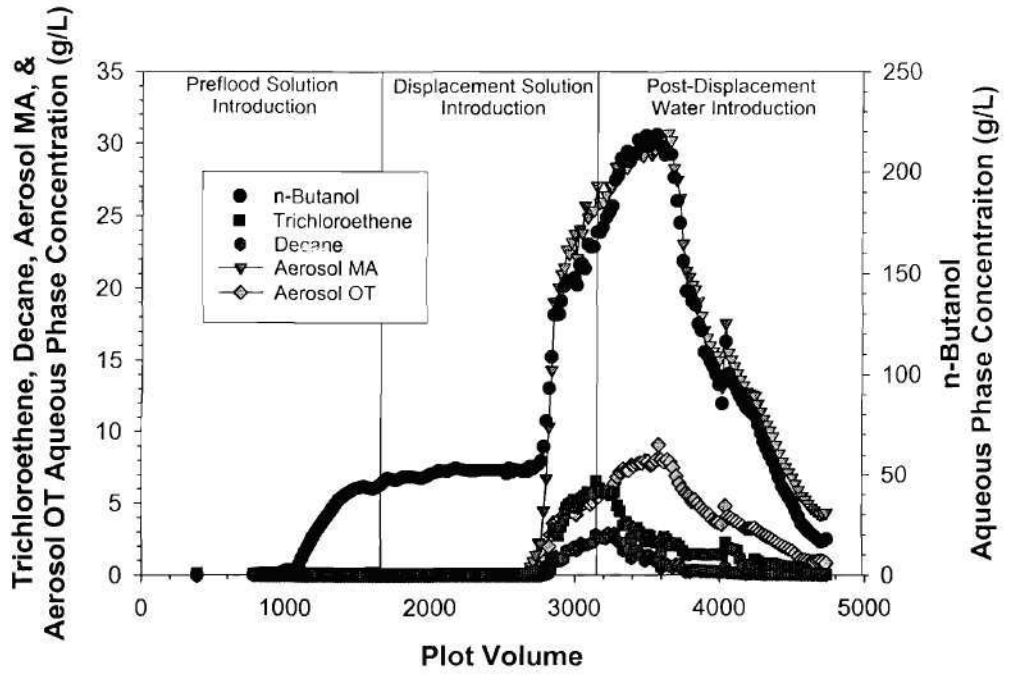

Figure 41. Aqueous phase concentrations of BuOH, TCE, decane, Aerosol MA, and Aerosol OT in the effluent from Box M1. Vertical lines represent the introduction of flushing solutions.

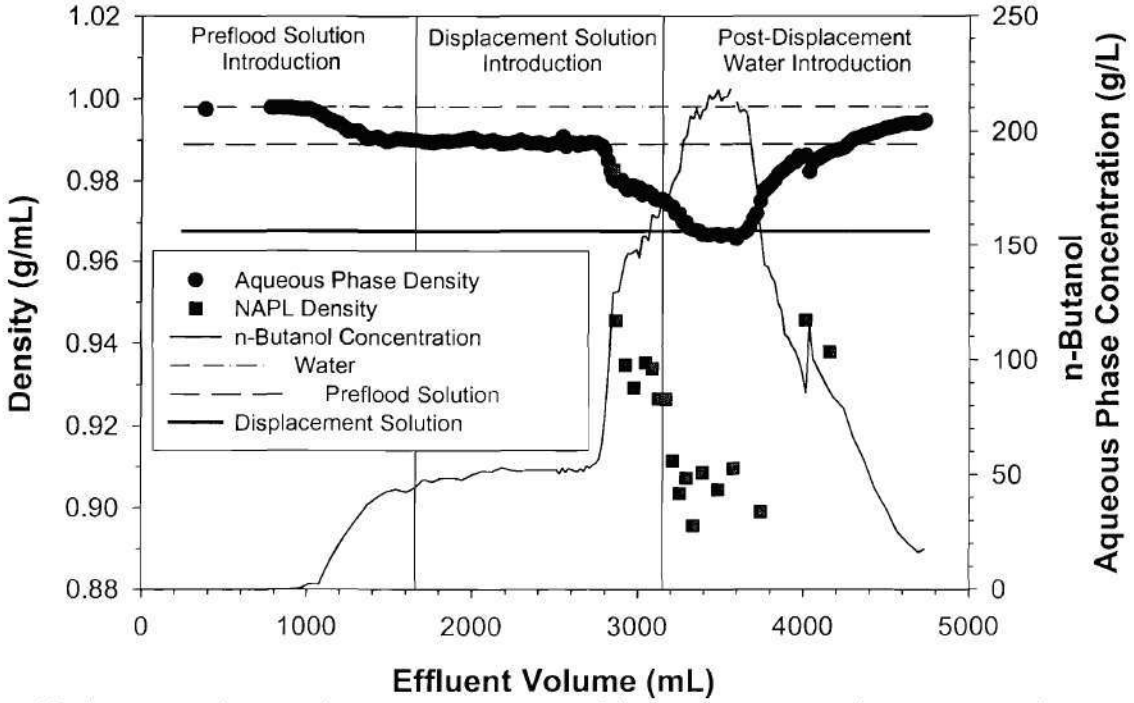

Figure 42. Aqueous phase and NAPL effluent densities and corresponding aqueous phase concentration on n-butanol from Box M1. Horizontal lines represent influent solution densities, and vertical lines represent the introduction of flushing solutions in the influent.

The second mixture considered consisted of 0.84 mole fraction TCE and 0.16 mole fraction decane and had a density of ~1.3 g/mL. While the mixture used in Box M1 had a higher fraction of decane, it was not necessarily representative of the density of a spent degreasing fluid. While the presence of decane appeared to have little impact on the partitioning behavior of n-butanol, the greater density reduction required for the relatively more dense mixture necessitated a *quantitative evaluation of the alcohol distribution. For these batch studies, various amounts of* n-butanol and NAPL (0.84 mole fraction TCE and 0.16 mole fraction decane) were contacted with water in 35 mL borosilicate centrifuge tubes. Each composition was generated in triplicate and equilibrated on shake trays for a minimum of 72 hours. Samples were subsequently centrifuged to promote coalescence of dispersed droplets in each phase. After centrifugation, the two phases in each tube were carefully removed, so as not to entrain any of the other phase, and placed in 20 mL scintillation vials. Samples were analyzed for density, viscosity, and composition using previously described methods.

Results of equilibrium compositional analysis of both phases are shown in the pseudo-phase diagram shown in Figure 43. Important to note is that the quaternary system of water, n-butanol, TCE and decane has been reduced to a ternary by assuming that the TCE and decane partition between the phases in a similar manner. This assumption is acceptable because the partitioning of water and n-butanol between the aqueous and organic phases are markedly different than that of TCE and decane. Measured tie lines compare with the phase behavior observed using the pure component NAPLs evaluated under Task 1A, and indicate that the aliphatic compound had little influence on the type (both exhibit Type II liquid-liquid equilibrium) and extent of alcohol partitioning (the two-phase region in each ternary diagram has similar shape). No compositional modeling (UNIQUAC) was conducted for this system and thus only measured tie lines are presented in Figure 3. A calculated tie line representing density conversion relative to water, however, has been included to demonstrate the relative size of the LNAPL region (see Figure 3, Task 1A). This tie line was based upon the mole fraction of n-butanol in the NAPL where the density reduction curve (NAPL density plotted against the mole fraction of n-butanol in the NAPL) intersects the density of water.

Following the batch experiments, a 2-D aquifer cell experiment was conducted to evaluate DMD of a TCE-decane NAPL mixture having 0.84 mole fraction TCE and 0.16 mole fraction decane, and a density of ~1.3 g/mL. Box M2 had a pore volume of 1325 mL and an overall permeability of 5.0×10^{-7} cm^2. After the NAPL injection and redistribution process, 31 mL of NAPL remained in the 2-D aquifer cell, corresponding to an overall NAPL saturation of 2.3%. A total of 4900 mL of an aqueous solution containing 6% (wt) n-butanol (dyed blue-green) were introduced through the partially screened injection well at an average flow rate of 4.3 mL/min. At early time (~400 mL) the preflood solution contacted the NAPL mixture and caused the NAPL to begin to swell (Figure 44). As noted previously, the influent solution appeared in the upper left-hand corner of the 2-D aquifer cell due to flow from the partially screened injection well into the fully screened end chamber, and back into the domain. At later time (~4860 mL), significant swelling and migration resulted from the IFT reduction associated with NAPL compositions near the point of density conversion. Migration of the NAPL, however, was not catastrophic (complete free product migration) as evidenced by the lack of NAPL in the fine layer and lenses. Additionally, capillary forces appear to have remained strong enough to re-entrap the NAPL, as no free product was collected in the effluent and migration did not continue during the flow interruption period of ~12 hours following the preflood. The inclusion of the flow interruption was not necessary for density conversion (discussed below with the effluent

concentration data), but rather the result of the length of the experiment. A total of 1400 mL of low-IFT solution consisting of 4% (4:1 wt) Aerosol MA/OT + 20% (wt) n-butanol + 500 mg/L $CaCl_2$ (not dyed) was introduced at an average flow rate of 4.3 mL/min through the partially screened influent well. At early time (~540 mL) and late (~1350 mL) time displacement and upward migration of the NAPL mixture was also observed (Figure 45).

Effluent aqueous phase concentrations from Box M2 are shown in Figure 46 as a function of effluent volume collected. Here the vertical lines represent the introduction of the preflood, low-IFT displacement flood and post treatment water flood solutions into the partially screened injection well. The x-axis of Figure 46 has been compressed below 6000 mL to improve the clarity of the low-IFT displacement flood data. After the appearance of preflood solution in the effluent, n-butanol concentrations increased steadily to values approaching the influent solution (~59 g/mL). Relatively minor reductions in the aqueous phase concentration of n-butanol can be seen following periods of flow interruption at ~2300 mL and ~4300 mL. The duration the reduced concentration (~100 mL), however is much less than the aqueous pore volume of the cell (~1300 mL) and therefore are more indicative of volatilization of n-butanol from the end chamber (having volume of ~60 mL) during periods of flow interruption. The prompt return of the n-butanol concentration to levels observed prior to periods of flow interruption suggests that the partitioning of n-butanol was relatively rapid, and thus the periods of flow interruption were not required for density conversion. Significant rate-limitations to n-butanol partitioning would have appeared as reductions in effluent n-butanol concentration following the resumption of flow, similar to that observed for rate-limited sorption processes. Upon arrival of the low-IFT solution in the effluent, as determined by increased Aerosol MA and Aerosol OT concentrations, the concentration of n-butanol began to rise again, and eventually exceeded the concentration of n-butanol in the influent low-IFT solution. Concentrations of n-butanol in excess of the influent value resulted in solubilization of NAPL containing n-butanol. Solubilization can be seen in Figure MIX8 as increases in both TCE and decane concentrations upon the arrival of the low-IFT solution. Displacement and solubilization are not mutually exclusive, and any solubilization of NAPL subsequent to the preflood would increase the mass of n-butanol in the aqueous phase.

Effluent densities from Box M2 are shown in Figure 47, where vertical lines represent the introduction of flushing solutions through the partially screened influent well, and horizontal lines represent the density of the influent solutions. Here again, the density of the aqueous phase was related to the concentration of n-butanol in the aqueous phase (hairline trace). Importantly, all NAPL densities were less than that of corresponding aqueous phase sample. This indicates that the NAPL density was reduced from 1.28 g/mL to values ranging from 0.942 g/mL to 0.914 g/mL and density conversion of the binary NAPL was successful.

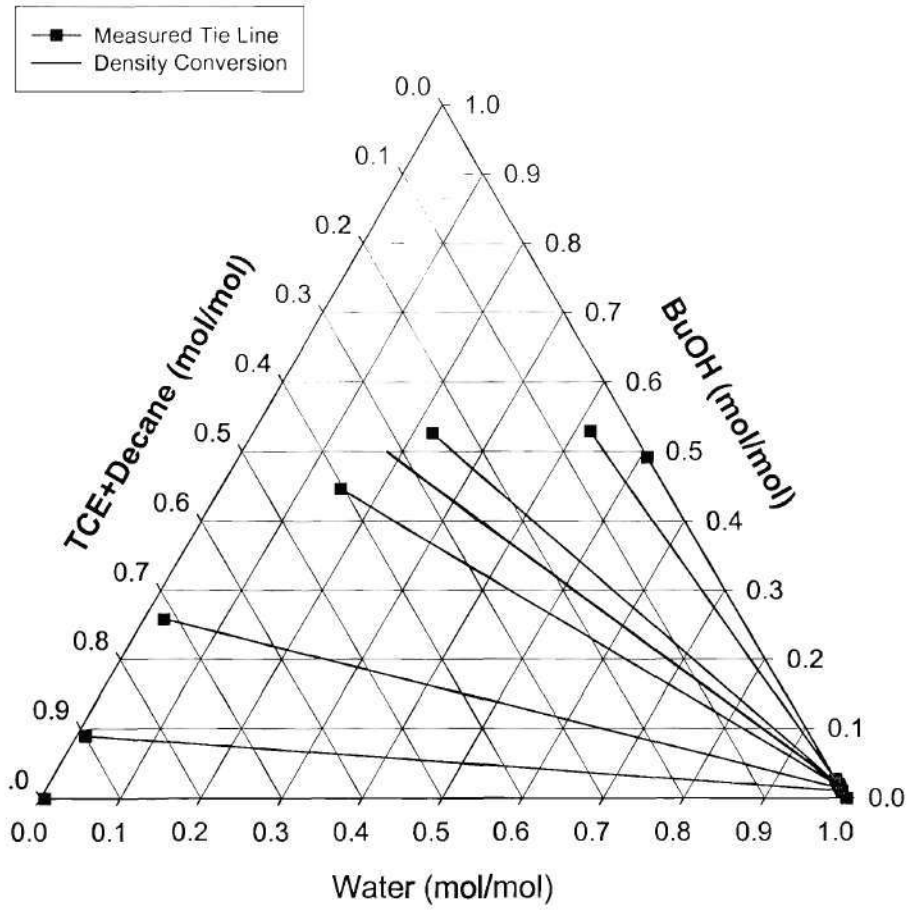

Figure 43. Pseudo-ternary phase diagram for the n-butanol, water, TCE and decane system. Molar ratio of TCE to Decane in the initial NAPL (i.e., before contact with water and n-butanol) was 5.25:1.

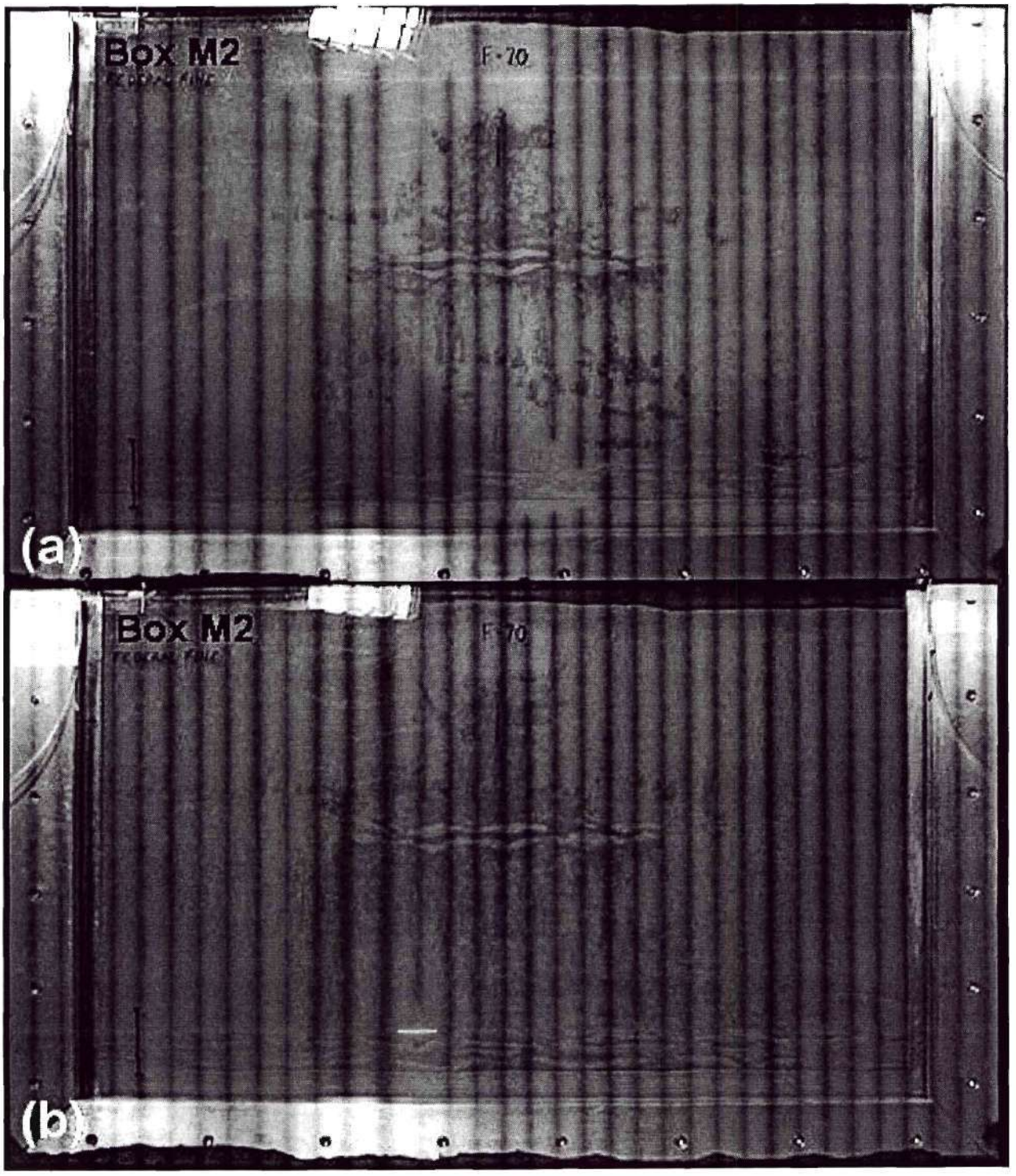

Figure 44. Representative early (a: ~400 mL) and late (b: ~4860 mL) time photographs during the 6% (wt) n-butanol aqueous preflood of Box M2 (initial NAPL composition was 0.84 mole fraction TCE and 0.16 mole fraction decane).

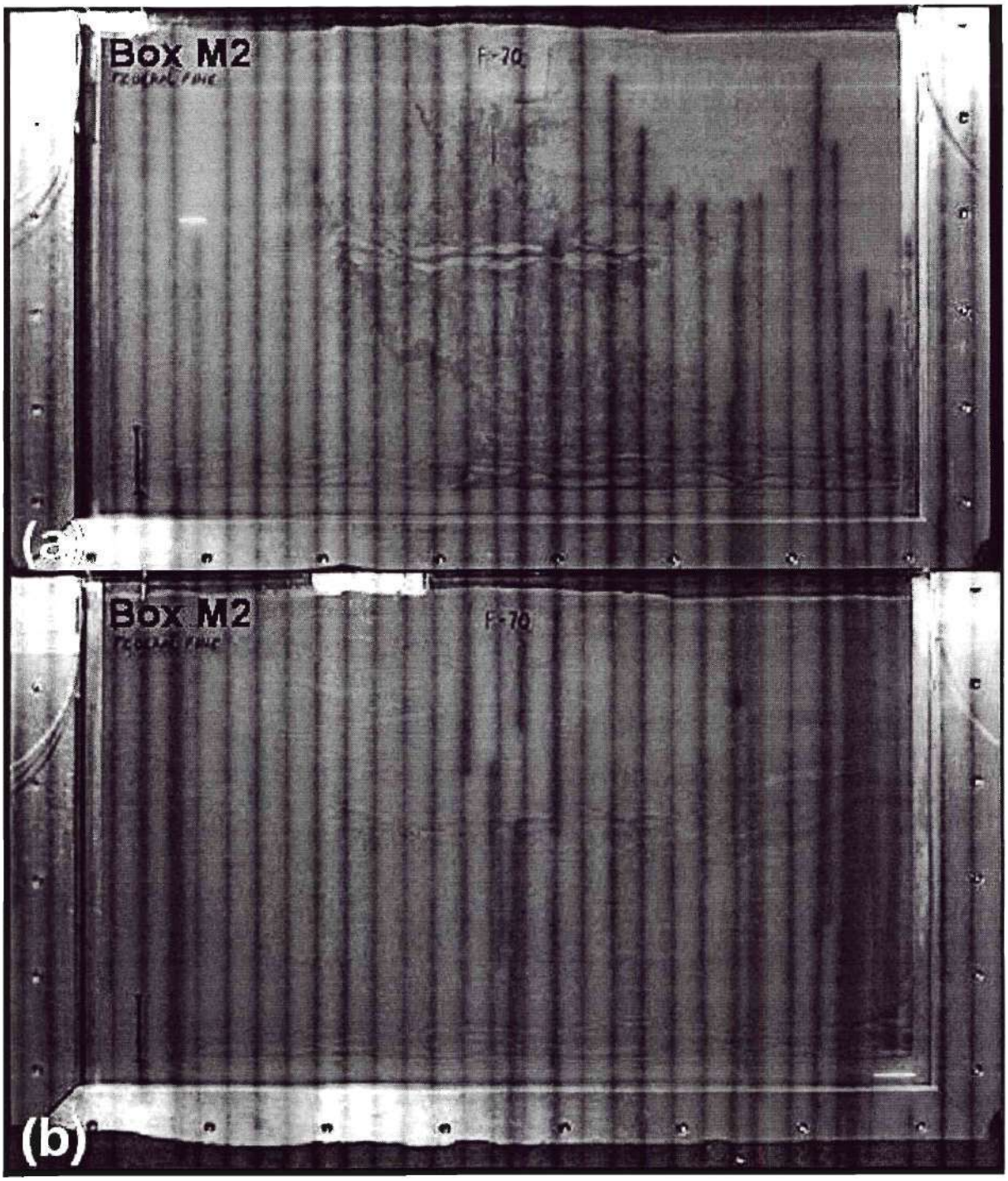

Figure 45. Representative early (a: ~540 mL) and late (b: ~1350 mL) time photographs during NAPL displacement in Box M2 (initial NAPL composition was 0.84 mole fraction TCE and 0.16 mole fraction decane).

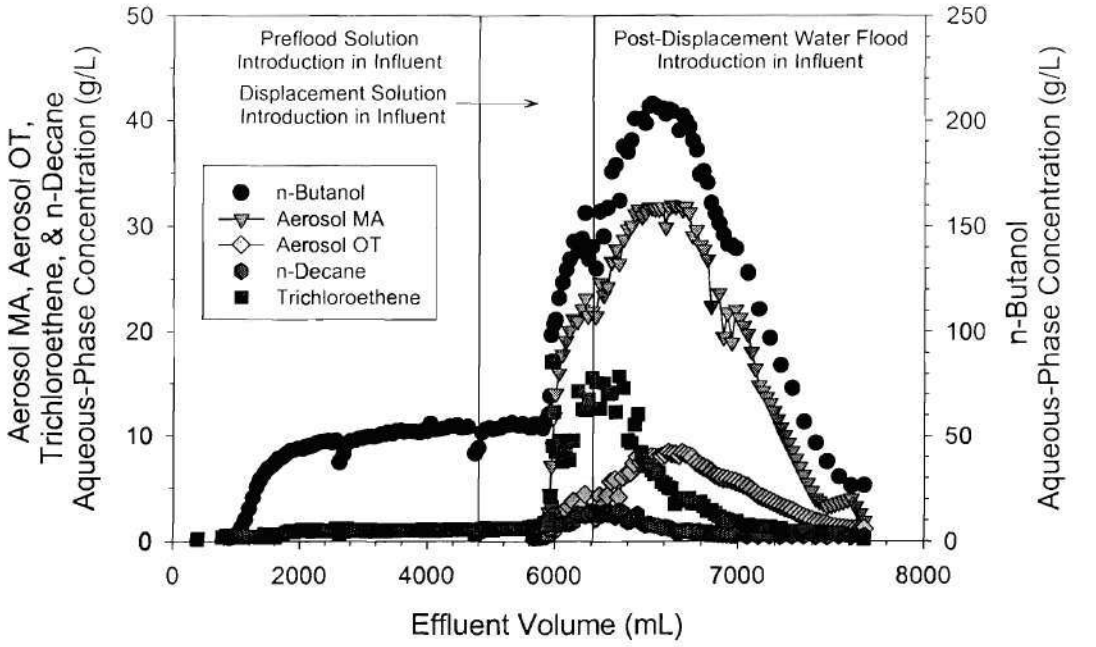

Figure MIX8. Aqueous phase concentrations of BuOH, TCE, decane, Aerosol MA, and Aerosol OT in the effluent from Box M2. Vertical lines represent the introduction of flushing solutions.

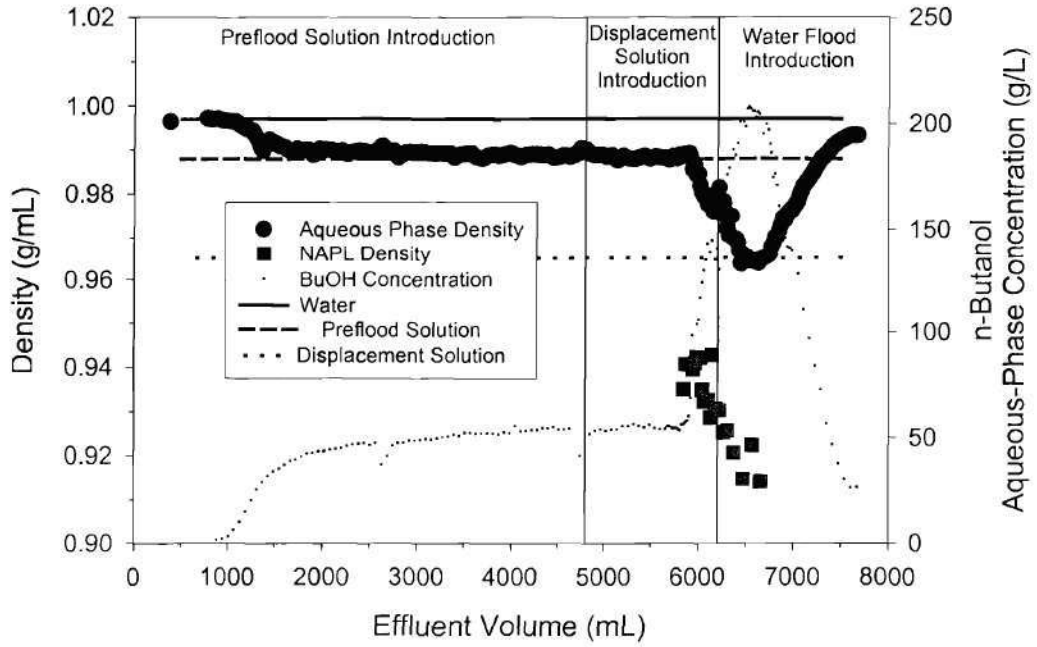

Figure 46. Aqueous phase and NAPL effluent densities and corresponding aqueous phase concentration of BuOH in Box M2. Horizontal lines represent influent solution densities, and vertical lines represent the introduction of flushing solutions.

(VII) TECHNOLOGY TRANSFER:

Technology transfer for Sub-Project IV is achieved through a combination of refereed publications, oral presentations, web-based presentations, as well as contact with consulting firms that may be interested in the DMD technology. A four page description of the DMD technology and photo sequences of the density modification and displacement processes are posted on the GLMAC HSRC web page by Shelley Armstrong and the main EPA-HSRC web page by Mark Hodges. In addition, Dr. Pennell has posted time-lapse photo sequences and descriptions of the DMD process on his university web page. A summary of project highlights, presentations and publications is provided below in chronological order.

(VIII) PROJECT HIGHLIGHTS:

- "Development, Mathematical Modeling and Field Testing of Surfactant Flushing for Remediation of NAPL-Contamination" presented at the U.S EPA Hazardous Substance Research Centers Five Centers Conference in Monterey, CA (2000).
- U.S. Patent No. 6,099,206, "Density Modification Displacement To Remediate Contaminated Aquifers" issued (2000).
- A pilot-scale field test of SEAR is successfully completed at the Bachman Road site in Oscoda, MI. The project involved a team of GLMAC-HSRC researchers from the University of Michigan, Georgia Institute of Technology, and HSI Geotrans, Inc. (May-August 2000).
- Two papers are published in the *Journal of Contaminant Hydrology* describing experimental and mathematical modeling of surfactant enhanced aquifer remediation (SEAR) in heterogeneous, two-dimensional aquifer cells (2001).
- A paper is published in *Ground Water Monitoring & Remediation* comparing two surfactant formulations considered for use at the Bachman Road site based on experimental tests and economic analysis (2001).
- Three papers are published in *Environmental Science & Technology* describing the development and testing of the Density Modified Displacement (DMD) method for recovery of TCE-DNAPL (2002).
- A provisional patent application submitted for "Macroemulsion Delivery of Partitioning Alcohols for Density Modified Displacement of DNAPLs" (2003)

(IX) PAPERS/PRODUCTS/PATENTS/OTHER:

1998-1999 Presentations:

Taylor, T.P., K.D. Pennell and L.M. Abriola. 1998. Surfactant/cosolvent enhanced recovery of tetrachloroethylene from porous media. American Geophysical Union Fall Meeting, December 6-10, 1998, San Francisco, CA.

Kibbey, T.C.G., K.D. Pennell, C.A. Ramsburg, K.F. Hayes. 1998. Effects of surfactant properties on equilibrium and nonequilibrium alcohol partitioning into dense nonaqueous phase liquids for in situ density modification applications. American Geophysical Union Fall Meeting, December 6-10, 1998, San Francisco, CA.

Loffler, F.E. Tiedje, J.M., Fathepure, B.Z., Hayes, K.F., Abriola, L.M., Pennell, K.D. and Adriaens, P. 1998. Remediation of Chlorinated Solvents at the Bachman Road Site Using Innovative Technologies. *In* Proceedings of the Abbua chlorierter Kohlenwasserstoffe Workshop, September 28-29, 1998, Fraunhofer-Institutszentrum, Stuttgart, Germany.

Pennell, K.D. 1998. Surfactant enhanced aquifer remediation. Vivendia Europea Academie des Sciences: Environmental European Forum of Young Researchers, August 27-31, 1998. Strasbourg, France *(invited)*.

Abriola, L. M. 1999. Surfactant-Enhanced Technologies for Subsurface Environmental Restoration: the Influence of Soil Textural Variations on System Performance. The Vth International Symposium, Chemistry Forum '99, Faculty of Chemistry, Warsaw University of Technology, Warsaw, Poland, April, 1999 *(Plenary Address)*.

Ramsburg, C.A. and K.D. Pennell. 1999. Refinement of the Density Modified Displacement (DMD) method for trichloroethylene remediation. American Geophysical Union Spring Meeting, May 30-June 3, 1999, Boston, MA.

Abriola, L. M., K. D. Pennell, K. F. Hayes, and E. A. Petrovskis. 1999. Surfactant Enhanced Remediation of DNAPLs at the Bachman Road Site. American Geophysical Union, Spring Meeting, May 30-June 3, 1999, Boston, MA.

Pennell, K.D. 1999. The Use of Surfactants to Enhance Subsurface Remediation Technologies. Savannah River Ecology Laboratory, Advanced Analytical Center for Environmental Sciences, October 8, 1999, Savannah River Site, SC *(invited)*.

Taylor, T.P., C.A. Ramsburg, and K.D. Pennell. 1999. Evaluation of Interfacial Area of Residual NAPL Compounds Using Anionic Surfactant Interfacial Tracers. American Geophysical Union National Meeting, December 13-17, 1999, San Francisco, CA.

1998-1999 Publications:

Rathfelder, K.M., T.P. Taylor, L.M. Abriola and K.D. Pennell. 1998. Simulation of the surfactant-enhanced solubilization of PCE in bench-scale laboratory studies. *In* Nonaqeuous Phase Liquids: Remediation of Chlorinated and Recalcitrant Compounds, G.B. Wickramanayake and R.E. Hinchee (eds.), Battelle Press, Columbus, OH pp. 91-96.

Singletary, M.A. 1998. Tetrachloroethylene (PCE) Infiltration and Entrapment in the Saturated Zone of a Two-Dimensional Aquifer System. Special Research Project Report, Master of Science in Environmental Engineering, Georgia Institute of Technology, Atlanta, GA.

Taylor, T.P. and K.D. Pennell. 1998. Surfactant enhanced recovery of PCE from heterogeneous porous media. *In* Proceedings of the 1998 Symposium on Environmental Models and Experiments Envisioning Tomorrow (EnviroMEET 98), July 20-23, 1998, Irvine, CA.

Rathfelder, K.M., Abriola, L.M., Singletary, M.A. and K.D. Pennell. 1999. Investigation of numerical prediction accuracy of multiphase flow in a laboratory sand tank. *In* Proceedings of ModelCARE 99, Calibration and Reliability in Groundwater Modelling, September 20-23, 1999 Zurich, Switzerland.

Singletary, M.A., Pennell, K.D. and C.A. Ramsburg 1999. Effects of soil layering and interfacial tension on DNAPL migration in subsurface environments. *In* Proceedings of the 1999 ASCE-CSCE Joint Conference on Environmental Engineering, July 25-28, 1999, Norfolk, VA.

Ramsburg, C.A. 1999. Development of Surfactant Formulations for In-Situ Remediation of a Tetrachloroethylene-Contaminated Aquifer: Treatability Studies and Economic Analysis. Special Research Project Report, Master of Science in Environmental Engineering, Georgia Institute of Technology, Atlanta, GA.

Taylor, T.P. 1999. Characterization and Surfactant Enhanced Remediation of Organic Contaminants in Saturated Porous Media. Ph.D. Dissertation, Georgia Institute of Technology, Atlanta, GA.

Ramsburg, C.A., T.C.G. Kibbey, K.D. Pennell and K.H. Hayes. 1999. Density Modified Displacement of Dense Nonaqueous Phase Liquids. *In* Proceedings of U.S. EPA Conference

on Innovative Clean-Up Approaches: Investments in Technology Development: Results and Outlook for the Future. November 2-4, 1999. Bloomingdale, IL.

2000 Presentations:

Ramsburg, C.A. and K.D. Pennell. 2000. Recovery of Trichloroethylene from Saturated Porous Media Using the Density Modified Displacement Method. American Institute of Chemical Engineers Spring Meeting, March 5-9, 2000. Atlanta, GA.

Pennell, K.D. 2000. Development of Efficient Flushing Strategies for Remediation of DNAPL-Contaminated Aquifers. Gordon Research Conference on "Modeling of Flow in Permeable Media", August 6-11, 2000, New Hampton, NH. *(invited)*

2000 Publications:

Ramsburg, C.A. and K. D. Pennell. 2000. Evaluation of Surfactant Formulations for Treatment of a PCE-Contaminated Field Site. *In* Treating Dense Nonaqueous Phase Liquids (DNAPLs): Remediation of Chlorinated and Recalcitrant Compounds. G.B. Wickramanayake, A.R. Gavaskar and N. Gupta (eds.), Battelle Press, Columbus, OH, pp. 211-218.

Luning Prak, D.J., L.M. Abriola, W.J. Weber, Jr., K.A. Bocskay, and K.D. Pennell. 2000. Solubilization Rates of n-Alkanes in Micellar Solutions of Nonionic Surfactants, Environmental Science and Technology, 34:476-482.

Rathfelder, K.M., L.M. Abriola, M.A. Singletary and K.D. Pennell. 2000. The influence of interfacial tension reduction on organic liquid migration: Numerical and experimental comparisons. *In* Calibration and Reliability of Groundwater Modelling: Coping with Uncertainty, F. Stauffer, W. Kinzelbach, K. Kovar and E. Hoehm (Eds.), International Association of Hydrological Sciences, Publication No. 256, Wallingford, England, pp. 439-447.

U.S. Patent No. 6,099,206, Density Modification Displacement To Remediate Contaminated Aquifers". Issued August 8, 2000. Inventor: Kurt D. Pennell, Assignee: GTRC.

2001 Publications:

Taylor, T.P., K.D. Pennell, L.M. Abriola, and J.H. Dane. 2001. Surfactant Enhanced Recovery of Tetrachloroethylene from a Porous Medium Containing Low Permeability Lenses. 1. Experimental Studies. *Journal of Contaminant Hydrology* 48:325-350.

Rathfelder, K.M., L.M. Abriola, T.P. Taylor, and K.D. Pennell. 2001. Surfactant Enhanced Recovery of Tetrachloroethylene from a Porous Medium Containing Low Permeability Lenses. 2. Numerical Simulation. *Journal of Contaminant Hydrology* 48:351-374.

Taylor, T.P. and K.D. Pennell 2001. Effects of Cosolvent Addition on Surfactant Enhanced Recovery of Tetrachloroethene (PCE) from a Heterogenous Porous Medium. *In* Physico-Chemical Groundwater Remediation, J.A. Smith and S.E. Burns (eds). Kluwer Academic Publishers, New York, pp. 285-306.

Kibbey, T.C.G., C. A. Ramsburg, K.D. Pennell and K.F. Hayes. 2001. In Situ Density Modification of Entrapped Dense Nonaqueous Phase Liquids (DNAPLs) using Surfactant/Alcohol Solutions. *In* Physico-Chemical Groundwater Remediation, J.A. Smith and S.E. Burns (eds). Kluwer Academic Publishers, New York, pp. 271-284.

Kibbey, T.C.G., K.D. Pennell and K.F. Hayes. 2001. Application of sieve-tray air strippers to the treatment of surfactant-containing wastewaters. *American Institute of Chemical Engineers Journal* 47: 1461-1470.

Ramsburg, C.A. and K.D. Pennell. 2001. Experimental and Economic Assessment of Two Surfactant Formulations for Source Remediation at a Former Dry Cleaning Facility. *Ground Water Monitoring & Remediation* 21:68-82.

2002 Presentations

Ramsburg, C.A., K.D. Pennell 2002. Density modified displacement of multi-component DNAPLs. American Institute of Chemical Engineers Fall Meeting, November 7-9, 2002. Indianapolis, IN.

Ramsburg, C.A., K.D. Pennell, T.C.G. Kibbey and K.F. Hayes. 2002. Delivery of n-butanol using a surfactant-stabilized o/w emulsion for density modified displacement of tetrachloroethene. Gordon Research Conference, Flow and Transport in Permeable Media, August 6-11, 2002, New Hampton, NH.

Drummond, C.D., E. Petrovskis, K.D. Pennell, and L.M. Abriola. 2002. Surfactant flushing pilot test results: Enhanced solubilization and biodegradability of PCE. 3rd International Conference on Remediation of Chlorinated and Recalcitrant Compounds, May 20-23, 2002, Monterey, CA.

Ramsburg, C.A., K.D. Pennell, T.C.G. Kibbey, and K.F. Hayes. 2002. Trichloroethene emulsification and recovery in saturated porous media. 76th American Chemical Society Colloid and Interface Science Symposium, "Interfacial and Colloidal Phenomena in Aquatic Systems", June 23-26, 2002, Ann Arbor, MI (*invited*).

Ramsburg, C.A. and K.D. Pennell. 2002. Density-modified displacement of DNAPLs using partitioning alcohol and low interfacial tension surfactant floods. 3rd International Conference on Remediation of Chlorinated and Recalcitrant Compounds, May 20-23, 2002, Monterey, CA.

2002-2003 Publications

Ramsburg, C.A. and K.D. Pennell. 2002. Density-modified displacement for dense nonaqueous phase liquid source-zone remediation: Density conversion and recovery in heterogeneous aquifer cells. *Environmental Science and Technology* 36:3176-3187.

Ramsburg, C.A. and K.D. Pennell. 2002. Density modified displacement for dense nonaqeuous phase liquid source zone remediation: Density conversion using a partitioning alcohol. *Environmental Science and Technology* 36:2082-2087.

Kibbey, T.C.G., C. A. Ramsburg, K.D. Pennell and K.F. Hayes. 2002. Implications of alcohol partitioning behavior for in situ density modification of entrapped dense nonaqueous phase liquids (DNAPLs). *Environmental Science and Technology*, 36:104-111.

Karagunduz, A. 2002. Influence of Surfactants on the Sorption and Transport of Contaminants in Saturated and Unsaturated Soils. Ph.D. Dissertation, Georgia Institute of Technology, Atlanta, GA.

Ramsburg, C.A. 2002. Development of Surfactant Based Immiscible Displacement Technologies for Remediation of Aquifers Contaminated with Dense Non-Aqueous Phase Liquids. Ph.D. Dissertation, Georgia Institute of Technology, Atlanta, GA.

U.S. Provisional Patent Application "Macroemulsion Delivery of Partitioning Alcohols for Density Modified Displacement of DNAPLs" submitted. Inventors: K.D. Pennell, C.A. Ramsburg, K.F. Hayes, and T.C.G. Kibbey (January 2003)

Rathfelder, K. M., L.M. Abriola, M.A. Singletary and K.D. Pennell. Influence of Surfactant-Facilitated Interfacial Tension Reduction on Organic Liquid Migration in Porous Media: Observations and Numerical Simulation. *Journal of Contaminant Hydrology* (in press).

Ramsburg, C.A., K.D. Pennell, T.C.G. Kibbey, and K.F. Hayes. 2002. Use of a surfactant-stabilized emulsion to deliver n-butanol for density modified displacement of trichloroethene-NAPL. *Environmental Science and Technology* (in review)

(X) STUDENTS SUPPORTED (degree, graduation date):

Michael A. Singletary, M.S. EnvE (August 1998)
Tammy P. Taylor, Ph.D. (August 1999)
Ahmet Karagunduz, Ph.D. (May 2002)
C. Andrew Ramsburg, Ph.D. (December 2002)